A Study for Leaching Synthetic Scheelite in H_2SO_4 And H_2O_2 Solution: An Investigation and Optimization

by

Idil Mutlu Tuncer

A thesis submitted in partial fulfillment of the requirements for the degree of

Master of Science

in

Materials Engineering

Department of Chemical and Materials Engineering

University of Alberta

ABSTRACT

Canada's 2021 Critical Minerals Strategy underscores the prominence of tungsten as a rare and critical element. Today, tungsten production relies on scheelite, categorized as a secondary resource due to its complex ore composition and lower-grade nature. This phenomenon stems from the depletion and utilization of high-grade wolframite reserves. In response to this context, the significance of synthetic scheelite has ascended, primarily due to its inherent advantages such as its low impurity content and enhanced accessibility, particularly in ongoing laboratory-based leaching investigations.

The most recent advancements in laboratory-scale research have yielded a feasible and environment-friendly approach for leaching synthetic scheelite utilizing a mixed acid solution of H_2SO_4 and H_2O_2. This process is carried out under normal pressure and moderate temperatures. Despite this notable progress, there persists a dearth of comprehensive inquiries into this novel leaching method. Furthermore, a comparative analysis between processes involving natural and synthetic ores remains underexplored. This existing gap in the literature underscores the need for a collaborative endeavor to achieve a comprehensive understanding of the novel leaching technique and a rigorous evaluation of the possibilities for optimizing operational parameters. Ultimately, the objective is to offer valuable insights and enhancements concerning the utilization of reagents, thereby fostering a more efficient, economically viable, and environmentally sustainable leaching process. To achieve this, a promising 2-step method for scheelite leaching was explored, aiming to minimize the thermal decomposition of H_2O_2 and subsequently reduce its concentration. The results showed that the 2-step method is infeasible as it requires a longer reaction time compared to the synergistic leaching approach, resulting in reduced productivity and energy efficiency.

Subsequently, a detailed investigation into the thermal decomposition process ensued, seeking to extract tungsten without compromising leaching efficiency. This was achieved by optimizing the operational conditions based on established literature for natural ore. The findings unveiled the potential for multiple recycling of lixivium, supplemented with depleted chemicals, thereby promoting an eco-friendly approach while reducing operational expenses. Notably, for an L/S (mL/g) ratio of 10, enhanced H_2WO_4 crystallization efficiency was achieved by optimizing the thermal decomposition duration, extended up to 6 hours. Moreover, experiments conducted without H_2SO_4 supplementation revealed the inherent optimization potential within the leaching system. Finally, optimization was undertaken in terms of reagent concentration, involving a reduction of H_2SO_4 concentration from 3 mol/L to 1 mol/L, an increase in temperature from 45°C to 60°C, and an additional 30-minute leaching duration. This collective effort culminated in proposing an environmentally conscious and cost-effective process for synthetic scheelite leaching in the solution of H_2SO_4 and H_2O_2.

PREFACE

This thesis is an original work by Idil Mutlu Tuncer under the supervision and edition of Dr. Jing Liu. Part of Chapter 3 has been presented as I. Mutlu Tuncer, J. Liu, "*Assessing the Feasibility of a 2-Step Method for Leaching Synthetic Scheelite in H_2SO_4 and H_2O_2 Solution*" The 34th Canadian Materials Science Conference, June 2023, Winnipeg, Canada.

ACKNOWLEDGMENTS

TABLE OF CONTENTS

LIST OF TABLES

LIST OF FIGURES

xii

LIST OF ABBREVIATIONS

ICP: Inductively coupled plasma spectroscopy

PTA: Peroxytungstic acid

XRD: X-ray diffraction

CHAPTER 1 INTRODUCTION

1.1 Research Background

Tungsten (W) is a strategically critical rare metal with a wide range of uses in the manufacture of high-performance metallic materials such as superalloys, cemented carbide, and specialty steels [1]. The escalating demand and increasing attention towards W in recent years have led to the exploration of novel production methods and applications [2]. Currently, hydrometallurgical methods are widely used, as they are considered the most effective, environmentally friendly, and favored approach in the W industry. In addition, hydrometallurgical methods offer high operational and production efficiencies for extracting W from complex and low-grade scheelite ($CaWO_4$) ores, which have become the primary source of this metal since high-grade and easily mineable wolframite ($[(Fe, Mn) WO_4]$) deposits have been exhausted progressively [3], [4]. Another important and popular W source is synthetic scheelite, which refers to a laboratory-made material with a crystal structure and chemical composition similar to natural scheelite, a calcium tungstate mineral. Synthetic scheelite can also be generated by pre-enrichment of $[(Fe, Mn) WO_4]$ by roasting in the presence of lime ($Ca(OH)_2/CaO$) or limestone ($CaCO_3$) [5]–[7].

In W extractive metallurgy, high temperature, and high-pressure required alkaline leaching is the traditional method and is still used in commercial W processing plants today. However, due to the environmental risks associated with alkaline leaching such as producing excess amounts of wastewater, acid leaching has garnered attention as a potential alternative eco-friendly method [8]. Subsequently, new laboratory-scale studies have focused on improving acid leaching as an alternative approach [4], [9]. Recently developed lab-scale acid leaching processes suggest shorter and cost-effective operation, high recovery of W, reduced environmental impact, a sharp reduction in disposal cost, and lower energy consumption due to no necessity for high pressure and temperature for W extract from the $CaWO_4$ mineral [9], [10]. HCl was the first acid-leaching reagent utilized in industrial processes, but its current application is limited due to being corrosive and having high volatility. Subsequently, attempts were made to employ HNO_3, but it presents a significant environmental hazard due to its toxic vapors, despite its high leaching efficiency and yield. For this reason, HNO_3 has never been adapted to the industry, and its use is considered risky [4], [8], [11]–[13]. Finally, H_2SO_4 has been presented as a possible alternative reagent to HCl in acid leaching, due to its affordability, ready availability, and reduced environmental risk due to its low volatility and corrosive properties relative to other acids [4], [13]. Using H_2SO_4 for $CaWO_4$

leaching has benefits, but it also leads to the precipitation of insoluble tungstic acid (H_2WO_4) and gypsum ($CaSO_4 \cdot 2H_2O$), similar to the use of HCl leaching. This results in the formation of an H_2WO_4 coating on unreacted $CaWO_4$ particles, which impedes further reaction and decreases leaching efficiency. Separating two insoluble solids can be challenging [4], [8]. To address this issue, a complexing agent is required to convert W into a water-soluble form, without precipitating as H_2WO_4 [4], [11]. Despite numerous attempts to find a suitable complexing agent, recent studies have shown that H_2O_2 is a promising option due to its strong oxidizing properties and eco-friendliness [11], [14], [15]. Thus, recent studies [8], [11], [13] showed that for $CaWO_4$ leaching H_2O_2-H_2SO_4 leaching solution proposes an effective and environmentally friendly process. This process is based on leaching synthetic scheelite in a mixture of H_2SO_4 and H_2O_2 at normal pressure and desired temperature. After leaching is completed the by-product $CaSO_4$ can be used as a direct raw material in the construction industry. On the other hand, W is obtained from the pregnant solution (peroxy/peroxo tungstic acid (PTA)) with H_2WO_4 precipitation by the thermal decomposition process. Moreover, the resulting leaching solution can be reused by supplementing fresh reagents after recycling. Therefore, hazardous waste or excessive amounts of wastewater are not generated throughout the leaching process [8], [11], [13]. Furthermore, this process does not require high temperature and pressure, making it energy-saving compared to other methods [13].

It is worth noting that despite the advantages of this leaching process, the poor thermal stability of H_2O_2 is one of the challenges. H_2O_2 is a self-decomposing chemical that starts to decompose when exposed to air and/or water. Moreover, increasing temperature enhances the decomposition rate of H_2O_2, and the leaching efficiency decreases as its concentration in the leaching medium reduces [14]. The other challenge is the poor stability of the resulting PTA since it is affected by H_2O_2 instability negatively [16]. Researchers have highlighted that the poor thermal stability of H_2O_2 and tungsten peroxide is affected by the leaching temperature, while the leaching efficiency is influenced by the concentration of H_2O_2 [13]. To address these challenges, in the recent study conducted by Zhang et al. [11], a 2-step method is suggested to minimize H_2O_2 decomposition in $CaWO_4$ leaching. However, no experimental proof exists of this method's effectiveness on $CaWO_4$ leaching. Therefore, further study is required to understand the leaching mechanism and increase the efficiency, test the feasibility of the 2-step method, and evaluate the impact of this method on the reagent consumption in the H_2SO_4 and H_2O_2 leaching system.

1.2 Problem Statement

During the leaching process of $CaWO_4$ using H_2SO_4 and H_2O_2 solution, the H_2SO_4 is primarily consumed in converting $CaWO_4$ to $CaSO_4$. H_2SO_4 does not decompose and has a long shelf life due to its stability and low volatility [13]. On the other hand, the addition of H_2O_2 to the leaching solution leads to the gradual decomposition of H_2O_2 into H_2O and O_2 due to its interaction with water, air, and H_2SO_4. This decomposition is further accelerated when heating the leaching solution, depleting H_2O_2 entirely during thermal decomposition. Consequently, the concentration and effectiveness of H_2O_2 decrease, negatively impacting the leaching rate [8], [11]. In essence, not all H_2O_2 concentrations remain active and efficient throughout the operation. Despite previous research suggesting a "2-step method" to minimize H_2O_2 decomposition and improve the process's cleanliness, practical evidence supporting the feasibility of $CaWO_4$ leaching in H_2SO_4 and H_2O_2 solution is lacking [11].

Previous studies [11], [13] have demonstrated the potential for recycling the leaching solution (lixivium) and renewing the consumed reagents through thermal decomposition. This approach reduces reagent consumption, minimizes waste generation, and promotes a cleaner operation. The leaching process can be repeated for up to 5 cycles without significant efficiency reduction by supplementing depleted reagents. However, specific details of this process are lacking. Therefore, understanding the recycling mechanism of the leaching solution is crucial for process improvement and assessing the economic impact of reagent consumption.

To evaluate the feasibility of the 2-step method proposed to minimize H_2O_2 decomposition and reduce reagent waste, it is necessary to lessen the residence time of H_2O_2 in the system. Further investigation is required to comprehensively understand the thermal decomposition process and reagent consumption, which would provide insights into the effect of chemical concentration and consumption on operation costs. Exploring high efficiency under different operating conditions and assessing the economic implications of these conditions is also important, as existing literature lacks approaches based on chemical consumption. Additionally, while studies have focused on investigating the kinetics such as reagent concentration and temperature to maximize leaching efficiency and yield, data regarding the reagent consumption on operating costs are currently lacking.

1.3 Research Objectives

The present work aims to test the feasibility of the practical application of the 2-step method in the leaching synthetic scheelite in H_2SO_4 and H_2O_2 solution to efficiently extract W. Additionally, it aims to gain a better understanding of lixivium recycling and reuse, as well as the impact of regent consumption and supplementation on the system. Moreover, it is significant to explore the feasibility of extracting W without compromising leaching efficiency by optimizing the operating conditions suggested in the existing literature. Ultimately, the objective is to provide insights and make improvements to the economic aspect of reagent use. The specific objectives of this work are addressed below:

(1)   To study the feasibility of the "2-step method" for leaching synthetic scheelite in the H_2SO_4-H_2O_2 solution system and investigate the time-dependent behavior of H_2WO_4 precipitation. Time measurements are used to evaluate the influence of leaching duration on efficiency and yield, while the color change in the slurry is recorded to emphasize the role of H_2O_2 in the leaching reaction.

(2)   To investigate lixivium's recycling and reuse mechanism and assess the reagent consumption in the operation. Changes in the physical properties of the lixivium, such as color, volume, mass, and pH, are recorded. An X-ray diffraction (XRD) analysis is conducted to evaluate the impact of reagent concentration on the leaching efficiency and the final product.

(3)   To optimize operating conditions based on the correlation of the findings from objective 1 and objective 2. Inductively coupled plasma mass spectrometry (ICP) is used to analyze the PTA. Overall, this study aims to improve our understanding of the synergetic leaching of synthetic scheelite in H_2SO_4-H_2O_2 solution and provide insight into the thermal stability of H_2O_2. Based on the results, further work needed will be determined.

1.4 Organization of the Thesis

Chapter 1 presents the research background, problem statement, and specific objectives of this dissertation.

Chapter 2 provides an overview of W and its industrial use, W ore resources, and traditional and modern extractive metallurgy methods in W production. This chapter focuses on the existing methodologies, progress, and knowledge gaps in the research of modern acid leaching in W extraction.

Chapter 3 presents the feasibility of the 2-step method of leaching $CaWO_4$ in H_2SO_4 and H_2O_2 solution. It includes detailed experimental procedures and interpretation of results. The second step, H_2O_2 addition, is performed in 30-minute intervals to investigate the leaching duration.

Chapter 4 presents detailed experimental procedures for lixivium recycling and reuse mechanism experiments, the reagent consumption in the leaching process, and a discussion of experimental findings. This chapter also covers the solid $CaSO_4$ and H_2WO_4 characterization by XRD.

Chapter 5 examines the optimization of leaching conditions by reducing the reagent concentration and analyzing the effects of temperature and leaching duration by correlating the results of Chapters 3 and 4. Post-experimental ICP characterization is used to explain the final leaching efficiency.

Chapter 6 exclusively summarizes experimental findings and provides recommendations for future work.

CHAPTER 2 LITERATURE REVIEW

2.1 Overview of Tungsten

W is a transition metal in Group 6 of the periodic table, known for its high melting point and density [17]. It is classified as a "less-common metal" and has limited economically extractable mineral resources compared to other metals [18], [19]. Recognized as a critical raw material, W ranks 54th in elemental abundance in the Earth's crust [18], [20]. It is considered one of the "3TG minerals" along with tin (Sn), tantalum (Ta), and gold (Au) [9]. Due to its exceptional chemical and physical properties, W plays a vital role in the production of high-quality tools used in aerospace, defense, optics-electronics, civilian, mining, and manufacturing [17], [18], [21]–[24]. It is particularly valuable for producing tungsten carbide (WC), a highly durable material widely used in lathe tools, cutters, drills, and dies for wire drawing [25]. W is also used in heat-resistant stainless steels, incandescent lamp filaments, electrical apparatus components, welding electrodes, and X-ray tube targets [18], [26]. **Figure 2.1** depicts the worldwide trend of concentrated tungsten production between 1960 and 2018 [27].
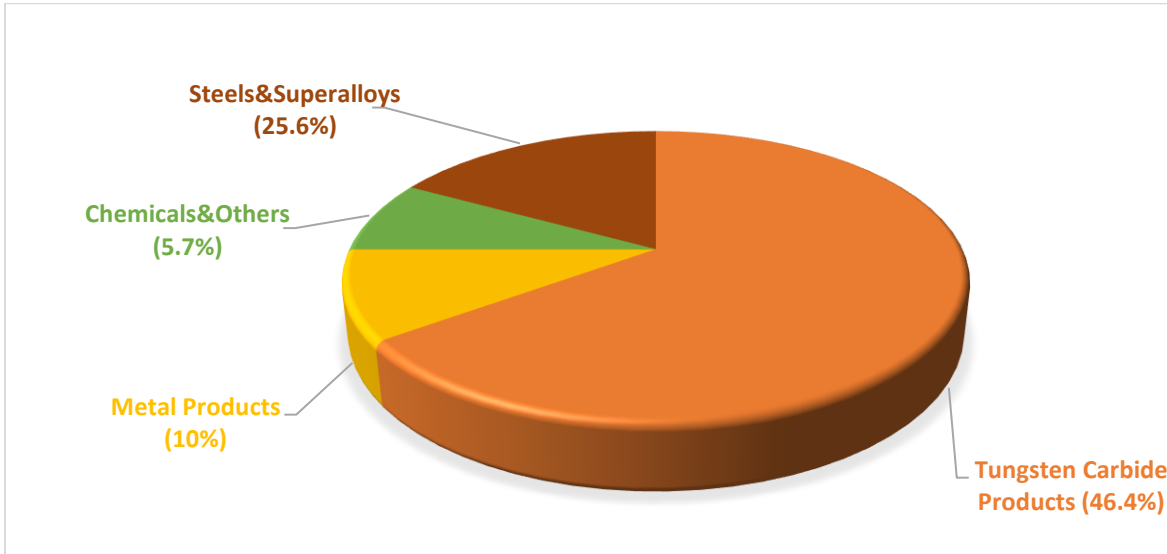
Figure 2. 1 Global analysis of concentrated W production from 1960 to 2018. Modified from [27].

In addition, W has been used as an eco-friendly alternative for lead (Pb) and uranium (U) in military applications for more than 50 years, and the demand is growing worldwide due to its non-solubility and non-toxicity [28]. Various W forms have also been extensively used in chemical

applications [25]. For example, ammonium para tungstate (APT) is used in the porcelain industry as a colorant and catalyst [24]; WO_3 (tungsten trioxide/ tungsten (VI) oxide/tungstic anhydride) is used as an inorganic pigment to add to ceramic glazes or paints to contribute physical strength of the catalyst and extend the catalyst's life. WO_3 is also used as part of selective catalytic reduction catalysts in coal-fired power plants to convert nitrogen oxides to N [18], [29]. Sodium tungstate (Na_2WO_4) is used to make fireproof fabrics [26]. The combination of unique chemical and physical characteristics of W and its key compounds, such as high density, high tensile strength, high melting point, high wear resistance, good thermal and electrical conductivity, low vapor pressure, and low expansion coefficient, make it an indispensable material for various applications [30], [31]. Consequently, the need for W resources in economic and social development is ineluctable [27].

2.2 W Resources

W has an average occurrence of about 1.5 ppm in the Earth's crust, making it rarer than most REEs [9]. Additionally, the majority of W sources are concentrated within the upper 3 km of the Earth's crust, accounting for approximately 0.01% [18]. While W resources are geographically widespread worldwide, as displayed in **Figure 2.2**, they are distributed unevenly. For instance, China holds the largest share with 54.3% of global W deposits, and is the leading producer, contributing 83.6% of primary W production. Canada follows with 8.3%, Russia with 7.1%, the USA with 4.0%, Bolivia with 1.5%, Austria with 0.3%, Portugal with 0.1%, and the remaining 24.4% distributed among other countries [27].

W does not exist in nature as an element; rather, it exists as a chemical compound with other elements [9], [26]. Despite W being present in more than 20 minerals, only two minerals, [(Fe, Mn) WO_4] and $CaWO_4$, are economically significant and extractable [9], [32]. The other minerals are rare and are mostly present in trace amounts [9]. Therefore, naturally occurring primary W resources are divided into wolframite groups and scheelite groups [29], [33]. According to data published by the US Geological Survey in 2018, the estimated global W reserves amount to approximately 3.3 million tons, primarily composed of $CaWO_4$ and [(Fe, Mn) WO_4] [34]. On the other hand, Shen et al. [9] reported that about one-third of the raw materials used in W metal production come from secondary resources, while the rest comes from primary resources.
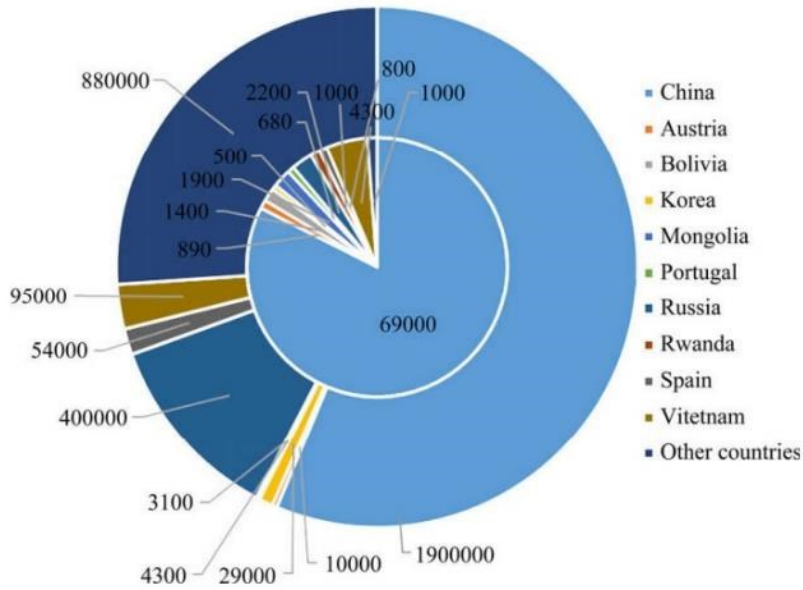
Figure 2. 2 Global W reserves and mine production in 2020 (unit: t) [27].

2.2.1 Primary Resources

Although there are various W-containing minerals in the earth's crust, most have low WO_3 content, ranging from 0.1 to 1.0 % [9]. W is primarily found in siliceous rocks as a tungstate (WO_4^{2-}) mixed with elements such as Fe, Mn, Ca, Cu, Pb, and Sn, and it is rarely present in other types of rocks [35], [36]. The main minerals that are well-known, abundant, and economically viable for mining are $CaWO_4$ and [(Fe, Mn) WO_4] [3], [8]. $CaWO_4$ accounts for 70% of the primary resources, while [(Fe, Mn) WO_4] [9] makes up the remaining 30%. The primary W minerals summarized by ITIA (International Tungsten Industry Association) are listed in **Table 2.1** [36].

Table 2. 1 Primary W minerals [29], [35]–[38].

Mineral	Formula	WO_3% Content
Ferberite	$FeWO_4$	76.3
Hubnerite	$MnWO_4$	76.6
Wolframite	(Fe, Mn) WO_4	76.5
Scheelite	$CaWO_4$	80.6
Stolzite and Raspite	$PbWO_4$	50.9

8

A WO_3 content of approximately 65% is required to produce W concentrate. $CaWO_4$ and [(Fe, Mn) WO_4] are richer in WO_3 content with 80.5% and 76.6%, respectively [5]. They are mostly found in five kinds of deposits: vein/stockwork, skarn, porphyry, strata bound, and disseminated [3]. The W mineralization is dominated by different origins [39]. For example, [(Fe, Mn) WO_4] is formed in veins, associated with cassiterite (SnO_2), pegmatite, and quartz (SiO_2) veins of hydrothermal origination genetically connected to granitic intrusive rocks, and its mineralization is based on greisen [36]. On the other hand, $CaWO_4$ is formed in various geologic settings, including granular masses in contact with metasomatic rocks, veins, and granite pegmatites [40].

2.2.1.1 Wolframite

[(Fe, Mn) WO_4] is an intermediate mineral between ferberite (Fe^{2+} rich) and Hubnerite (Mn^{2+} rich) [41]. It can be associated with apatite ($Ca_5(PO_4)$), arsenopyrite (FeAsS), and quartz [30]. The mineral crystals of [(Fe, Mn) WO_4] are in the monoclinic system, exhibiting perfect cleavage. They have a dark gray to brown-black color and a submetallic shining luster. Its fracture is uneven to rough, with a reddish-brown streak [42]. Additionally, with a specific gravity of 7.0–7.5 and a hardness of 4.0 to 4.5, [(Fe, Mn) WO_4] has paramagnetic properties [42], [43]. Due to its density and paramagnetic properties, gravity and magnetic separation methods are the most preferred and easily applied methods to enrich [(Fe, Mn) WO_4] [44]. The obtained concentrates have a WO_3 content of 76.5% [18]. Therefore, [(Fe, Mn) WO_4] ores have been used as the main source of W metal production for many years because of their high grade and quality, and ease of mining and processing [45]. However, the increased exploitation and consumption of [(Fe, Mn) WO_4] deposits over the years have resulted in the deposits becoming finer grains and containing complex ore [46], [47].

2.2.1.2 Scheelite

$CaWO_4$ has become the primary main mineral to produce W due to the continuous mining and overexploitation of high-quality [(Fe, Mn) WO_4] deposits and other high-grade W resources [48]. It includes 63.65% W in the purest form [42], and the concentrates obtained from $CaWO_4$ contain approximately 80.6% WO_3 [18]. $CaWO_4$ is easily identifiable by its white, brown, green, red, and honey-yellow colors and vitreous luster [42]. Under shortwave UV light characteristically, it emits sky-blue light, particularly the pale white to brown-orange varieties [49], [50].

The crystals of $CaWO_4$ are in the tetragonal crystal system and appear as dipyramidal pseudo-octahedra [42]. It has a specific gravity of 5.9–6.1 and a hardness of 4.5–5, with distinct cleavage and a subconchoidal to uneven fracture [51]. Furthermore, $CaWO_4$ deposits are found alongside calcium-bearing oxidized minerals such as apatite, fluorite, and calcite [45]. These gangue minerals negatively affect the smelting process when mixed into $CaWO_4$ concentrate, requiring a time-consuming and difficult separation process [51]. Flotation is the preferred method to remove calcium-bearing gang minerals during mineral beneficiation [3], [52].

While [(Fe, Mn) WO_4] and $CaWO_4$ minerals have been the main raw resources of W, synthetic scheelite, specifically calcium $CaWO_4$, has emerged as a strong competitor as an alternative W source [5], [53]. Synthetic scheelite is produced through various processes, including (a) roasting [(Fe, Mn) WO_4] with $Ca(OH)_2/CaO$) or $CaCO_3$ at 800 °C [6], the stoichiometric ratio of calcium carbonate 1.3 and holding time 2 h as shown in **Equation (2.1)** [5]–[7]; (b) precipitating $Na_2WO_4 \cdot 2H_2O$ using calcium solutions/salts after low-grade W concentrates were alkaline-leached, as shown in **Equation (2.2) and (2.3)** [5], [7], [54], [55]; (c) recycling W from scraps and spent catalysts by pyrometallurgical pretreatment; (d) treating waste liquors from the flowsheets of APT production [13]. Historically, it was produced by recovering W from [(Fe, Mn) WO_4] or low-grade $CaWO_4$ concentrates that had been digested with NaOH or Na_2CO_3 [56].

$$2FeWO_{4(s)} + 2CaCO_{3(s)} + 1/2O_{2(g)} = 2CaWO_{4(s)} + Fe_2O_{3(s)} + 2CO_{2(g)}\uparrow \textbf{ (2.1)}$$

$$CaCl_{2(aq)} + Na_2WO_{4(aq)} = CaWO_{4(s)} + 2NaCl_{(aq)} \textbf{ (2.2)}$$

$$Na_2WO_{4\ (aq)} + Ca(OH)_{2\ (s)} = CaWO_{4\ (s)} + 2\ NaOH_{(aq)} \textbf{ (2.3)}$$
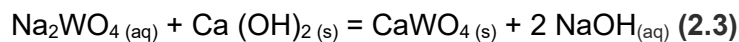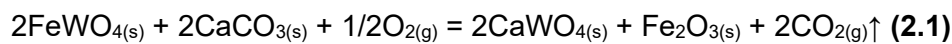
2.2.2 Secondary Resources

W scrap is the only secondary resource in W manufacturing [57]. There are three types of W scrap: new scrap (by-products of W materials), old scrap (spent W-bearing materials), and unrecovered scrap (excess reactants) [9]. The grade of W scrap varies between 40–95 wt.% [57], and recycling of the secondary resources contributes to meeting 30% of the world's W demand [58]. Approximately 34% of W consumption comes from secondary resources, including recycled scrap, worn-out WC components, waste generated during processing, and used components in

the industry. Low-grade W scrap, such as low-grade sludge, contains significantly higher W content, ranging from 10-75 wt.% WO_3 [31].

In addition, W tailings are another potential secondary resource for W recovery. Because in ore beneficiation, due to the low W content in the ore, 7-10 tons of waste containing about 0.4-0.6% WO_3 is generated to produce 1 ton of W concentrate (50-65% WO_3). Worldwide, tailing deposits are estimated to contain more than 100 Mt of tailings, with approximately 96,000 tons of WO_3. However, a great part of the [(Fe, Mn) WO_4] in the tailings is below 25 µm and $CaWO_4$ is below 74 µm. It is hard to reprocess by conventional processes due to fine and ultrafine fractions [36].

2.3 Intermediate Products in W Production

Metallurgical methods are essential for W production, particularly for complex W ores. The extraction technology for W has undergone significant advancements since Oxland invented a process to produce Na_2WO_4, WO_3, and solid W in 1847. Subsequently, solvent extraction (SX) and ion exchange (IX) methods were adopted with the advancement of industrial technologies. Today, to meet strict environmental standards, numerous novel laboratory procedures have been suggested as the commercial growth of the W industry picks up speed [9].

Ideally, around 65% WO_3-containing concentrate is aimed to be obtained by extractive metallurgy methods from natural W-containing minerals to be sold as a commodity in the industrial chain [29]. Therefore, except for the high-quality concentrate, W concentrates must be pretreated at the mine site to stabilize the output and increase the W content before metallurgical processing [9], [29]. The simplified illustration of the generic steps in the W processing flowsheet is represented in **Figure 2.3**.
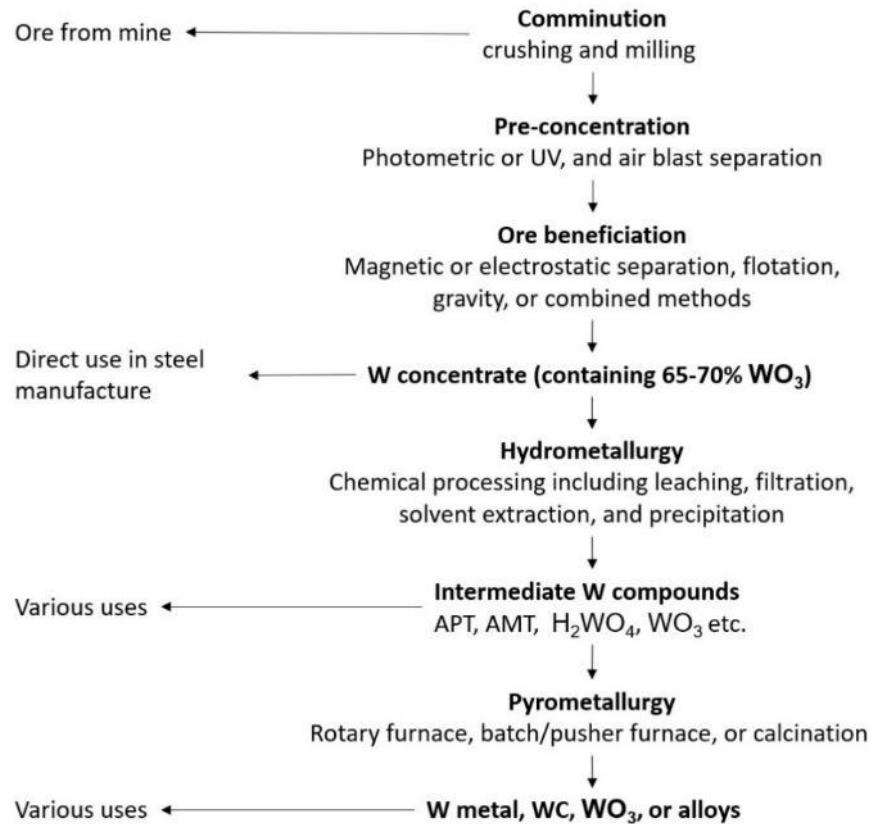
Figure 2. 3 Flow diagram of the generic steps in W processing. Modified from [29], [59].

In the mine site, the first step is comminution including crushing the ore in a jaw, cone, or impact crusher and then milling in a ball or rod mill operating in a closed circuit with vibrating screens and classifiers in the grinding circuit to produce more liberated particles. Also, in some processing plants, to remove impurities, and improve efficiency a pre-concentration step can be applied, such as ore separation, photometric detection, and air blast separation [9], [29], [34], [36]. For example, $CaWO_4$ ore can be separated from the dark W ore by photometric method, due to its UV light reflection ability. After preconcentration methods, the ore is concentrated in the beneficiation step by using techniques including gravity, flotation, magnetic, and electrostatic separation, depending on the properties of the ore. Thereafter, $CaWO_4$ can be concentrated by gravity methods (spirals, cones, and/or vibrating tables) frequently combined with flotation, due to its amenability of flotation [29], [36]. On the other hand, $[(Fe, Mn) WO_4]$ ore can also be concentrated by gravity methods, occasionally the gravity method is combined with magnetic separation due to being paramagnetic and dense material [29]. At the end of the ore beneficiation, a minimum of 65% WO_3-containing concentrate occurs [59], this product can be directly used in ferrotungsten (FeW) and steel

manufacturing. For example, while [(Fe, Mn) WO$_4$] concentrates can be smelted directly with coke or charcoal in an electric furnace for FeW productions, pure CaWO$_4$ concentrate is added directly to molten steel [29], [59].

In modern processing plants, pretreated W concentrates are processed by hydrometallurgical methods to produce intermediate compounds [18], [29], [59]. Industrially, W can be traded in diverse forms, the following list describes the well-known intermediate products [29]:

APT: It serves as a principal intermediate product in the manufacture of W metal, WC, and other W-based materials, making it one of the main commodities in the W market [59], [60]. It has the [(NH$_4$)$_{10}$(W$_{12}$O$_{41}$).5H$_2$O) · 4H$_2$O] chemical formula and is a highly crystalline powder containing 71.6 % W, or 89.5% WO$_3$ [18], [61]. APT is typically not directly converted into metal due to excessive water vapor and NH$_3$ generation during the reduction process. Instead, it is transformed into tungsten blue oxide (W$_{20}$O$_{58}$) or tungsten yellow oxide (WO$_3$) by calcination [29], [62], then reduced to a W metal [33].

AMT: Ammonium metatungstate has the chemical formula of [(NH$_4$)$_6$(H$_2$W$_{12}$O$_{40}$) ·nH$_2$O] and is a highly soluble white crystalline powder [29]. In general, numerous methods can be used to produce AMT such as thermal decomposition, ion exchange, or liquid–liquid extraction. The traditional AMT production process is based on the removal of NH$_3$ by thermal decomposition of APT crystals [63], [64].

Tungsten metal powder (W): To produce W metal powder, tungsten oxide is reduced in hydrogen reduction/rotary furnaces at 700-1000 °C or in pusher kilns. Although W is sometimes used in powder form, it frequently needs to be solidified [29].

Tungsten heavy-metal alloys (WHAs): WHAs are W-based materials commonly containing 90-98 % wt. W along with varying amounts of Ni, Fe, Cu, and/or Co [65]. These heavy metal alloys, produced through liquid phase sintering, act as binders to hold the W particles in place. Conversely, pure W is easier to manufacture and does not require milling for improved properties [29].

WC or semi-carbide (W$_2$C): WC, an affine gray powder can be pressed and shaped for a wide range of applications. To produce WC, W metal powder is carburized with pure C powder at 900-

2200°C in pusher or batch furnaces [29]. Due to its high melting point (2870°C), high hardness (8.5–9.0 on the Mohs scale, making it as tough as sapphire or corundum), high strength, and good wear resistance [66], WC is most frequently used in cutting and mining tools [29], [67].

WO_3: Tungsten oxide or tungsten trioxide, also called tungstic anhydride, can be produced as a light-yellow powder by oxidatively calcining APT in a rotary furnace that operates at 500–700 °C. Additionally, it is possible to produce it by calcination of H_2WO_4, which is a hydrated form of tungsten trioxide [29]. It is commonly utilized in a variety of applications, such as organic dye adsorbents, gas sensors, photocatalysts, and electrochromic devices, making it an important representative electrochromic material [16].

Tungsten blue oxide (TBO; WO_{3-x}): It has a dark blue or black powder appearance with a nominal chemical formula of $WO_{2.97}$. However, its chemical formula changes with the amount of oxygen present and has different chemical and physical characteristics based on the environment and machinery used during production. APT is calcined under moderate reducing conditions to produce TBO. Blue tungsten oxide (TBO) has largely taken the position of WO_3 as a forerunner in the production of W metal and WC [29].

H_2WO_4: Typically, yellow and existing as a powder or crystals tungstic acid is an intermediate compound in the production of W metal [68]. It is also known as tungsten trioxide hydrate is a hydrated oxide that exists in many forms, compositions, and structures, such as $WO_3 \cdot 2H_2O$, $WO_3 \cdot H_2O$, and $WO_3 \cdot 0.33H_2O$. All crystalline phases have different physical and chemical properties and are affected by the formation conditions [69]. Obtaining H_2WO_4 as a final product at the end of the acidic leaching process is one of the main methods that have been used to extract W [68].

2.4 W Extractive Metallurgy and Industrial Leaching Methods

The extensive exploitation of easily accessible high-grade W resources has resulted in the depletion of these resources and the emergence of complex, low-grade ore deposits. Consequently, conventional flotation methods alone are insufficient to address these challenges, necessitating the use of extractive metallurgy techniques [3]. Extractive metallurgy involves extracting valuable metals from ores and refining them into purer forms [70]. Hydrometallurgy, a branch of extractive metallurgy, employs aqueous solution technologies to extract metals or

metallic compounds from ores, concentrates, or intermediates in an environmentally friendly and cost-effective manner [71], [72]. A commonly used hydrometallurgical method is leaching, which selectively dissolves the target mineral using chemical reactants (leachants) in the ore, concentrates, or intermediate product [72], [73]. **Figure 2.4** provides an overview of a typical flowsheet for hydrometallurgical processes, which typically involve comminution and physical concentration or ore beneficiation steps. In modern W extractive metallurgy processing plants, pretreated W concentrates are subjected to hydrometallurgical methods to produce intermediate compounds for the W supply chain [18], [29], [59].
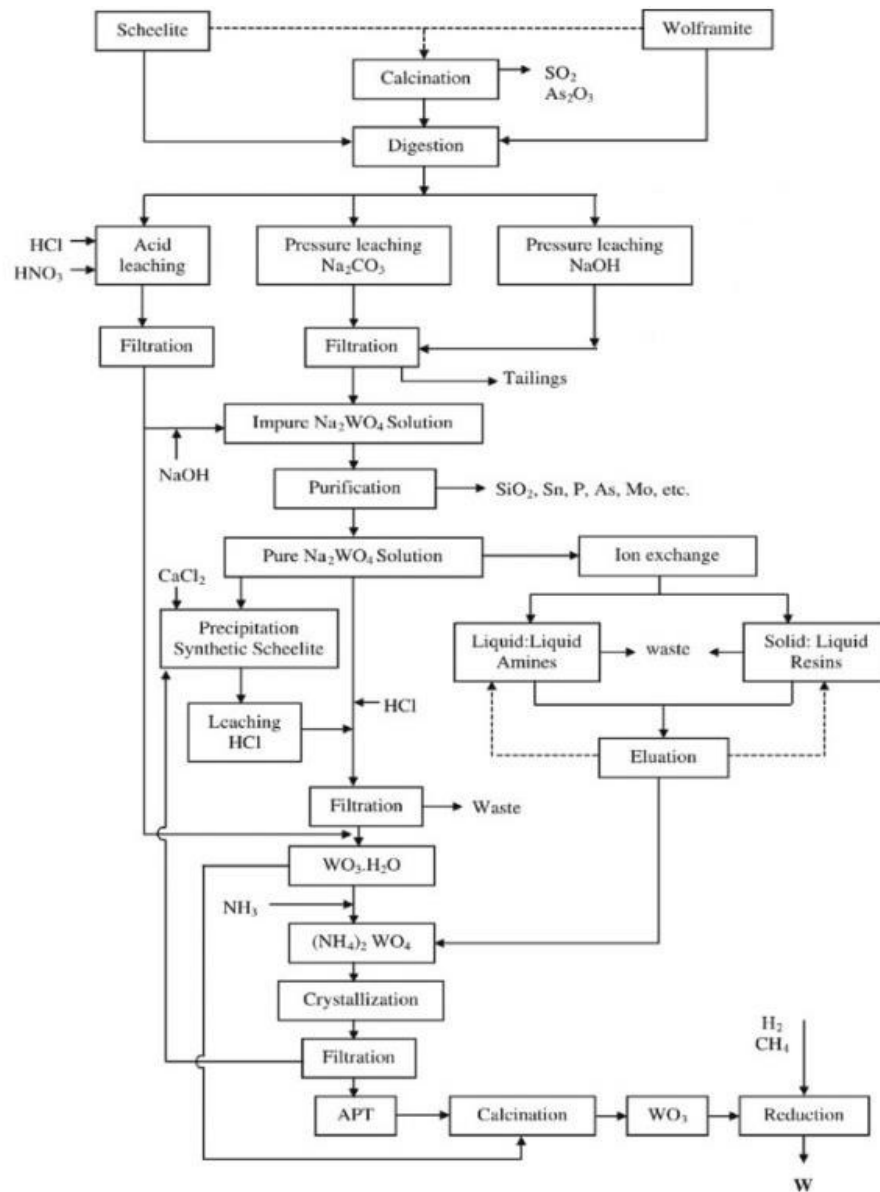
Figure 2. 4 Flowsheet of the generalized W production process in detail [38].

The traditional method in W extractive metallurgy involves decomposing W ores through alkaline leaching, typically using NaOH or Na_2CO_3. However, this approach has drawbacks such as increased leaching costs due to the high price of NaOH and harmful alkali decomposition residue formation, which requires separate waste disposal processes [9], [10]. Additionally, excessive use of NH_3-containing reagents in alkaline leaching leads to the production of ammonia wastewater during IX and crystallization steps, resulting in large volumes of high-salinity wastewater discharge per ton of APT production [9], [10]. These factors contribute to environmental concerns, resource limitations, increased costs, and the need for specialized operations [11], [74]. In contrast, acid leaching offers several advantages over alkaline leaching. It is a shorter process, reduces the purification steps of IX or SX, facilitates impurity separation, and generates smaller amounts of hazardous waste. According to the Chinese government, the waste residue produced by acid leaching does not fall under the classification of hazardous waste, resulting in significant cost reductions for disposal [10]. Acid leaching, especially with HCl, is suitable for decomposing $CaWO_4$, showing higher decomposition rates compared to [(Fe, Mn) WO_4] ores [1], [21]. Although acid leaching has numerous advantages in W production, the separation of HCl, the only acid commonly used in the industry, is not widely implemented [75]. However, there is an increasing interest in the use of acid leaching in modern W metallurgy, as it demonstrates promising results and significant advantages, particularly in laboratory-scale investigations [10].

2.4.1 Alkaline Leaching

Advancements in W metallurgy have introduced a widely utilized method called autoclaved alkali leaching, which effectively decomposes W minerals [76]. This method is particularly effective in treating high-grade W resources but still presents challenges [77]. Some of these challenges include the generation of large amounts of leaching residues during mineral digestion, excessive reagent consumption to achieve high WO_3 recovery, and the presence of valuable metals such as W, Mo, Mn, Sn, Ta, and Nb in the residues [9], [76]. Moreover, autoclaved alkali leaching requires significant energy input due to high reaction temperatures, and the difficulty in recycling the alkaline reagent contributes to increased costs and environmental concerns [77]. Nevertheless, compared to the traditional HCl process, current commercial alkaline leaching methods offer higher WO_3 recovery with lower energy consumption and reduced labor requirements, producing high-quality products [9]. **Table 2.2** provides an overview of the current state of acid and alkali industrial processes, considering factors such as ore type, gangue and

WO$_3$ grade, reagent consumption, labor, auxiliary materials, energy and water usage, wastewater, solid residues, exhaust gas discharge, recycling, and production cost [9], [68], [78].

Table 2. 2 The state of the art of present industrial processes [9].

Process		Raw materials	Consumption	Discharge	Recycling	Others
Classical process		Scheelite concentrates with fewer impurities	2–2.5 stoichiometric ratio HCl	High salinity acidic wastewater	No recycling	High volatility and corrosion; Low WO$_3$ recovery
Modern process	Caustic soda digestion	Various raw materials, more suitable for wolframite	>1.6 stoichiometric ratio NaOH; Normally ≥ 100 °C; Need diluted water	High salinity wastewater; Alkaline leaching residue with <3% WO$_3$	Only mother liquor recycling	Yield between 97 and 99%
	Soda digestion	Various raw materials, more suitable for scheelite	2.5–4.5 stoichiometric ratio Na$_2$CO$_3$; 190–225 °C with 12–26 bar pressure; Chemical cost higher than Na$_2$CO$_3$	High salinity wastewater; Leaching residue with ~1% WO$_3$	Only mother liquor recycling	Yield between 97 and 99%; Na$_2$CO$_3$·CaCO$_3$ or Na$_2$CO$_3$·2CaCO$_3$ may form
	With solvent extraction	–	>25 t-H$_2$O/t-APT; 0.54–1.3 t H$_2$SO$_4$/t-APT	>25 t high salinity acidic wastewater /t-APT	Solvent recycling	More auxiliary material consumption
	With ion exchange	–	80–125 t-H$_2$O/t-APT	>80 t- high salinity wastewater/t-APT	Resin recycling	–

2.4.2 Acid Leaching

The utilization of acid extraction for W has notable advantages, addressing the limitations of traditional alkali processes [21]. Acid leaching offers a shorter process by reducing the purification steps in SX and IX [10] and mitigating environmental pollution and waste issues [79]. Proper selection and control of the acid type and quantity can prevent the discharge of high-salinity wastewater during the recovery of W from $CaWO_4$ ore [74]. Acid leaching is appealing due to the non-hazardous nature of the waste generated, resulting in low disposal costs, and reduced environmental impact [10]. Additionally, acid leaching allows for reduced reagent consumption and eliminates the need for high temperatures or pressures during the reaction [20], [78]. In summary, the acidic leaching process for $CaWO_4$ has emerged as a solution to overcome the drawbacks of alkaline methods, leading to cost reduction, and minimized waste generation [8], [10] Reagents such as HCl, HNO_3, and H_2SO_4 are commonly used due to their reasonable cost and widespread availability, enabling the production of H_2WO_4, WO_3, or APT [1], [9]. The reaction mechanisms between various acidic mediums and $CaWO_4$ are depicted in **Equations (2.4) and (2.5)** [79].

$$CaWO_{4(s)} + 2H^+_{(aq)} = Ca^{2+}_{(aq)} + H_2WO_{4(s)} \text{ (Using HCl or HNO}_3) \textbf{ (2.4)}$$

$$CaWO_{4(s)} + 2H^+_{(aq)} + SO_4^{2-}_{(aq)} = CaSO_{4(s)} + H_2WO_{4(s)} \text{ (Using } H_2SO_4) \textbf{ (2.5)}$$
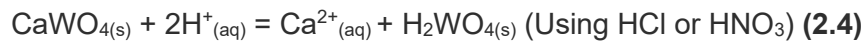
The use of acidic leaching agents (HCl, HNO_3, and H_2SO_4) for $CaWO_4$ decomposition leads to the formation of insoluble H_2WO_4 [79]. This solid yellow H_2WO_4 covers the surface of undecomposed $CaWO_4$ particles, obstructing further reactions and slowing down the mass transfer process, resulting in reduced W recovery [1], [8]–[10], [80]. Therefore, it is necessary to filter and wash the H_2WO_4 to remove acidity or dissolve it [33]. Several attempts have been made to dissolve H_2WO_4 and enhance leaching rates, such as reducing particle size, increasing temperature, raising reagent concentration, and utilizing heated ball mill reactors for mechanical activation. However, these approaches increase production costs due to the requirement for corrosion-resistant equipment [9], [55], [81].

Equation (2.6) demonstrates the dissolution reaction of H_2WO_4 products by $NH_3.H_2O$, resulting in the formation of an ammonium tungstate [$(NH_4)_2WO_4$] solution from which W can be extracted. However, obtaining a [$(NH_4)_2WO_4$] solution is challenging due to secondary $CaWO_4$ precipitation.

To address this issue, selective leaching of H_2WO_4 can be achieved by using a mixture of $NH_3.H_2O$ and $(NH_4)_2CO_3$. The CO_3^{2-} ion in $(NH_4)_2CO_3$ promotes the conversion into a $CaSO_4 \cdot nH_2O$ compound instead of secondary $CaWO_4$, as shown in **Equation (2.7)** [1], [79]. The proposed optimal concentrations for $NH_3.H_2O$ and $(NH_4)_2CO_3$ are 3 mol/L and 2 mol/L, respectively. Another approach involves preferentially combining Ca^{2+} by adding suitable amounts of additives such as Na_3PO_4 and/or NaF to the NaOH solution, forming a more stable passivation layer of $Ca_5(PO_4)_3OH$, CaF_2, or $Ca_5(PO_4)_3F$ [1]. It has been reported that W in $CaWO_4$ concentrates cannot be selectively dissolved using an acidic leaching process [82]. To prevent H_2WO_4 formation, promote the extraction of W through water-soluble complex salts, and enhance leaching yield and rate, various methods have been proposed, including co-leaching $CaWO_4$ concentrates with complexing/chelating agents such as H_2O_2, oxalic, oleic, ethyl alcohol, tartaric, citric, and phosphoric acids [55], [80]–[84]. The process kinetics align with the mechanism of particle shrinkage as the ore particles disintegrate under the influence of acid and complexing agents, gradually reducing in size until only insoluble residue remains [80].

$$H_2WO_{4\,(s)} + 2NH_3 \cdot H_2O_{\,(aq)} + CaSO_4 \cdot nH_2O_{\,(s)} = CaWO_{4\,(s)} + (NH_4)_2SO_{4\,(aq)} + (n+2)\,H_2 \textbf{(2.6)}$$

$$CaSO_4 \cdot nH_2O_{(s)} + (NH_4)_2CO_{3\,(aq)} = (NH_4)_2SO_{4\,(aq)} + CaCO_{3\,(s)} + nH_2O,\ n=0,0.5,2 \ \textbf{(2.7)}$$
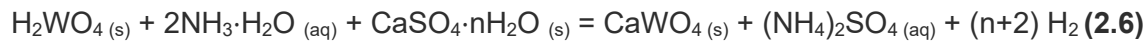
Considering key issues such as slowed mass transfer rates caused by colloidal H_2WO_4, side reactions, and the strong volatility of corrosive acids, the first acid that was adapted for commercial processing plants is HCl, which is still limitedly used. HCl decomposition was introduced in the early 20th century, gradually being replaced by the alkaline process by the end of the same century [1]. On the other hand, although HNO_3 is less corrosive than HCl, it has never been widely adopted in the industry due to the generation of toxic NO_2 gas during the process and its strong oxidation properties, which hinder the recycling of HNO_3 through SX or IX [1], [85], [86]. Furthermore, the recently developed method of leaching CaWO4 in a mixed acid, including H_2SO_4 and H_3PO_4, has also been adapted for industrial use [1], [87]. A comparison of two commercial acidic leaching methods for $CaWO_4$ digestion is presented in **Table 2.3**. The table emphasizes that parameters or indicators such as principles and practices, laboratory and facility considerations, environmental aspects, and cost should be considered for practical industrial applications. Additionally, ongoing laboratory-scale research and optimization studies are being conducted to utilize existing acid types and explore other potential acids [1].

Table 2. 3 Parameters of two industrialized acid decomposition processes of W ore [1].

Items	HCl decomposition method	H_2SO_4-H_3PO_4 synergistic decomposition method
Current application scale	No	Medium
Feedstock (Mineral adaptability)	High-quality $CaWO_4$ concentrate	$CaWO_4$
Decomposition conditions	HCl:200–350 g/L; T: 50–110 °C (~0.1 MPa); L/S ratio: (1–2):1	H_2SO_4:200–300 g/L; H_3PO_4: 50–250 g/L; T: 80–90 °C (0.1 MPa); L/S ratio: (3–8):1
Reagent price (RMB/t)	≥ 30% HCl: 200–500	98% H_2SO_4: 300–800 85% H_3PO_4: 5000–10,000
Reagent cost* (RMB/t)	150–350	250–500
Waste	Wastewater with strong acidity and high salinity.	/
Advantages	Low energy consumption, simple operation	Low energy consumption, low cost, available $CaSO_4$ residue
Disadvantages	Poor mineral adaptability, acid mist volatilization, and corrosion	Introduced P needs to be subsequently removed
Analogous process	H_2SO_4 decomposition method to avoid volatile acid mist.	H_2SO_4-oxalate/H_2O_2 synergistic decomposition method to avoid the introduction of P impurity.

*Theoretical consumption cost of decomposition reagent based on 1 t standard W concentrate with 65% WO_3.

2.4.2.1 Industrial Acid Leaching Methods

The HCl decomposition method is the first of two industrially adapted acid leaching methods for $CaWO_4$. It was used as the main traditional acid process for industrial $CaWO_4$ leaching in the early 20th century and is still used for pure tungstic acid and metatungstic acid production, as

shown in **Figure 2.5** [1], [8], [9]. Although this method yields good digestion results and has a thermodynamically fast reaction rate [87], its high capital costs, harsh operating environment, and generation of acid fog are its main disadvantages [8], [9]. Additionally, this method has been banned by the Chinese government due to its high consumption of HCl, which causes corrosion of equipment at high temperatures (85-100 °C), high volatilization, and difficulties in solid-liquid separation of colloidal H_2WO_4, leading to poor operational environments [1], [9], [69], [78], [88]. As a result, it is rarely adopted by W metallurgical companies today [75], [89]. To produce APT or W intermediates from W ores by HCl decomposition, alkaline digestion/roasting pretreatment and subsequent purification are applied before HCl leaching to remove impurities from [(Fe, Mn) WO_4] ore and to form $CaWO_4$. The first pure synthetic scheelite is produced by alkaline digestion following purification. $CaWO_4$ is then decomposed by HCl, and insoluble H_2WO_4 particles and layers are produced, as shown in **Equation (2.8)** [9]. The formation of H_2WO_4 caused by using HCl needs to be directly filtered out from the system [33]. At the end of the process, H_2WO_4 can be calcined to WO_3 or re-dissolved in ammonia (NH_4OH) solution to produce APT, as shown in **Equation (2.9)** [9], [34], [81].
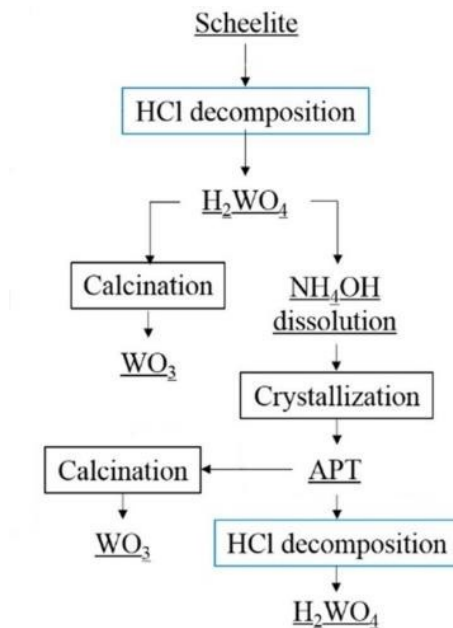
Figure 2. 5 Generalized flowsheet of traditional HCl leaching of $CaWO_4$. Based on [9].

$CaWO_{4(s)}$ + $2HCl_{(aq)}$ ↔ $H_2WO_{4(s)}$ + $CaCl_{2(aq)}$ **(2.8)**

$H_2WO_{4(s)}$ + $2NH_4OH_{(aq)}$ → $(NH_4)_2WO_{4(aq)}$ +$2H_2O_{(aq)}$ **(2.9)**
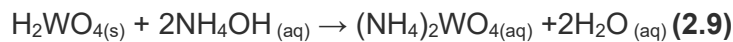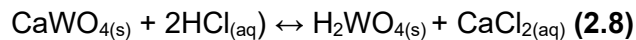
Another industrially adapted acid leaching method is the mixed acid of H_2SO_4 and H_3PO_4 [1], [87], which was patented by Zhongwei et al. [87]. This method aims to address the disadvantages of HCl digestion by proposing H_2SO_4 as a low-volatile and less corrosive substitute for HCl. However, the presence of a large amount of H_2SO_4 leads to the wrapping effect on the products, inhibiting further decomposition by the fast nucleation of supersaturated gypsum. As a result, yellow H_2WO_4 precipitation still forms. To overcome these challenges and increase leaching efficiency, H_3PO_4 is used as a complexing agent. H_3PO_4 has the advantages of low volatility and less corrosive effects compared to HCl [87]. In this mixed-acid system (H_2SO_4–H_3PO_4–W), W is extracted in the form of soluble phosphotungstic heteropoly acid (HPW), as shown in **Equation (2.10)** [87], [90]. Furthermore, it has been confirmed that although this method can be applied to [(Fe, Mn) WO_4], the leaching speed of $CaWO_4$ is significantly faster than that of [(Fe, Mn) WO_4] in the H_3PO_4-H_2SO_4 solution [91].

$$12CaWO_4 + 25H_3PO_4 = 12Ca(H_2PO_4)_2 . H_2O + H_3[PW_{12}O_{40}] + 11H_2O \quad \textbf{(2.10)}$$
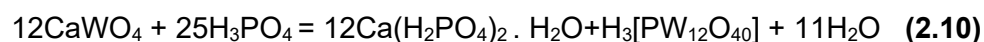
In this leaching process, a mixed acid is prepared with H_2SO_4 concentration ranging from 150 to 500 g/L and P_2O_5 concentration ranging from 15 to 35 wt. %. The mixed acid is then heated to the desired temperature (70-100°C), and a calculated amount of $CaWO_4$ is added to the solution with a liquid-to-solid ratio (L/S) of 3-8 L per kg of $CaWO_4$. The leaching process is allowed to proceed for 1-6 hours. Once the leaching is completed, filtration is employed to separate the liquid and solid components, obtaining a mother solution containing phosphotungstic acid. The phosphotungstic acid crystals are dissolved in water to obtain a phosphotungstic acid solution. The resulting solution can be further treated with Na_2WO_4 to convert it into APT. The mother liquor, containing the residual acid, can be reused for subsequent rounds of ore leaching by supplementing it with the same concentrations of H_2SO_4 and P_2O_5 [96]. Additionally, a study conducted by Li et al. [12] reported that a mixture solution with an H_2SO_4 concentration of 250 g/L and H_3PO_4 concentration of 350 g/L, heated to 90°C for 40 minutes, resulted in approximately 99% digestion of $CaWO_4$ [12] **Figure 2.6** illustrates the industrial production of APT intermediates from $CaWO_4$ ores using the H_2SO_4 and H_3PO_4 mixed acid process.

The described leaching process offers several advantages and is well-suited for industrialization. One of the key advantages is that the high concentrations of H_3PO_4 effectively mitigate the issue of $CaSO_4$ supersaturation by complexing Ca^{2+} ions and increasing solubility. This, in turn, prevents the nucleation and formation of compact $CaSO_4$ particles. Additionally, compared to the

traditional HCl process, this leaching method significantly reduces problems related to corrosion and volatilization. While it is true that H_3PO_4 is relatively expensive [12], the recycling and reuse of both H_3PO_4 and H_2SO_4 contribute to cost reduction and minimize the generation of wastewater during the leaching process [87]. However, it is important to note that the presence of phosphorus negatively impacts the subsequent APT preparation process, necessitating a separate dephosphorization step [8], [21].
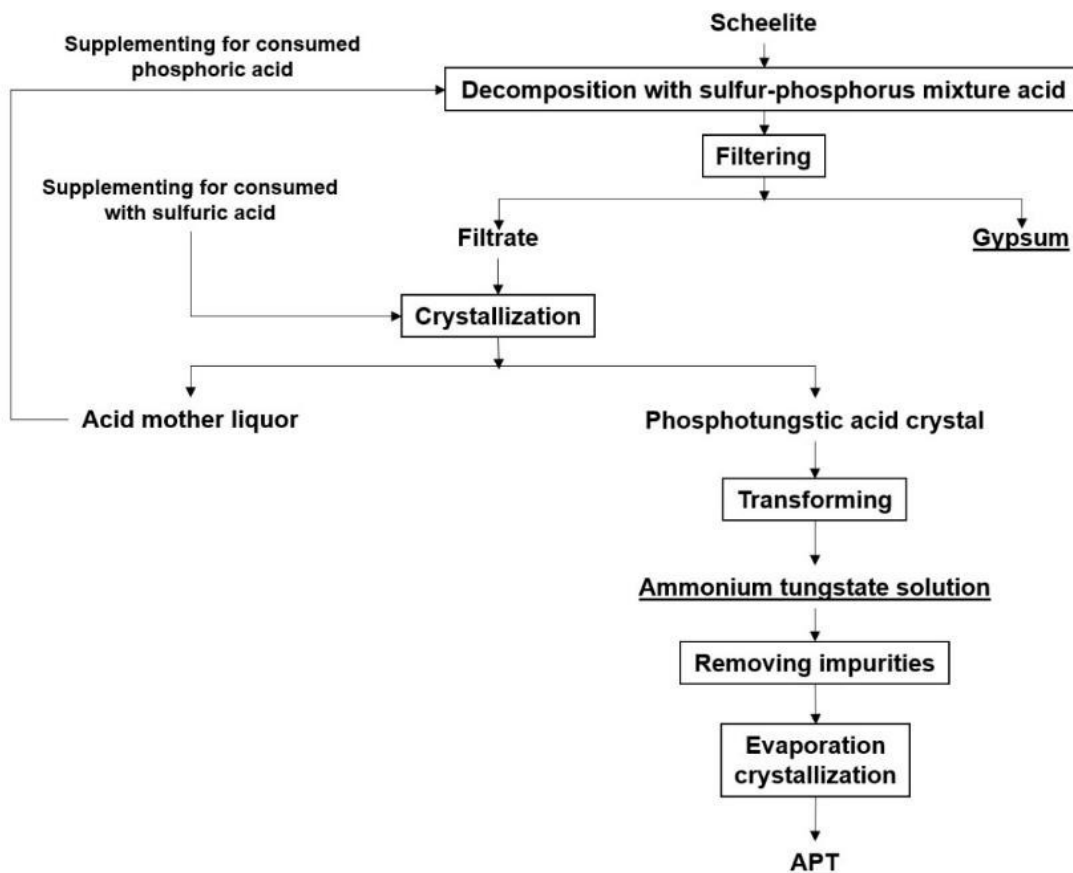
Figure 2. 6 Flowsheet of the leaching $CaWO_4$ in H_2SO_4 and H_3PO_4 mixed acid process for APT production [87].

2.4.2.2 Recently Developed Lab-Scale Acid Leaching Processes

To provide a cost-effective, eco-friendly, and more energy-efficient leaching process new laboratory-scale studies are carried out. It should be noted that while novel lab-scale studies have made significant progress in reducing reagents used and increasing recycling efficiency, their

industrial applicability needs to be tested on a larger scale process [9]. There are several attempts to dissolve W in acidic solutions by co-leaching in the presence of acid combinations, acid-alkaline combinations, or complexing agents [9], [81]–[84]. Due to their widespread availability and reasonable cost, the three inorganic strong acids HCl, HNO_3, and H_2SO_4 are the most often used reagents for leaching as summarized in **Table 2.4**. The fact that its volatility and corrosiveness are low and relatively cheap and that the mother liquor is recycled and reused after the leaching process makes H_2SO_4 more remarkable compared to the others [1]. Moreover, recently it has been discovered that the addition of H_2O_2 to the H_2SO_4 solution as a complexing agent enables the production of a soluble W compound, and the inhibition of the production of a solid H_2WO_4 layer is eliminated, resulting in a higher leaching efficiency and yield [11]. This method forms the research topic of this thesis and is detailed in the next section.

Table 2. 4 The state-of-the-art recently developed laboratory scale processes for synergetic/co-leaching leaching $CaWO_4$ in an acidic environment.

Decomposition acid media	Complexing acid	Reaction Equation	Operating Temperature (°C)
HCl	H_2O_2 [10], [55], [81]	$CaWO_{4(s)} + 2HCl_{(aq)} + 2H_2O_{2(aq)} \rightarrow$ $[WO(O_2)_2(H_2O)_2]_{(aq)} + CaCl_{2(aq)} + H_2O_{(l)}$ [81]	30 [55] - 50 [81]
HCl	H_3PO_4 [84], [91]	$(1/2) CaWO_{4(s)} + HCl_{(aq)} + (1/24)$ $H_3PO_{4(aq)} \rightarrow (1/24) H_3PO_412WO_{3(aq)}$ $+ (1/2) CaCl_{2(aq)} + (1/2) H_2O_{(l)}$ [84]	37 - 90 [84] >90 [91]
HNO_3	H_3PO_4 [86], [91]	$(1/2) CaWO_{4(s)} + HNO_{3(aq)} + (1/24)$ $H_3PO_{4 (aq)} c (1/24) H_3PO_412WO_{3(aq)} +$ $(1/2) Ca (NO_3)_{2(aq)} + H_2O_{(l)}$	50 - 70 [86]
H_2SO_4	H_2O_2 [8], [11], [13]	$CaWO_{4(s)} + H_2SO_{4(aq)} + 2H_2O_{2(aq)} \rightarrow$ $H_4[WO_3(O_2)_2]_{(aq)} + H_2O_{(l)} + CaSO_{4(s)}$ [8]	45 - 60 [8], [11]

2.4.3 Leaching Synthetic Scheelite $CaWO_4$ in H_2SO_4 and H_2O_2 Solution

2.4.3.1 The Leaching System

In recent studies, the operating procedure of synergistic leaching of $CaWO_4$ in H_2SO4 and H_2O_2 solution has been reported in various optimal operating conditions. The first study conducted by Yin et. al. [8], is based on heating the reactive aqueous media prepared with 3 mol/L H_2SO_4 and 1.5 mol/L H_2O_2 to 45 °C and adding the appropriate amount of ore with an L/S ratio of 10 mL/g. The leaching process was continued for 90 minutes under atmospheric pressure and continuous stirring with a magnetic stirrer. The $CaSO_4$ product is obtained by filtering from the resulting slurry to separate the solid $CaSO_4$ residue from the pregnant solution, which is cooled to room temperature after the leching is finished to allow precipitation as illustrated in **Figure 2.7** [13]. Afterward, the byproduct $CaSO_4$ is washed and used directly in the construction industry. The filtrate PTA obtained is an intermediate product in liquid form containing W. The leaching efficiency for this study was reported as 99.7%. In a separate study by Zhang et al. [11], it was reported that the leaching efficiency was over 98% when the procedure in the preceding study was applied in the same way but under different leaching operating conditions. For example, the concentrations of H_2SO_4 and H_2O_2 are 2 mol/L and 2.5 mol/L, respectively. While the temperature increased to 60 °C in this study, the L/S ratio was kept at 10mL/g. Furthermore, the leaching duration was suggested to be 180 minutes, which is twice as long as the previous study. Additionally, it has been confirmed and reported that the $CaSO_4$ byproduct obtained by filtration from the slurry cooled to room temperature after the filtration process can be used directly in the construction industry. The filtrate obtained is an intermediate in liquid form containing PTA, as described in **Equation (2.11)**.

$$CaWO_{4(s)} + H_2SO_{4(aq)} + 2H_2O_{2(aq)} = H_4[WO_3(O_2)_2]_{(aq)} + H_2O_{(l)} + CaSO_{4(s)} \textbf{ (2.11)}$$

The by-product $CaSO_4$ residue has low solubility in water [92], and in aqueous solutions, crystallizes into various types with the chemical names hemihydrate (HH, $CaSO_4 \cdot 0.5H_2O$), dihydrate or gypsum (DH, $CaSO_4 \cdot 2H_2O$), and anhydrite (AH, $CaSO_4$). In the leaching operation, the formation depends on the solution conditions, such as temperature and H_2SO_4 concentration, which complicate the prediction and control of calcium sulfate scaling [93]. Furthermore, it can be used in building materials, which is another advantage of this leaching process [8], [55]. The content of W in the pregnant solution is determined by chemical analysis (ICP analysis), and the composition and morphology of the precipitate are examined by XRD, SEM [11], [13].
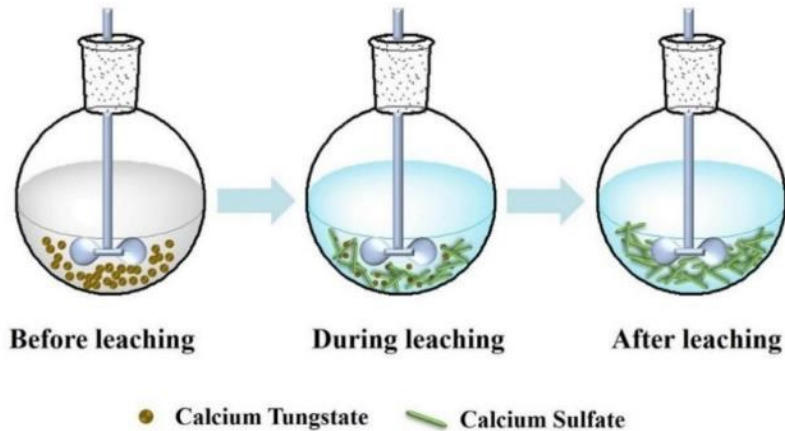
Figure 2. 7 Schematics of the leaching mechanism of $CaWO_4$ in H_2SO_4-H_2O_2 solution [13].

The following step after liquid-solid separation is decomposing the soluble PTA thermally at 90°C for 4 hours, to precipitate the final product H_2WO_4 [11]. After thermal decomposition, H_2WO_4 is filtered out from the lixivium. It was reported that lixivium contains immoderate H_2SO_4 due to having low volatilization and high boiling point [10], and a small amount of dissolved $CaSO_4$ but does not contain H_2O_2 [13]. Because the self-decomposing H_2O_2 and the peroxotungstic acid decompose when the temperature exceeds 50°C [81]. Instead of treating the resulting solution from thermal decomposition with lime and discharging, it is possible to recycle and reuse the lixivium by supplementing the consumed reagents [13]. Zhang et al. [13], reported that Lixivium can be recycled and reused for up to 5 cycles without reducing the leaching efficiency. After 5 cycles, the efficiency of leaching started to decrease slightly around 2%. In conclusion, the lixivium can be recycled and reused, and it results in creating an advantage for the leaching system by decreasing the reagents consumption and cost of leaching [13], and also reducing the environmental risks [11]. In light of the above experimental results, a flowsheet for leaching synthetic scheelite in an H_2SO_4-H_2O_2 solution was proposed by Zhang et al. [13], as illustrated in **Figure 2.8**.
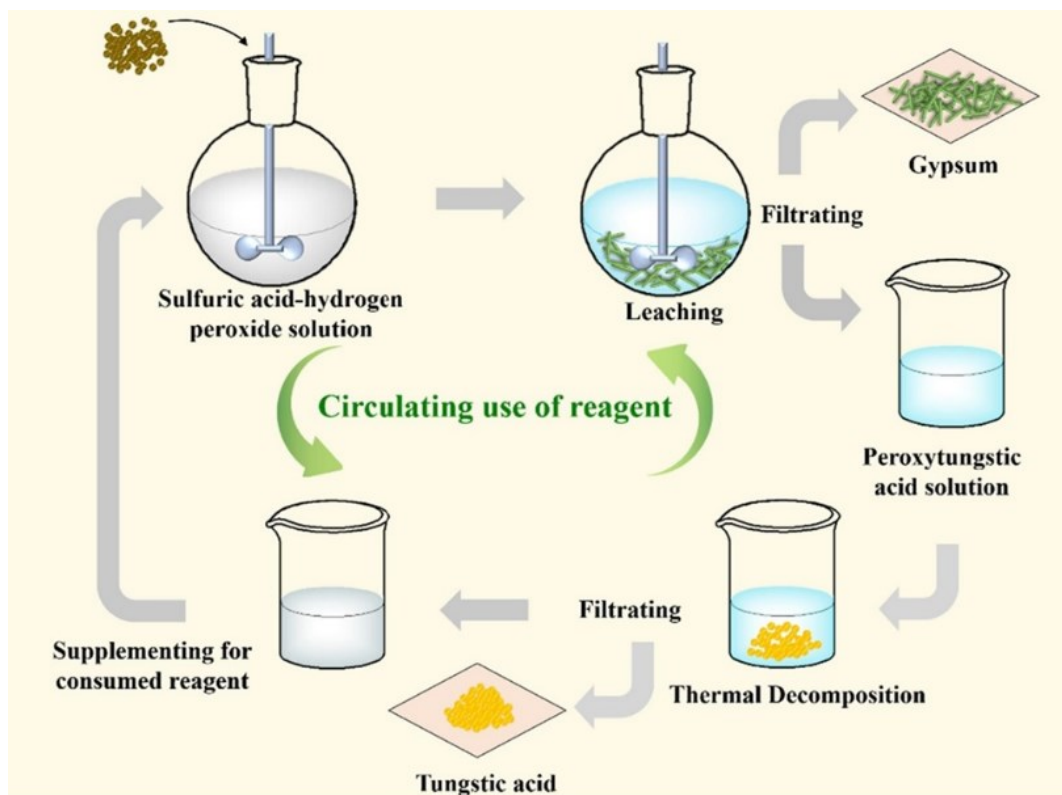
Figure 2. 8 Proposed flowsheet of synergetic leaching $CaWO_4$ in H_2SO_4-H_2O_2 solution [13].

In a word, the novel lab-scale development, leaching $CaWO_4$ in an H_2SO_4-H_2O_2 solution system is advantageous in terms of the following aspects:

1.   It provides an energy-efficient and shorter process because it does not require high pressure and temperature compared to traditional methods, and the reaction can take place at atmospheric pressure and moderate temperatures such as 50-60 °C. Furthermore, The $CaSO_4$ product obtained by filtration can be used directly in the construction industry, simplifying downstream processing [11].

2.   The H_2SO_4-H_2O_2 solution is proposed as a green and non-toxic aqueous medium and provides an environmentally friendly process. While the lower volatility and corrosiveness of H_2SO_4 and the minimal discharge of high-salinity wastewater increase the safety of the working environment [4], also, the lixivium can also be recycled and reused [13]. Furthermore, the precipitated $CaSO_4$ byproduct can be used as cement raw material in the construction industry, thereby preventing waste residue pollution and realizing the utilization of calcium resources [8], [12], [55], [94]. In addition, this method is advantageous because it does not produce any hazardous W residue or harmful ions in the experimental procedure [8].

3.   It proposes a cost-effective and easy-to-operate process since H_2SO_4 is cheap and easy to achieve, and the aqueous medium used in the system is recyclable and reusable. Furthermore, the process easily operated under atmospheric pressure and moderate temperatures, with no need for high-pressure or high-temperature equipment. Additionally, there is no excessive requirement for anti-corrosion protection for equipment, and the system is energy efficient [8], [13].

2.4.3.2 The Role of H_2O_2

$CaWO_4$ is the primary raw material currently in W production, and the most newly discovered W ore deposits are $CaWO_4$-dominated. However, hydrometallurgical methods are required because the high impurity content in the raw resources ore beneficiation methods are insufficient to extract W efficiently. Due to the disadvantages such as the need for special operations to deal with the waste caused by alkaline leach for industrial W production, the cost increases. Thus, new lab-scale studies have focused on acid leaching to treat $CaWO_4$ cost-effectively and try to limit waste generation [8]. In the traditional acid decomposition method, $CaWO_4$ is treated with HCl to produce H_2WO_4 [13]. But recently, H_2SO_4 proposed as an appropriate and favored candidate reagent for leaching $CaWO_4$ to avoid the use of HCl because being low cost, low volatility, long shelf life, and minimal discharge of high-salinity wastewater [4], [10], [68], [74]. Consequently, using H_2SO_4 reduced the reagent cost and increased the safety of the operating environment [4]. However, the chemical reaction between H_2SO_4 and $CaWO_4$ results in an insoluble yellow H_2WO_4 layer as in the HCl process [68], also insoluble $CaSO_4$ is produced as shown in **Equation (2.12)** [11]**.** The insoluble solid-colloidal layer of H_2WO_4 slows down the leaching rate by preventing the transport of H_2SO_4 inside the unreacted $CaWO_4$ particles as shown in **Figure 2.9** [55], [56]. Furthermore, as the reaction time is prolonged, the thickness of the product layer increases thereby impeding the interaction of H_2SO_4 and $CaWO_4$ [55]. Conversely, the other solid product, $CaSO_4$, has the property of covering the surface of mineral particles [1].

$$CaWO_{4(s)} + H_2SO_{4(aq)} \rightarrow CaSO_{4(s)} + H_2WO_{4(s)} \quad \textbf{(2.12)}$$
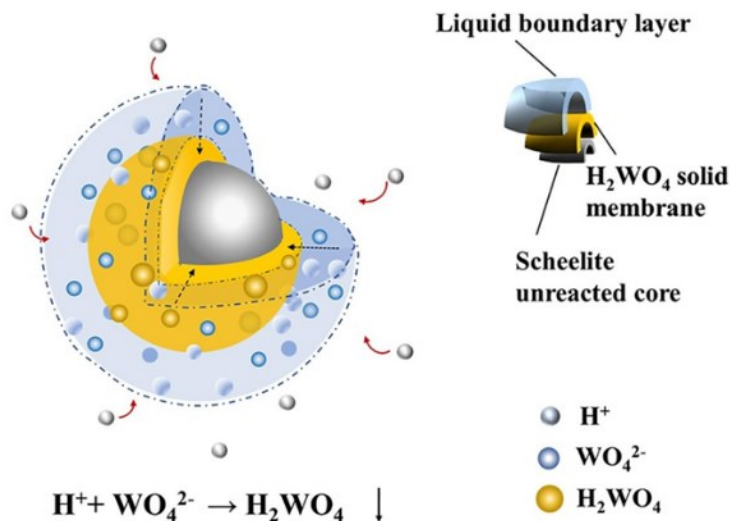
Figure 2. 9 Illustration of W combined with H^+ ion to form stable tungstic acid solid [95].

However, since the two insoluble products cannot be separated [12], the adaptability of some strategies to the process has been proposed to reduce the diffusion control imposed by H_2WO_4 on unreacted core particles: a) working with the particles finer than 44 mm; (b) use of heated ball mill reactors to decompose the H_2WO_4 ash layer, but this will be corrosive from acid and high temperature; (c) dihydric or polyhydric aliphatic alcoholic solutions can be employed and the reaction should be carried out under pH regulation and to dissolve the H_2WO_4 generated during the leaching [96]; (d) complexing reagents can be used to promote soluble compounds during the acid leaching such as H_3PO_4, $C_2H_2O_4$, H_2O_2 [78]. Using a complexing agent is the common and most preferred method because for a W^{6+} ion, binding to negatively charged ionic ligands is facile due to its high charge, small radius, and strong polarization ability. Therefore, in the presence of a ligand, WO_4^{2-} can form a complex ion by coordinating with a complexing agent [10]. For example, one of the industry-adapted novel methods proposes that using H_3PO_4 was advantageous because phosphorus can coordinate with W easily to form a soluble heteropoly acid [21]. Despite the promising results of the H_3PO_4 complexing agent, the phosphotungstic heteropoly acid was dissolved in ammonia water to create a crude ammonium tungstate solution after being separated from the leaching solution by cooling crystallization [97]. Thus, a separate phosphorus removal process is required due to the negative impact on the subsequent APT preparation process [21]. Instead of H_3PO_4, a green and pollution-free H_2O_2 was proposed by Yin et al. [8] to form PTA to extract W from the H_2SO_4 decomposition residue as shown in **Equation (2.13)** [21] inspired by the synergistic leaching of $CaWO_4$ with mixed H_2SO_4 and H_3PO_4 solution [1]. In addition, with this environmentally friendly leaching medium created by the mixture of H_2O_2

with H_2SO_4, it is possible to obtain the final product of pure H_2WO_4 by thermal decomposition from PTA [21], while minimizing the amount of ammonia wastewater formed [97]. In acidic solutions, O_2^{2-} ions can replace O^{2-} ions that are within the structure of WO_4^{2-} ions and are connected to W as a bidentate ligand. This enables W to combine with H_2O_2 to form a water-soluble PTA without aggregation, while Ca forms an insoluble compound with SO_4^{2-} to create $CaSO_4 \cdot nH_2O$. Therefore, W dissolves in the solution, while Ca remains in the residue. In conclusion, the role of H_2O_2 is to create a chelating effect to prevent the formation of solid H_2WO_4 and promote the reaction, resulting in a faster reaction rate than conventional methods, as shown in **Figure 2.10** [55].

$$H_2WO_{4(s)} + 2H_2O_{2(aq)} \rightarrow H_4WO_3(O_2)_{2(aq)} + H_2O_{(l)} \text{ (2.13)}$$
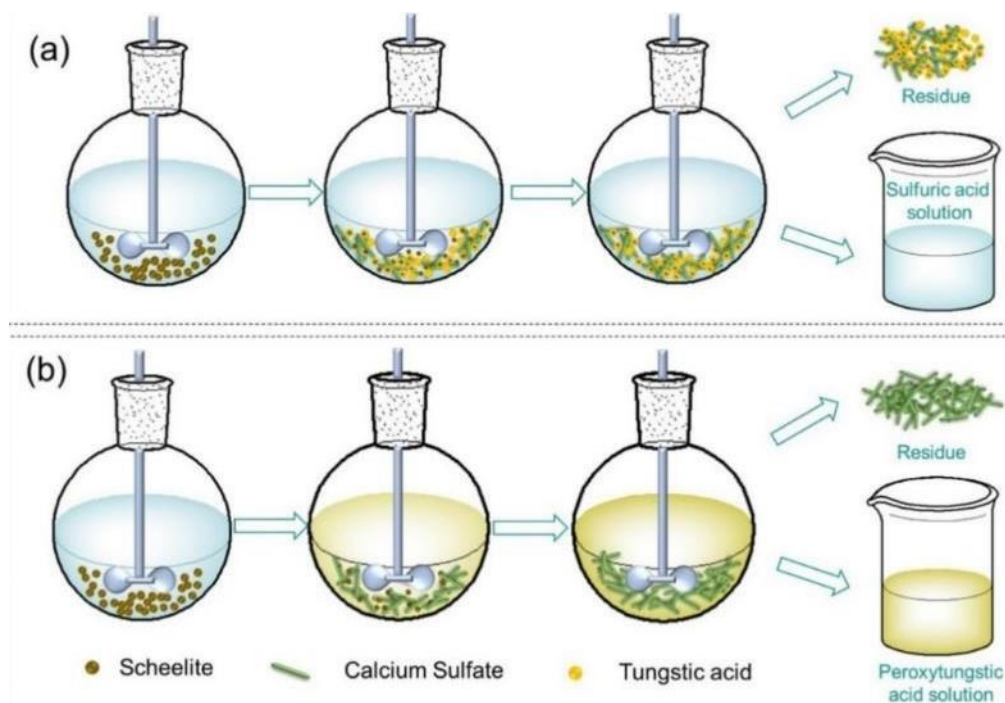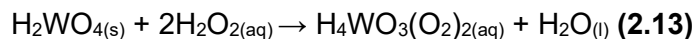
Figure 2. 10 The role of H_2O_2 in the leaching synthetic scheelite $CaWO_4$ in H_2SO_4 and H_2O_2 solution system [11]: (a) in the presence of an H_2O_2 complexing agent, (b) the lack of an H_2O_2 complexing agent.

In a study conducted to observe the dissolution behavior of H_2WO_4 in H_2O_2, by Gong et al. [69], it is reported that different forms of H_2WO_4 react with H_2O_2 during extraction of W. It is suggested controlling the decomposition conditions is necessary when using H_2SO_4. The findings of the study indicate that an increase in H_2O_2 concentration leads to a higher collision frequency

between H_2O_2 and H_2WO_4 molecules, which can adversely affect the system. For example, the dissolution rate of $WO_3 \cdot H_2O$ and $WO_3 \cdot 2H_2O$ is highest at an H_2O_2 concentration of 1 mol/L, while $WO_3 \cdot 0.33H_2O$ has a lower dissolution rate and requires a higher H_2O_2 concentration of 3 mol/L to achieve maximum dissolution. Moreover, high dissolution percentage the optimal dissolution temperature in H_2O_2 is 60°C for $WO_3 \cdot H_2O$, $WO_3 \cdot 2H_2O$, and $WO_3 \cdot 0.33H_2O$. In addition, it is reported that, at 40 °C for 30 minutes the dissolution rate is more than 95% for $WO_3 \cdot H_2O$ and $WO_3 \cdot 2H_2O$ in H_2O_2 while the dissolution percentage of $WO_3 \cdot 0.33H_2O$ was less than 25%. Therefore, $WO_3 \cdot H_2O$ and $WO_3 \cdot 2H_2O$ have better dissolution behavior in H_2O_2 better than that of $WO_3 \cdot 0.33H_2O$ [69].

Another study conducted by Li et al. [68] revealed that H_2SO_4 concentration affects the solubility limit of H_2WO_4 and the conversion of $CaWO_4$. Accordingly, the initial H_2SO_4 concentration should be determined by the free H_2SO_4 concentration in the resulting solution to ensure both the full conversion of $CaWO_4$ concentrate to H_2WO_4 and $CaSO_4.nH_2O$ and the lowest possible WO_3 content in the filtrate. The conversion ratio rises noticeably until it reaches around 100% at about 250 g/L H_2SO_4, but surprisingly, it reduces sharply with further increasing H_2SO_4 concentration. Therefore, to complete the conversion the optimum concentration of free H_2SO_4 is 50-100 g/L, ideally about 100 g/L [68].

Consequently, H_2O_2 can selectively dissolve W from H_2WO_4 and $CaWO_4$ acid decomposition residue, which is clean and inexpensive compared to other complexing agents and does not leave impurity in subsequent processes [10], [13]. Thus, H_2O_2 can easily coordinate with H_2WO_4 to form soluble $H_4[WO_3(O_2)_2]_{(aq)}$, and H_2WO_4 film formation can be avoided, as shown in **Equation (2.14)** [8]. Additionally, it works well with H_2SO_4 on converting $CaWO_4$ into a residue of fibrous, plank-shaped $CaSO_4.nH_2O$ and a water-soluble PTA solution in the H_2SO_4 - H_2O_2 system [8], [55], [97].

$$CaWO_{4(s)} + H_2SO_{4(aq)} + 2H_2O_{2(aq)} = H_4[WO_3(O_2)_2]_{(aq)} + H_2O_{(l)} + CaSO_{4(s)} \textbf{ (2.14)}$$

2.4.3.3 Poor Stability of H_2O_2 and Peroxytungstic Acid (PTA) Solution

Despite the H_2SO_4-H_2O_2 solution leaching system being advantageous in terms of proposing a cost-efficient, energy-efficient, shorter, and green process to extract W from $CaWO_4$ efficiently, there are two main challenges mentioned in the literature, thermal instability of H_2O_2 and PTA solution [11]. First, the non-toxic complexing agent H_2O_2 also known as peroxide plays a major

role in providing a clean and environment-friendly process while preventing the precipitation of H_2WO_4 by converting it into a water-soluble W intermediate product, PTA solution. Although it helps to increase the leaching efficiency [8], it is disadvantageous in terms of being a self-decomposing chemical, and it is thermally unstable in acidic solutions and can rapidly decompose [14]. It is well known that H_2O_2 has a short shelf life and is sensitive to temperature, its stability starts to decrease when the temperature exceeds 40 °C. The decomposition ratio is reported to be 3–4% within 1 hour when the temperature rises to 50 °C. After a series of experiments to examine the effect of reaction temperature on the dissolution ratio it is concluded that to reduce the loss of H_2O_2, the optimal decomposition temperature range was 40–45 °C [10]. In addition, exposure to impurities or catalysts such as Fe^{3+} and MnO_2 can speed up the decomposition reaction. Thus, the natural W ore's chemical composition and mineral structure should be carefully considered during the acid H_2O_2 complexation decomposition process [1]. The additional factors that can affect the decomposition reaction rate are pressure, the concentration of the solution, type, activity, and surface area of the catalyst, exposure to sunlight, and the existence of inhibitors. The exothermic reaction of H_2O_2 decomposition generates a significant amount of heat production (ΔH = - 2884.5 kJ/kg H_2O_2 for pure compound), which leads to an acceleration of the reaction and makes the reaction self-sustaining after the phase of catalytic initiation [14]. Therefore, controlling the amount of H_2O_2 and improving its utilization ratio is significant because, after the decomposition process, it is challenging to recover and expensive the oxygen in H_2O_2 [10]. The decomposition reaction is described in **Figure 2.11**.

$$O^{-1} + e^{-} \longrightarrow O^{-2}$$
$$2H_2O_2 \longrightarrow 2H_2O + O_2$$
$$O^{-1} \longrightarrow O^{0} + e^{-}$$
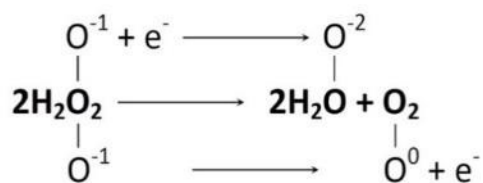
Figure 2. 11 Decomposition reaction of H_2O_2 [14].

The other challenge is the thermal instability of the resulting peroxytungstic acid solution [98]. Even though tungstic acid solutions are simple to handle and low-priced, it has been reported that none of the PTA are stable [5]. PTA gradually decomposes over time same as H_2O_2 when it is exposed to impurities or catalysts, and other environmental factors because of having poor stability. A study conducted by Park et al.[16], demonstrate the self-decomposing behavior of PTA by time, in the experimental procedure the prepared PTA solution was sealed and then aged for

3-21 days at room temperature to provoke the precipitation of WO_3. It is reported that an increase in the aging time results in color change; the color of the PTA solution changed from pale yellow to vibrant yellow, indicating an increase in the precipitation of WO_3 nanoparticles.

In the leaching of $CaWO_4$ in H_2SO_2 and H_2O_2 solution, Ca^{2+} ions generate $CaSO_4$ residues while W is converted into PTA in solution, as shown in **Equations (2.15) and (2.16)** [1], [8]. PTA is a compound that is created by substituting the -O-O- bond $(O_2)^{2-}$ in the H_2O_2 for O^{2-} in WO_4^{2-} [1]. It is synthesized *in situ* by reacting W or H_2WO_4 with H_2O_2 and is commonly utilized in the manufacture of prepared tungsten oxide and W powder or film forms in various forms [98].

$CaWO_{4(s)} + mH_2O_{2(aq)} + 2H^+_{(aq)} = H_2[WO_{4-m}(O_2)_m]_{(aq)}$ m=1,2,3,4 **(2.15)**

$CaWO_{4(s)} + mH_2O_{2(aq)} + H_2SO_4 (aq) = H_2[WO_{4-m}(O_2)_m]_{(aq)} + CaSO_{4(s)} . nH_2O_{(s)}$ m m=1,2,3,4; n=0,0.5,2 **(2.16)**
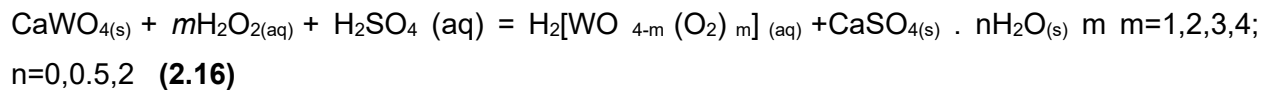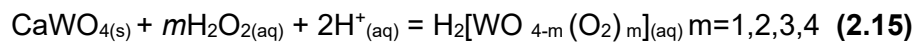
To extract the purified H_2WO_4, increasing the temperature or decreasing the ratio of $n(O_2^{2-})$ to $n(W)$ is required [1]. However, in the presence of excess peroxy ions, stable solutions can be formed [99]. In this synergistic leaching system, the PTA is heated to produce the yellow H_2WO_4 precipitation at temperatures greater than 55 °C [55], and the optimum conditions are stated as 4 hours at 90°C with 99.3% efficiency [13]. Based on the experimental phenomena, the elongation of the reaction time in thermal decomposition leads to a progressive transformation of the solution, transitioning from clarity to turbidity. Subsequently forming a white paste, and ultimately culminating in a yellow H_2WO_4 solid which indicates that the process starts with the decomposition of the PTA and then the polymerization process of H_2WO_4. Therefore, the W concentration in the leaching solution experiences a rapid reduction [81]. Additionally, H_2O_2 is completely decomposed during the thermal decomposition reaction, and there is no left in the resulting lixivium [13]. The degree of instability of PTA decreases as the W: O_2 molar ratio in the solution rises, resulting in the precipitation of H_2WO_4 as shown in **Equation (2.17)** [81]. In the presence of PTA, pH decreases to values between 2.6 and 3, due to acid dissociation [98], as shown in **Equation (2.18)**.

$H_4WO_3(O_2)_{2(aq)} = H_2WO_{4(s)} + H_2O_{(l)} + O_{2(g)}$ **(2.17)**

$PTA = PTA^-_{(aq)} + H^+_{(aq)}$ **(2.18)**
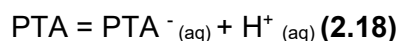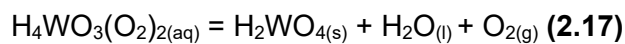
2.5 Summary

In conclusion, the $CaWO_4$ mineral has become the primary source of critical and rare metal W due to the overexploitation of high-grade and easily accessible [(Fe, Mn) WO_4] minerals. The generic flowsheet for leaching synthetic scheelite in H_2SO_4 and H_2O_2 solution is illustrated in **Figure 2.12**. However, the increasing complexity and lower grade of ore deposits pose challenges in W extraction. Throughout history, hydrometallurgical methods, including acid and alkaline leaching, have been employed to extract W minerals, and these methods continue to be explored as technology advances. Nevertheless, the successful transition from laboratory-scale studies to industrial-scale processing plants is challenging and requires further comprehensive research.
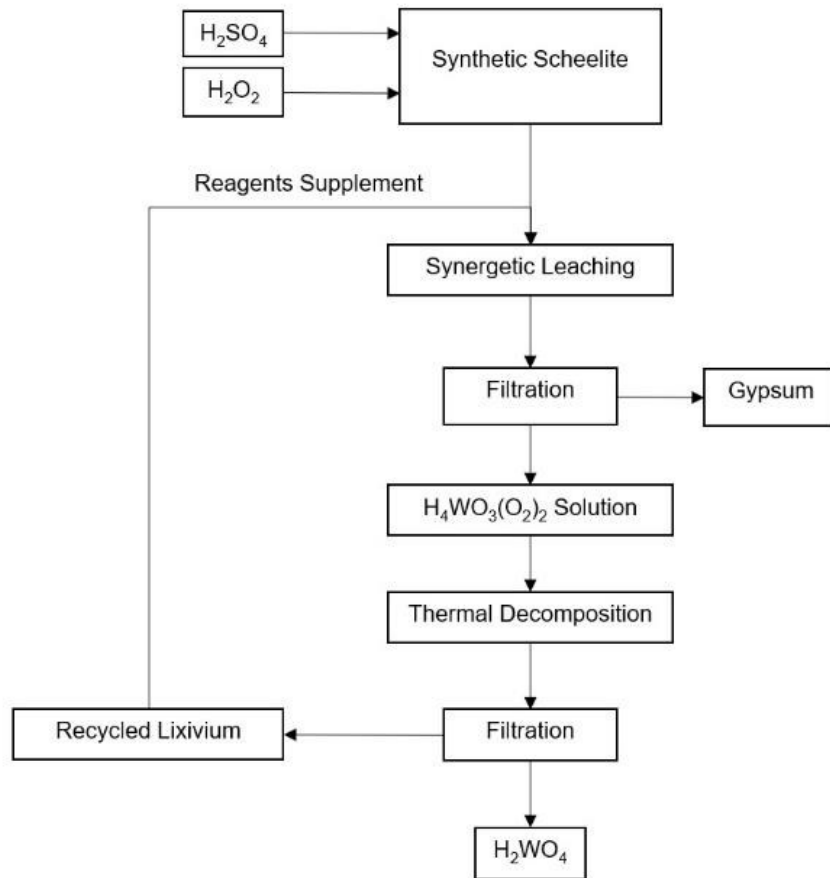
Figure 2. 12 Generic flowsheet of synergetic leaching synthetic scheelite in H_2SO_4 and H_2O_2 solution. Based on [55].

Currently, high-pressure and high-temperature alkaline leaching is predominantly used in W processing plants due to its efficiency, despite its known drawbacks and stringent environmental regulations. Acid leaching, on the other hand, is viewed as a potential solution to the issues

associated with the alkaline process and offers more effective and advantageous production alternatives. Notably, HCl, HNO_3, and H_2SO_4 have been extensively studied in the laboratory for their applicability in W extraction. However, only HCl is commonly used in industrial settings, albeit with limited adoption due to its drawbacks. HNO_3, with its high volatility and environmental risks, has not been widely adopted in the industry and is rarely utilized in laboratory studies. Consequently, recent laboratory-scale investigations have primarily focused on H_2SO_4, which exhibits low volatility, accessibility, compatibility with complexing agents, and energy efficiency due to its lower temperature and pressure requirements.

The latest studies have discovered that using an H_2O_2 complexing agent in combination with an H_2SO_4 solution provides a green and advantageous alternative. Although H_2O_2 exhibits selectivity in W extraction, resulting in high leaching efficiency and yield, its poor thermal stability and the presence of PTA pose limitations for the leaching process. Therefore, ongoing research aims to address these challenges and optimize the acid leaching method for sustainable and efficient W extraction.

Although the leaching method mentioned is effective and eco-friendly, there is a lack of differentiation in the operating conditions applied to natural and synthetic scheelite. A recent study [8] examined the leaching efficiency and kinetics of both ore types, aiming to understand the effect of operational variables. However, without considering the characteristic differences of both ore types, the same operating conditions are suggested for natural and synthetic ore. In essence, the selected and proposed leaching conditions were considered identical for both ore types, regardless of unique ore properties. Moreover, the literature provides limited information on the recycling mechanism of lixivium, with a focus primarily on experimental parameters. Therefore, in the existing studies [11], [13], there is a lack of detailed results and discussion regarding the products obtained from thermal decomposition operations specific to synthetic and natural ore types.

In addition to the lack of knowledge, some things have not yet been attempted. For instance, the 2-step method was proposed for low-grade scheelite ore leaching in the study conducted by Zhang et al. [11], in 2021. It has been suggested that this application would be beneficial in improving the thermal stability of H_2O_2. However, although it is recommended, there is no scientific proof of the feasibility of this method. Moreover, since leaching scheelite in the H_2SO_4 and H_2O_2 solution method is already a novel method, the published studies focus on understanding the

impact of the operating conditions on the leaching efficiency and kinetics [8], [11]. No work has been presented for the optimization of this leaching system.

CHAPTER 3 FEASIBILITY STUDY OF THE 2-STEP METHOD FOR LEACHING SYNTHETIC SCHEELITE

The main objective of this chapter is to investigate the feasibility of the suggested sequential 2-step method for leaching synthetic scheelite in H_2SO_4 and H_2O_2 solution. To achieve this, it is crucial to first develop a fundamental understanding of the synergistic leaching of $CaWO_4$ in the H_2SO_4-H_2O_2 solution. Therefore, the initially published synergistic leaching methods in the literature were replicated to validate their effectiveness [8], [11]. Subsequently, the suggested 2-step method experiment was conducted to assess its feasibility. Part of this chapter has been presented as I. Mutlu Tuncer, J. Liu "Assessing the Feasibility of a 2-Step Method for Leaching Synthetic Scheelite in H_2SO_4 and H_2O_2 Solution" CMSC 2023, Canada.

3.1 Validation of The Synergistic $CaWO_4$ Leaching in H_2SO_4 and H_2O_2 Solution Method

The recent synergistic leaching of $CaWO_4$ in H_2SO_4 and H_2O_2 solution has garnered significant attention due to its ability to achieve high leaching efficiency and yield at normal temperatures and pressures [8], [11]. To comprehend and evaluate the leaching mechanism and validate the synergistic leaching of $CaWO_4$ in H_2SO_4 and H_2O_2 solution, two tests were performed based on the latest references [8], [11].

3.1.1 Experimental

For the following tests, all the chemical reagents and synthetic ore utilized were shown in **Table 3.1**. The experimental procedure consists of 2 different leaching conditions presented in the most recent studies as described in **Table 3.2.** In the scope of validation tests, 250 mL scale leaching experiments were performed in a closed Pyrex® reaction flask, which was heated thermostatically by a water bath and stirred by a magnetic stirrer. In each experiment, the mixed-acid solution of H_2SO_4–H_2O_2 was introduced into the cell and heated to the desired temperature ($\pm$ 0.5 °C). When the conditions were attained, the reaction was initiated with the addition of a specific amount (L/S: 10 mL/g) of synthetic scheelite, and the timing was started. At the end of the leaching process, the resulting slurry cooled to room temperature in the cell and was filtered with Whatman grade 5 filter paper to remove by-product $CaSO_4$ from PTA, and then washed with DI water. After filtration, washing is important to remove the pregnant solution remaining in $CaSO_4$ collected on the filter. Otherwise, the pregnant solution remaining in the $CaSO_4$ during drying in the oven undergoes

thermal decomposition and precipitates as yellow H_2WO_4 and contaminates the white $CaSO_4$ concentrate.

The washed residue obtained from the filtration process was dried in an oven under specified conditions. Once dried, the residue was weighed using an electronic balance. The tungsten (W) content in the solution was determined through analysis using inductively coupled plasma (ICP). The final "leaching efficiency" (λ), which represents the proportion of W in the $CaWO_4$ that entered the solution, was calculated using **Equation (3.1)** [11]:

$$\lambda = \frac{m_0\,w_0 - m_1\,w_1}{m_0\,w_0} \times 100\% \qquad \textbf{(3.1)}$$

Where m_0 and m_1 are the mass of scheelite and leaching residues, respectively; w_0 and w_1 are the WO_3 content in scheelite and leaching residues, respectively.

Table 3. 1 Description of utilized compounds for all the leaching experiments in this study.

Compound	Formula	Concentration (w/w)	CAS-No	Supplier
Sulfuric acid	H_2SO_4	24.95%	7664-93-9	Fisher Scientific
Hydrogen peroxide	H_2O_2	27%	7722-84-1	Fisher Scientific
Synthetic scheelite	$CaWO_4$	98%	7790-75-2	Fisher Scientific

Table 3. 2 Operating conditions of reference tests based on the literature.

Conditions	Reference 1 [8]	Reference 2 [11]
H_2SO_4 (mol/L)	3	2
H_2O_2 (mol/L)	1.5	2.5
L/S ratio (mL/g)	10	10
Temperature (°C)	45	60
Leaching duration (min)	90	180
Stirring rate (r/min)	400	300
Drying temperature (°C)	70	80
Drying time (h)	24	8
Leaching efficiency (%)	99.7	98

To obtain the final product, W is precipitated as an H_2WO_4 intermediate from PTA by thermal decomposition [13]. For reference 1 [8] and reference 2 [11], the thermal decomposition procedure was conducted under the same conditions, in a thermostatically heated water bath Pyrex® reaction flask under vigorous stirring. The PTA solution obtained from the leaching process was added into the flask, which was heated to the desired temperature of 90°C and decomposed for 4 hours [13], at a stirring speed of 300 r/min [11]. After the reaction was completed, the slurry was cooled down to room temperature, filtered, and washed with DI water. The resulting filter cake was dried in an oven at 70°C for 24 hours in sequence, and the dried residue was weighed by an electronic balance. The resulting $CaSO_4$ and H_2WO_4 products were characterized using X-ray diffraction using an X-ray diffractometer (Rigaku Ultima IV).

3.1.2 Results and Discussion

Upon the addition of the synthetic scheelite ore to the solution, bubbles appeared on the surface of the solution, and within a few minutes, white, stick-like morphology $CaSO_4$ crystals precipitated. During this precipitation, no visible insoluble yellow H_2WO_4 was observed in the slurry or on the filtered-out solid residue, as shown in **Figure 3.2 (a) and (b)**. This observation indicates that the H_2O_2 complexing agent effectively interacts with the H_2SO_4 leaching agent, preventing the formation of H_2WO_4, as stated in the literature [8], [11], [13]. In other words, the solid residue collected on the filter consists solely of white $CaSO_4$, and the absence of yellow H_2WO_4 precipitate confirms the conversion of W to PTA solution. Moreover, as depicted in **Figure 3. 1 (a) and (b)**, the absence of turbidity in the resulting PTAs and their light yellow and transparent appearance further corroborates the $CaSO_4$ filter cake visual observation findings.
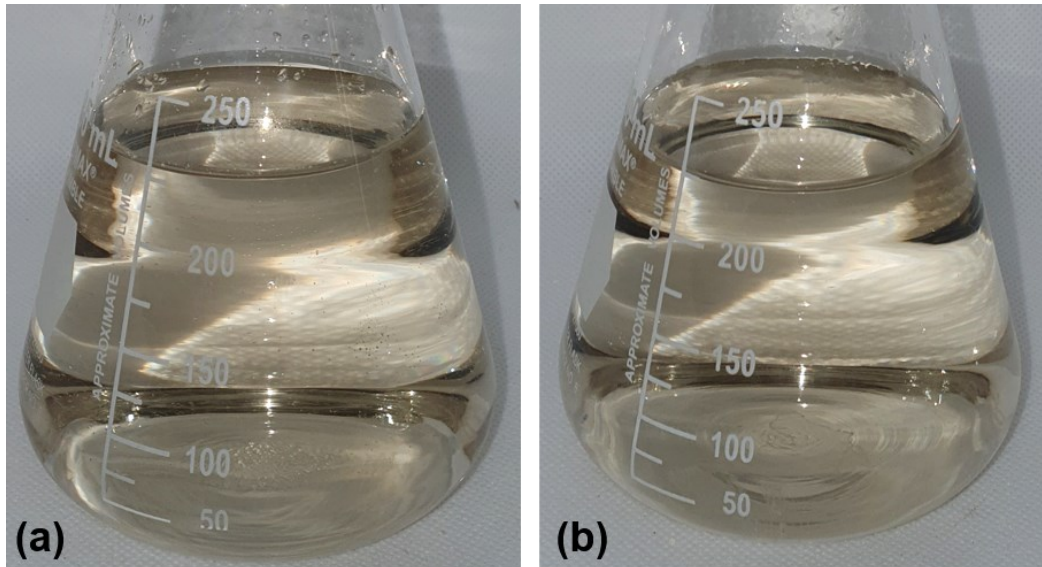
Figure 3. 1 Resulting PTAs obtained from validation of the synergistic $CaWO_4$ leaching in H_2SO_4 and H_2O_2 solution method tests: (a) reference 1 [8], (b) reference 2 [11].
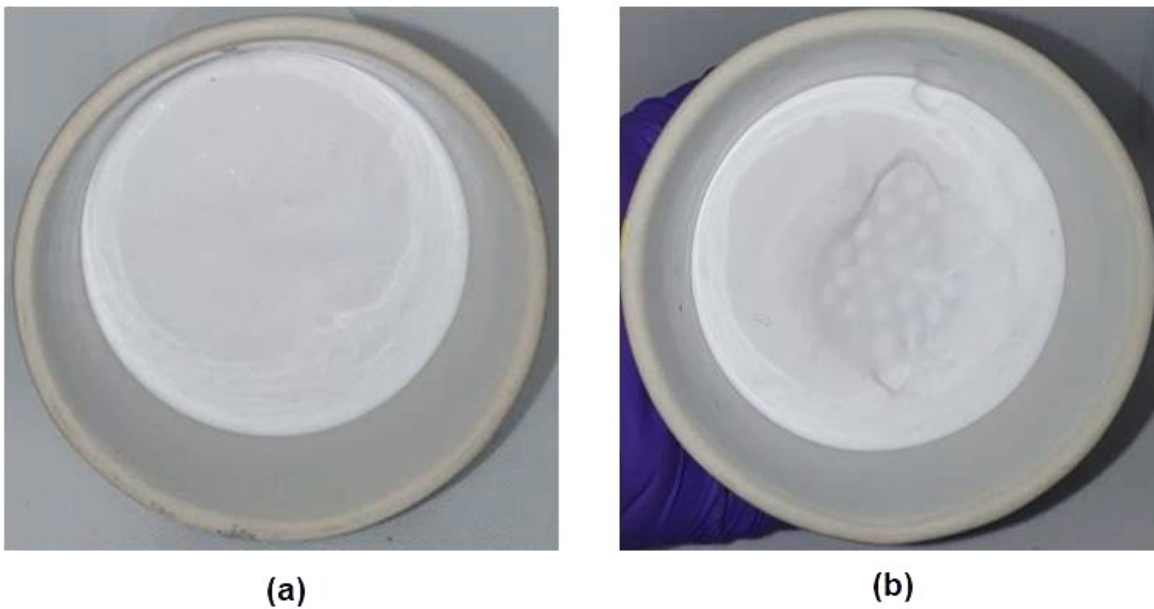
Figure 3. 2 Resulting $CaSO_4$ filter cakes obtained from validation of the synergistic $CaWO_4$ leaching in H_2SO_4 and H_2O_2 solution method tests: (a) reference 1 [8], (b) reference 2 [11].

After leaching is completed, to extract W from the solution in the form of a solid H_2WO_4 intermediate product, the pregnant solution **(Figure 3.3 (a))** was treated by thermal decomposition [11]. As the temperature was around 80 °C degrees, a color change and turbidity were observed in the transparent pregnant solution **(Figure 3.3 (b))**. As the temperature exceeded 90 °C, visible

yellow H_2WO_4 precipitations began to form, as shown **in Figure 3.3 (c).** Once the thermal decomposition process was completed, the bright, yellow-colored non-sticky formed H_2WO_4 **(Figure 3.3 (d))** was collected through filtration, while the resulting lixivium **(Figure 3.3 (e))** was prepared for reuse. **Chapter 4** provides an in-depth examination of the mechanism behind lixivium recycling and reuse. The investigation focuses on unraveling the intricacies of this process and offers comprehensive insights into the feasibility and potential benefits of recycling and reusing lixivium.
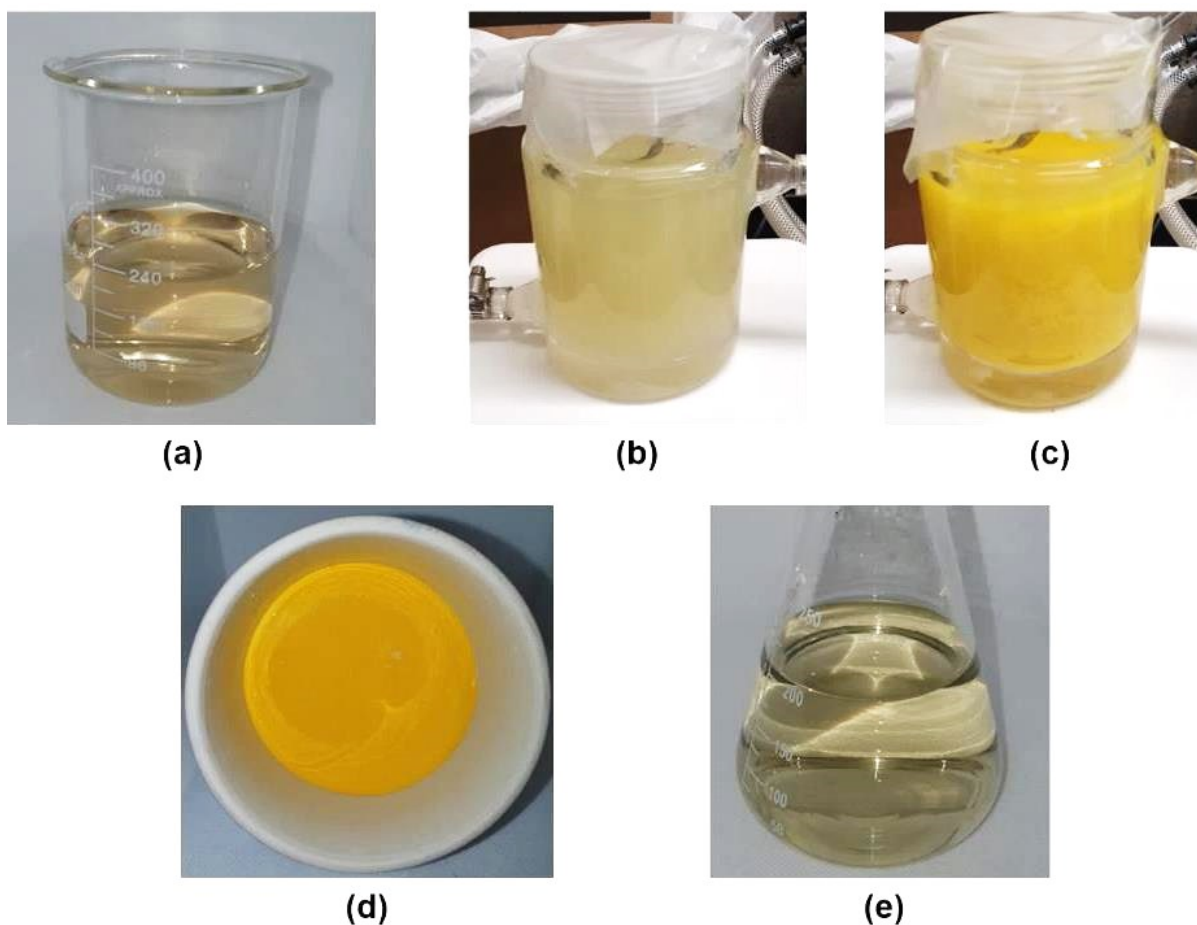
Figure 3. 3 Sequential steps of thermal decomposition to obtain H_2WO_4 intermediate from PTA: (a) PTA solution to be decomposed thermally, (b) color change and precipitation started, (c) after thermal decomposition completed, (d) yellow H_2WO_4 on the filter paper, (e) recycled and reusable lixivium.

XRD analysis was employed to ascertain the chemical composition and crystal structure of the solid products, namely the filter cakes obtained after the leaching and thermal decomposition procedures. It is a highly versatile technique that provides the identification of distinct chemical compounds for elemental analysis as well as for phase analysis [100]. **Figure 3.4 (a)** reveals that the main diffraction peaks in the resulting filter cakes after leaching correspond to fibrous, plank-shaped monoclinic phases of $CaSO_4 \cdot 2H_2O$ [8] for both tests. Moreover, the absence of any impurities or unreacted $CaWO_4$ particles indicates that the entire synthetic ore has been converted to $CaSO_4.2H_2O$. Likewise, **Figure 3.4 (b)** illustrates that the prominent diffraction peaks observed in the filter cakes obtained after thermal decomposition correspond to pure orthorhombic phases of tungstite ($WO_3.H_2O$) [13] for both tests, indicating a high degree of similarity between the resulting products, while no impurity phases are observed in the pattern.
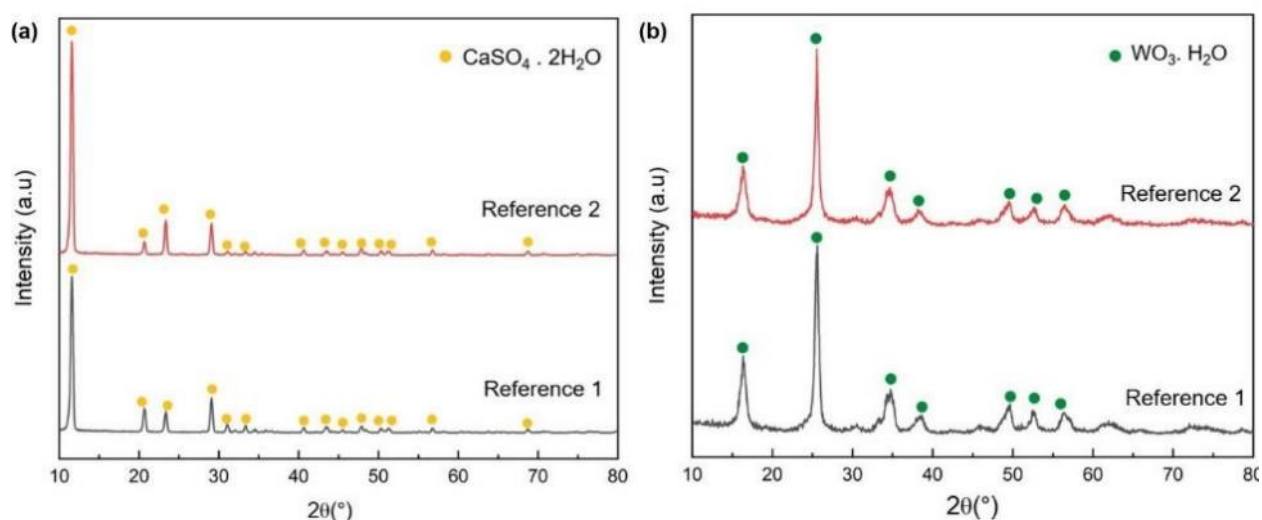
Figure 3. 4 XRD patterns of the resulting filter cakes after leaching and thermal decomposition were obtained by reference 1 [8] and reference 2 [11]: (a) $CaSO_4$ filter cakes, (b) H_2WO_4 filter cakes.

There are remarkable differences between the two leaching conditions in reference tests 1 [8] and 2 [11]. Reference test 1 [8] is conducted at 45°C for 90 minutes, while reference test 2 [11] is conducted at 60°C for 180 minutes. Furthermore, the concentrations of the reagents used in these tests are notably different. The use of 1.5 mol/L H_2O_2 in reference test 1 [8] is considered to be more environmentally friendly and cost-effective compared to the 2.5 mol/L H_2O_2 used in reference test 2 [11]. This is because the self-decomposing oxidizing reagent H_2O_2 exhibits poor thermal stability and decomposes upon contact with water/air [14]. During leaching, it naturally

decomposes and is completely consumed during thermal decomposition, requiring its entire concentration to be replenished for preparing a new leaching solution. In contrast, the stable H_2SO_4 remains undecomposed during leaching and thermal decomposition only converting $CaWO_4$ to $CaSO_4$ and providing acidity [13].

According to ICP results, despite the variations in operating parameters, reference test 1 [8] achieved a leaching efficiency of 95.98%, while reference test 2 [11] presented a leaching efficiency of 97.05%, both of which are in proximity to the reported efficiencies. However, these values are slightly lower than the reported values of 99.7% for reference test 1 [8] and 98% for reference test 2 [11]. To further investigate this difference, considering the absence of impurities in the $CaSO_4$ filters according to the XRD results, the ICP results of the washing waters were examined, revealing a W content of 2.34% for reference test 1 [8] and 2.05% for reference test 2 [11]. Consequently, the total leaching efficiency, including the loss of material in the washing water, amounted to 95.98% for reference test 1 [8] and 97.05% for reference test 2 [11], whereas the literature reports values of 99.7% for reference test 1 [8] and 98% for reference test 2 [11]. This minor reduction in the achieved leaching efficiencies could potentially be attributed to various environmental factors inherent to the laboratory setting.

Besides validating the reported tests, to observe the aging behavior of PTA mentioned in the literature [16], the pregnant solution was stored for 24 hours in a sealed HDPE bottle at room temperature. Although there was no remarkable color change observed, the presence of oxygen gas bubbles in the solution was visible, as shown in **Figure 3.5. (a).** The bottle also exhibited signs of deterioration due to gas expansion. Upon opening the bottle as in **Figure 3.5. (b)**, there was an audible release of gas, indicating the presence of accumulated oxygen gas in the PTA. This resulted in a slight weight difference between the PTA weighed after the leaching process and the PTA stored for 24 hours, around 0.10 grams. Oxygen bubbles continued to form even after an additional 24 hours of storage, as shown in **Figure 3.5 (c)**, indicating ongoing gas release in the re-ventilated PTA. In addition, color changes were observed in all stored PTAs after 3 days in all experiments. It was confirmed that the color of the PTA solution changed from faded yellow to bright yellow as the aging time increased, due to an increment in the precipitation of WO_3 nanoparticles [16].
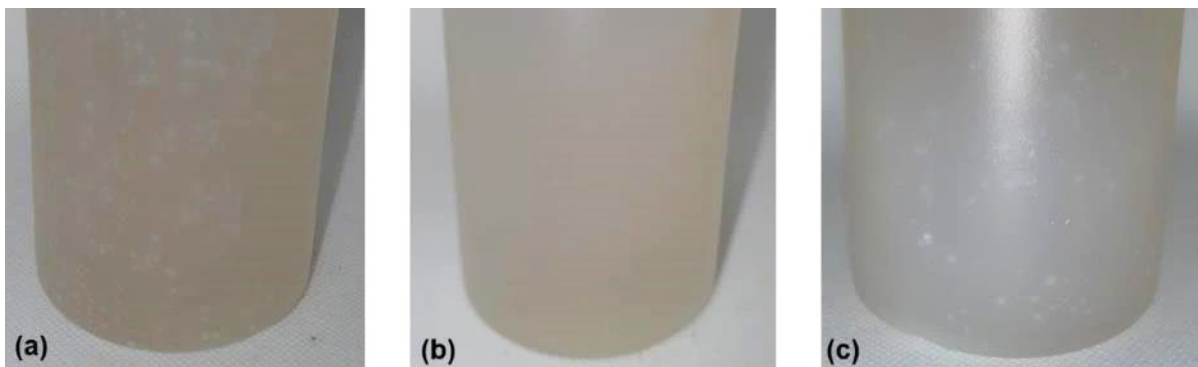
Figure 3. 5 Aging observation in stored PTA: (a) oxygen bubbles produced by peroxide decomposition in PTA stored for 24 hours, (b) PTA after opening the lid of the 24-hour stored PTA and aeration, (c) re-formation of oxygen bubbles after an additional 24 hours of storage of the aerated PTA**.**

Based on the findings from this chapter, it was concluded that the synergistic leaching of synthetic scheelite in the mixed H_2SO_4-H_2O_2 system is feasible, as previously reported in recent publications [8], [11], [13]. Moreover, the leaching conditions of reference test 1 [8] were selected as the basis for further experimentation due to their potential for creating a more eco-friendly and cost-effective process. This is attributed to the lower temperature, reduced H_2O_2 concentration, and shorter leaching duration required in this approach. Building upon this knowledge, **Chapter 3.2** delves deeper into the investigation of the 2-step method leaching of synthetic scheelite using this aqueous leaching media, providing a comprehensive analysis of the process.

3.2 Feasibility Study of the 2-Step Method

To conduct the 2-step method experiment, the leaching conditions of reference 1 [8] were used due to requiring lower temperature, and less H_2O_2 concentration requirement, as discussed in **Chapter 3.1.1.** By comparing the reaction conditions of the reference tests 1 [8] and 2 [11], which exhibit differences in temperature, leaching duration, and reagent concentration, it is feasible to explore the possibility of achieving the leaching process in a shorter time with reduced reagent usage through the implementation of the 2-step method. The objective of this experiment is to assess the feasibility of the 2-step method and observe its impact on the leaching efficiency and final product. Additionally, the study aims to investigate whether it is possible to effectively operate the leaching system by minimizing H_2O_2 decomposition, reducing the concentration of the relatively expensive H_2O_2, and increasing the W production rate per unit time by shortening the

leaching duration. The limited information in this area can be considered a hindrance to the efficiency of this method. Therefore, this study focuses on determining the slow reaction and evaluating the reaction time of the 2nd step to assess its influence on the overall leaching efficiency.

3.2.1 Experimental

The experimental procedure involved conducting leaching experiments on a 250 mL scale using a Pyrex® reaction flask, which was heated by a water bath and stirred with a magnetic stirrer. In the 1st step, a 3 mol/L H_2SO_4 solution was introduced into the flask and heated to 45 °C (± 0.5 °C). Once the desired temperature was reached, 25 grams of synthetic scheelite was added to initiate the leaching reaction, which continued for 60 minutes. Considering that the reaction time of 90 minutes used for synergistic leaching in reference 1 [8] would not be sufficient to apply the 2-step method, the reaction time for the 1st step was chosen as 60 minutes. This adjustment allows for the elimination of concerns regarding insufficient reaction time for the 2nd step and provides a suitable environment for visual observation. Following the completion of a 60-minute leaching process in the 1st step, a 1.5 mol/L H_2O_2 solution was heated to the leaching temperature and was introduced into the flask to initiate the 2nd step. To observe the dissolution behavior of H_2WO_4 and the reaction duration of the 2nd step, the leaching time was observed at 30-minute intervals. Therefore, slow reactions in the leaching mechanism can be identified. The leaching times chosen for the 2nd step were 30, 60, 90, and 120 minutes, ensuring that the total leaching time did not exceed 180 minutes, the maximum leaching duration specified in reference test 2 [11]. The precipitation of H_2WO_4 was visually observed and recorded during these intervals.

After the completion of the leaching, the slurry present in the reactor was cooled to room temperature and subjected to filtration using Whatman grade 5 filter paper. This filtration step aimed to separate the solid products, namely the yellow H_2WO_4 and the white $CaSO_4$, from the PTA. The filtered residue was then washed with DI water. Subsequently, the washed residue was dried in an oven set at 70 °C for 24 hours. The resulting dried residue was weighed using an electronic balance. Since $CaSO_4$ and H_2WO_4 could be visually distinguished in the slurry and filter cake, no further XRD or ICP characterization analyses were performed in the 2-step method tests. The low efficiency of the leaching process was confirmed by the detection of visible yellow H_2WO_4 in the final filter, therefore the thermal decomposition step was not applied for the 2-step method test.

3.2.2 Results and Discussion

In the 1st step, after adding the ore to the heated H_2SO_4, yellow H_2WO_4 and white $CaSO_4$ precipitates started forming within a few minutes. The white $CaSO_4$ precipitation was not easily visible due to the dominant presence of yellow H_2WO_4 in the system, as shown in **Figure 3.6 (a)**. The color of the slurry remained unchanged throughout the 1st step. After completing the 60-minute 1st step reaction, the addition of heated H_2O_2 in the 2nd step resulted in the slurry turning into a lighter yellow color within a few minutes.

During the 2nd step, observations were made at 30-minute intervals to assess the solubility of H_2WO_4 and determine the reaction duration. At the end of the 30-minute reaction, the $CaSO_4$ and H_2WO_4 products were separated from each other **in Figure 3.6 (b)**, with the H_2WO_4 accumulating at the bottom of the flask, as shown in **Figure 3.7 (a).** However, the 30-minute reaction time was insufficient for the complete conversion of H_2WO_4 to PTA. Therefore, the reaction time for the 2nd step was extended to 60 minutes. At the end of 60 minutes, the amount of yellow H_2WO_4 decreased, but it was not completely dissolved, as shown in **Figure 3.6 (c)** and **Figure 3.7 (b)**. Thus, it was concluded that the total leaching time of 90 minutes specified in reference test 1 [8] was insufficient for the application of the 2-step method.

(a)   (b)   (c)   (d)   (e)
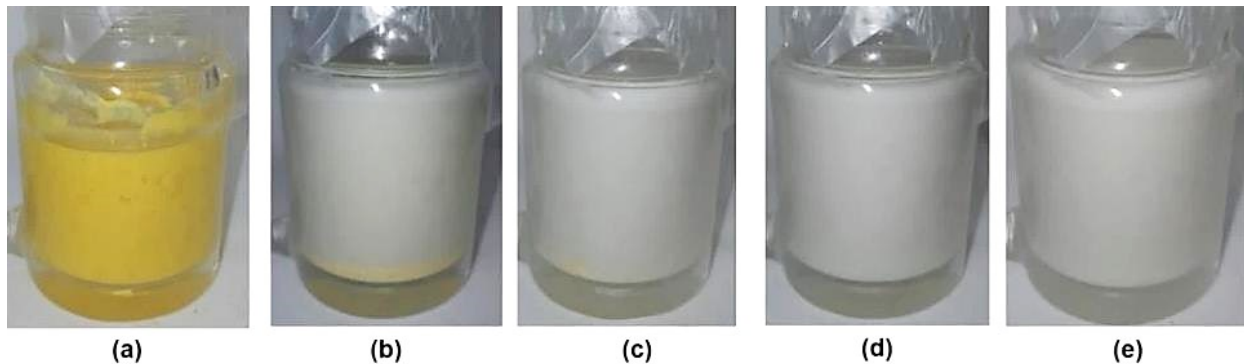
Figure 3. 6 Evolution of H_2WO_4 precipitation in the slurry during the 2nd step with H_2O_2 addition: (a) after the completion of 1st step, (b) after 30 minutes, (c) after 60 minutes, (d) after 90 minutes, (e) after 120 minutes in the 2nd step.
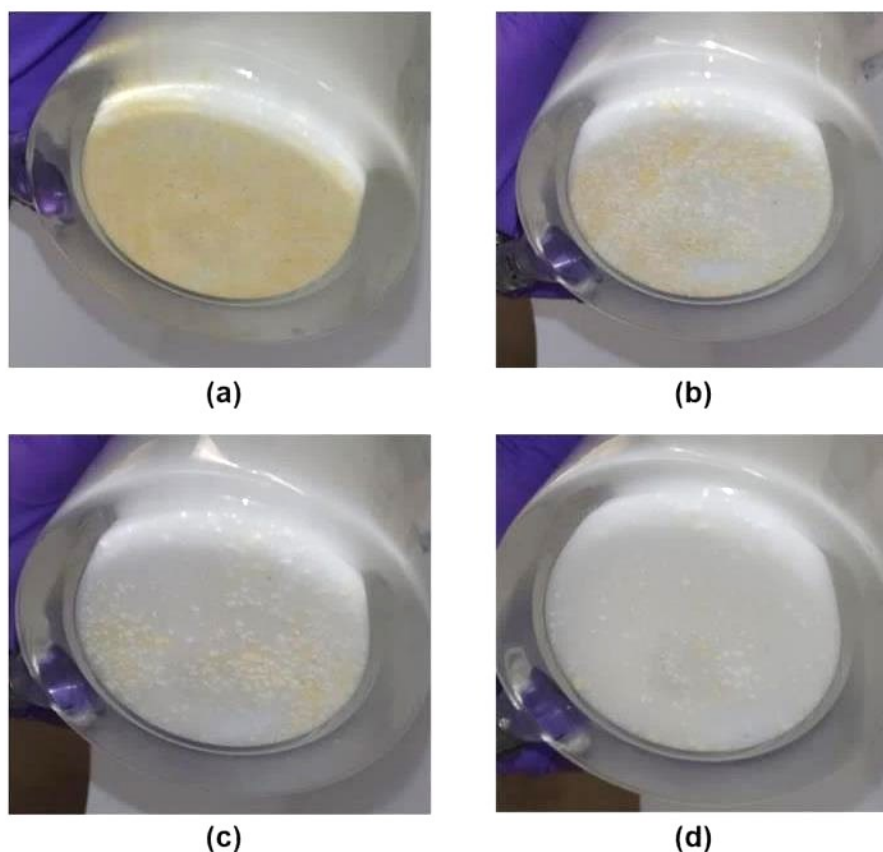
Figure 3. 7 Accumulation of H_2WO_4 precipitation at the bottom of the flask during the 2nd step with H_2O_2 addition: (a) after 30 minutes, (b) after 60 minutes, (c) after 90 minutes, and (d) after 120 minutes in the 2nd step.

To further investigate the dissolution of H_2WO_4, the reaction time for the 2nd step was increased to 90 minutes. After 90 minutes, the visible amount of H_2WO_4 decreased significantly as shown in **Figure 3.6 (d) and Figure 3.7 (c)**, but it was still not completely dissolved. This indicated that the total leaching time of 90 minutes specified in reference test 1 [8] was insufficient for the application of the 2-step method. To explore the dissolution further, the reaction time for the 2nd step was extended to 120 minutes. However, even after 120 minutes, the yellow precipitate of H_2WO_4 was still visible at the bottom of the flask as shown in **Figure 3.7 (d)**, indicating incomplete dissolution. Therefore, it can be concluded that 120 minutes was also insufficient to dissolve H_2WO_4 in the 2nd step under the given leaching conditions. Additionally, as shown in **Figure 3. 8**, the resulting filtrate after leaching exhibits a yellow appearance. This indicates that the white $CaSO_4$ byproduct, which can be directly used as a cement raw material after leaching, is

negatively affected by the yellow H_2WO_4 precipitation, making it challenging to effectively separate them from each other.

Figure 3. 8 Yellow H_2WO_4 precipitates contamination in the resulting $CaSO_4$ filter cake obtained from the 2-step method.

It is concluded that in the 2-step method for leaching $CaWO_4$ in H_2SO_4 and H_2O_2 solutions, the slow reaction occurs in the 2nd step, which involves the addition of H_2O_2. Experimental tests conducted at 30-minute intervals demonstrated that H_2WO_4 requires more time to transform into the PTA form during this step. This delay in the reaction can be attributed to the formation of colloidal H_2WO_4, which covers the surface of unreacted $CaWO_4$ particles and hinders further reaction, as described in the literature [13]. Although the maximum leaching time of 180 minutes, as specified in the literature [11] for synergistic leaching of synthetic scheelite in H_2SO_4 and H_2O_2 solution, was completed in the 2-step method experiment, the presence of visible unreacted H_2WO_4 particles indicates that complete conversion was not achieved under the specified leaching conditions.

The 2-step method, despite being recommended to minimize the decomposition of thermally unstable H_2O_2, requires more time to complete the reaction, resulting in energy loss and a decrease in the production of the final product per unit of time. It has been demonstrated that

H_2O_2 works more effectively in synergy with H_2SO_4, where the presence of H_2SO_4 enhances the leaching reaction efficiency. In contrast, the synergistic leaching method requires a shorter reaction time as it converts the ore to PTA without the need for complete conversion to H_2WO_4. However, further investigation is required to explore the 2-step method in leaching $CaWO_4$ in H_2SO_4 and H_2O_2 solutions under different operating conditions. This research would help identify potential improvements and optimize the process for better efficiency and productivity.

3.3 Summary

The feasibility of the sequential 2-step method for leaching $CaWO_4$ in H_2SO_4 and H_2O_2 solution was investigated, and the following conclusions were drawn from the experimental results:

- The importance of H_2O_2 was emphasized in this study. In synergistic leaching, the addition of ore leads to the formation of insoluble solid products, H_2WO_4, and $CaSO_4$, within a few minutes. The role of H_2O_2 as a complexing agent is to convert W to PTA by preventing the precipitation of H_2WO_4. However, with the 2-step method, it is not practical or beneficial to precipitate H_2WO_4 in the 1st step and then attempt to convert it to PTA by adding H_2O_2 in the 2nd step.

- The 2-step method requires more time compared to the synergistic leaching method, primarily due to the slow reaction occurring in the 2nd step. The 2-step method necessitates a longer leaching duration than the maximum specified in the literature for synergistic leaching. This is because the precipitated H_2WO_4 covers the unreacted $CaWO_4$ particles, inhibiting further reaction. Consequently, it is not possible to reduce the retention time of H_2O_2 in the leaching system with the 2-step method.

- Synergistic leaching demonstrates superior leaching efficiency and higher yields compared to the 2-step method. The 2-step method, despite its aim to reduce H_2O_2 decomposition, requires more time to complete the reaction, leading to energy loss and decreased productivity. In contrast, synergistic leaching achieves satisfactory results by converting the ore to PTA without the need for complete conversion to H_2WO_4.

In conclusion, further investigation is necessary to explore the 2-step method for leaching $CaWO_4$ in H_2SO_4 and H_2O_2 solutions under different operating conditions. This research would provide valuable insights to enhance the efficiency and productivity of the process.

CHAPTER 4 INVESTIGATION STUDY OF THE LIXIVIUM RECYCLE AND REUSE MECHANISM

The lixivium's reusability, generated by precipitating H_2WO_4 by thermal decomposition in the synergistic leaching approach, enhances eco-friendliness [11], [13] [11]. It also reduces reagent consumption and operational costs [13]. Current data [13] shows lixivium can be recycled through thermal decomposition and reused with replenished reagents for 5 cycles. After 5 cycles, leaching slightly drops (about 1-3%). Despite emphasizing lixivium's recyclability and reusability, comprehensive information on its recycling, reuse mechanism, and decomposition parameters is lacking. Understanding thermal decomposition, lixivium recycling, and reuse processes is crucial.

The experimental results show that self-decomposing H_2O_2 reacts with air, water, and heat during leaching, depleting entirely in thermal decomposition [14]. As a result, the recycled lixivium obtained after thermal decomposition does not contain H_2O_2. It contains excess H_2SO_4, small amounts of dissolved $CaSO_4$, and water. On the other hand, H_2SO_4 is only consumed for $CaSO_4$ production during leaching, matching the ore's Ca content, and isn't used up in thermal decomposition [13]. Additionally, **Chapter 3.2** highlights the impracticality of reducing H_2O_2 concentration by minimizing its thermal decomposition with a 2-step approach. Given this information, the chapter aims to explore cycles achievable by only adding consumed H_2O_2 to the lixivium, without extra H_2SO_4. This investigates the feasibility of decreasing H_2SO_4 concentration in the process and its effects on final leaching efficiency. The study also assesses the potential for recycling lixivium multiple times without needing H_2SO_4 supplementation, evaluating its sustainability and efficiency.

4.1 Experimental

The experimental procedure involved conducting complete leaching cycles, including thermal decomposition, using the conditions specified in reference 1 [8]. Each leaching cycle used consistent conditions (temperature, duration, cooling, filtering, and filter cake drying), as outlined in **Table 4.1**.

In the 1st cycle, a 250 mL scale leaching experiment was performed in a Pyrex® reaction flask, heated by a water bath and stirred magnetically. A fresh mixed-acid solution of H_2SO_4–H_2O_2 was added to the flask and heated to a precise temperature of 45°C (± 0.5 °C). Once the conditions were met, synthetic scheelite was introduced at a specific ratio (L/S: 10 mL/g), initiating a 90-

minute leaching process. After leaching, the slurry cooled and was filtered using Whatman grade 5 filter paper to remove the $CaSO_4$ by-product from PTA. Subsequently, the $CaSO_4$ filter cake was dried at 70 °C for 24 hours. The resulting PTA filtrate underwent thermal decomposition to precipitate yellow H_2WO_4 at 90°C under 300 r/min [11], with stirring for 4 hours [13]. After completion, the slurry was cooled, filtered, and washed with DI water. The resulting H2WO4 filter cake was then dried at 70 °C for 24 hours. The 1st cycle concluded upon obtaining and storing the resulting filtrate, recycled lixivium.

In the 2nd cycle, the recycled lixivium was reused by supplementing the consumed H_2O_2 (1.5 mol/L) and preparing a new 250 mL leaching solution. Notably, H_2SO_4 supplementation was not carried out. The newly prepared leaching solution was utilized in the 2nd cycle, following the identical operating conditions as the 1st cycle. Once the leaching concluded, the resulting slurry cooled to room temperature within the flask. Subsequently, it was filtered using Whatman grade 5 filter paper to remove the $CaSO_4$ by-product from PTA, followed by rinsing with DI water. The resulting $CaSO_4$ filter cake underwent drying at 70 °C for 24 hours. The same thermal decomposition process as in the 1st cycle was applied to the PTA, resulting in the precipitation of H_2WO_4. The 2nd cycle was deemed complete upon acquiring and storing the resulting filtrate, recycled lixivium.

In the 3rd cycle, given the successful 2nd cycle, 1.5 mol/L of H_2O_2 was supplemented to match the H_2O_2 concentration of the new leaching solution in the 1st cycle, omitting H_2SO_4 supplementation. The newly prepared leaching solution was employed for leaching, following the same operating conditions and procedure as the 1st cycle. Following leaching, the resulting slurry cooled and was filtered with Whatman grade 5 filter paper to remove the $CaSO_4$ by-product from PTA, then washed with DI water. The $CaSO_4$ filter cake was dried at 70 °C for 24 hours. Similarly, the pregnant solution underwent thermal decomposition for H_2WO_4 precipitation, as in the 1st cycle. The 3rd cycle concluded upon obtaining and storing the resulting filtrate, recycled lixivium.

After the 3rd cycle, it was determined that further cycles were unfeasible. Visual observation of H_2WO_4 precipitates in the obtained lixivium revealed significant decreases in leaching efficiency and product yield from thermal decomposition. XRD analysis was conducted to identify mineral phases in solid products. Furthermore, a mass balance was executed to ascertain the reagent concentrations required for a new leaching solution. This prompted the discontinuation of the test after the 3rd cycle.

4.2 Results and Discussion

During each cycle, the leaching process resulted in transparent PTA. However, with increasing cycles, there was an observable darkening effect in the color of the PTAs, illustrated in **Figure 4.1 (a), (b), and (c).** In contrast, the white $CaSO_4$ filter cakes maintained consistent appearances across all cycles, as depicted in **Figure 4.1 (d), (e), and (f)**, without any indication of yellow H_2WO_4 precipitates. Nevertheless, as cycles increased, the $CaSO_4$ product exhibited a noticeable fine grain structure, with the 3rd product displaying finer grain size and greater viscosity than usual. This finer grain size presented challenges during filtration. It's understood that the presence of fine particles generated under low H_2SO_4 concentration prompts quicker crystal nucleation, affecting the reaction between H_2SO_4 and unreacted ore while complicating subsequent filtration processes [8]. This phenomenon gains additional support from the XRD analysis.
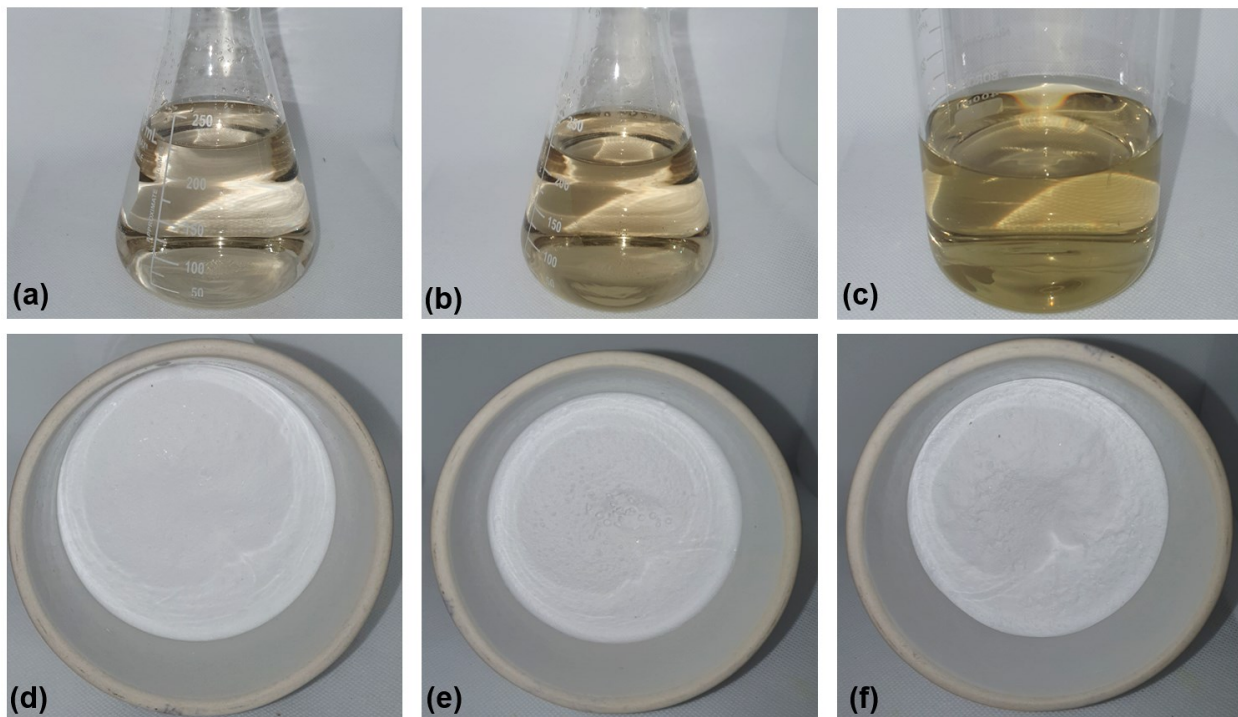
Figure 4. 1 Resulting PTAs, and $CaSO_4$ filter cakes after leaching in each cycle obtained from investigation study of the lixivium recycle and reuse mechanism tests: (a) PTA of the 1st cycle, (b) PTA of the 2nd cycle, (c) PTA of the 3rd cycle, (d) $CaSO_4$ product of the 1st cycle, (e) $CaSO_4$ product of the 2nd cycle, (f) $CaSO_4$ product of the 3rd cycle.

According to XRD characterization, all the diffraction peaks of samples are in perfect agreement with the standard pattern of $CaSO_4.2H_2O$ crystals for all cycles [8], with no impurity phases, as shown in **Figure 4.2**. Furthermore, no unreacted $CaWO_4$ was identified in the filter cakes, confirming the complete conversion of synthetic scheelite ore to gypsum, indicating full $CaWO_4$ decomposition. Additionally, the absence of diffractions consistent with H_2WO_4 supports the observation that yellow H_2WO_4 precipitation didn't occur during leaching.

In the XRD pattern, strong and sharp diffraction peaks signify high-degree crystallization [11]. However, in the 3rd cycle, the diffractions weren't as strong as in the 1st and 2nd cycles. This suggests that when H_2SO_4 concentration decreased, the crystals formed—mainly manifesting as small rods—were relatively small, disordered, and dense. Furthermore, it's noted that leaching efficiency suffered at low H_2SO_4 concentrations [8]. This underscores the influence of H_2SO_4 concentration on crystal growth, nucleation ratio, shape, and size, with significant implications.
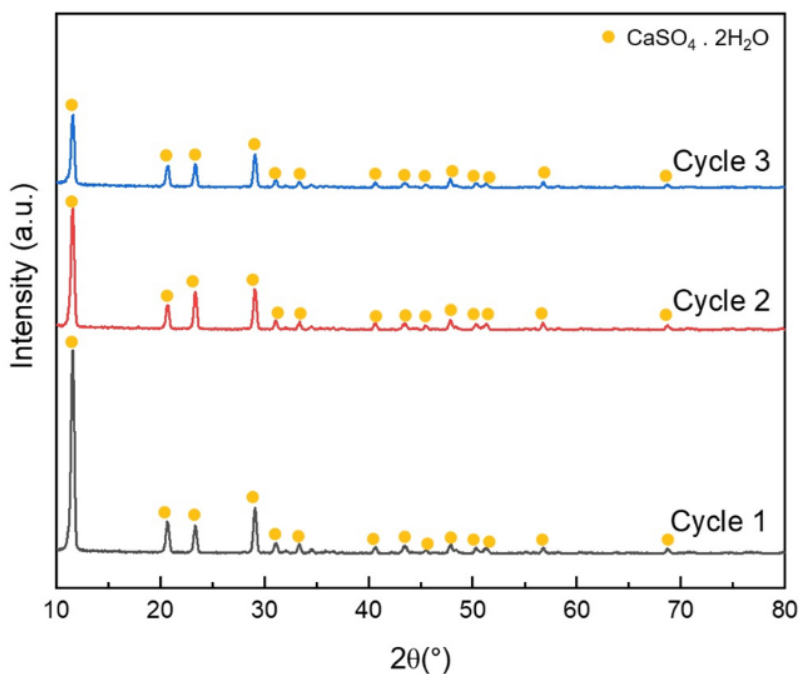
Figure 4. 2 XRD patterns of the resulting $CaSO_4$ filter cakes after leaching were obtained by 3 cycles.

The thermal decomposition process of the 1st and 2nd cycles yielded a similar slurry **(Figure 4.3 (a) and (b))** and yellow H_2WO_4 filter cake **(Figure 4.3 (d) and (e))**, as observed visually. However, in the 3rd cycle, despite favorable results in leaching based on visual observation and XRD analysis, a surprising light-green color formation was observed in the slurry during thermal

decomposition with increased temperature. Within a few minutes, an exceedingly fine-grained, sediment-free slurry with a muddy appearance formed, as depicted in **Figure 4.3 (c)**. Consequently, upon completion of thermal decomposition, no yellow H_2WO_4 precipitation was observed. The fine-grained mud posed filtration challenges due to clogging, leading to incomplete separation of lixivium and solid product during filtering, as shown in **Figure 4.3 (f).**
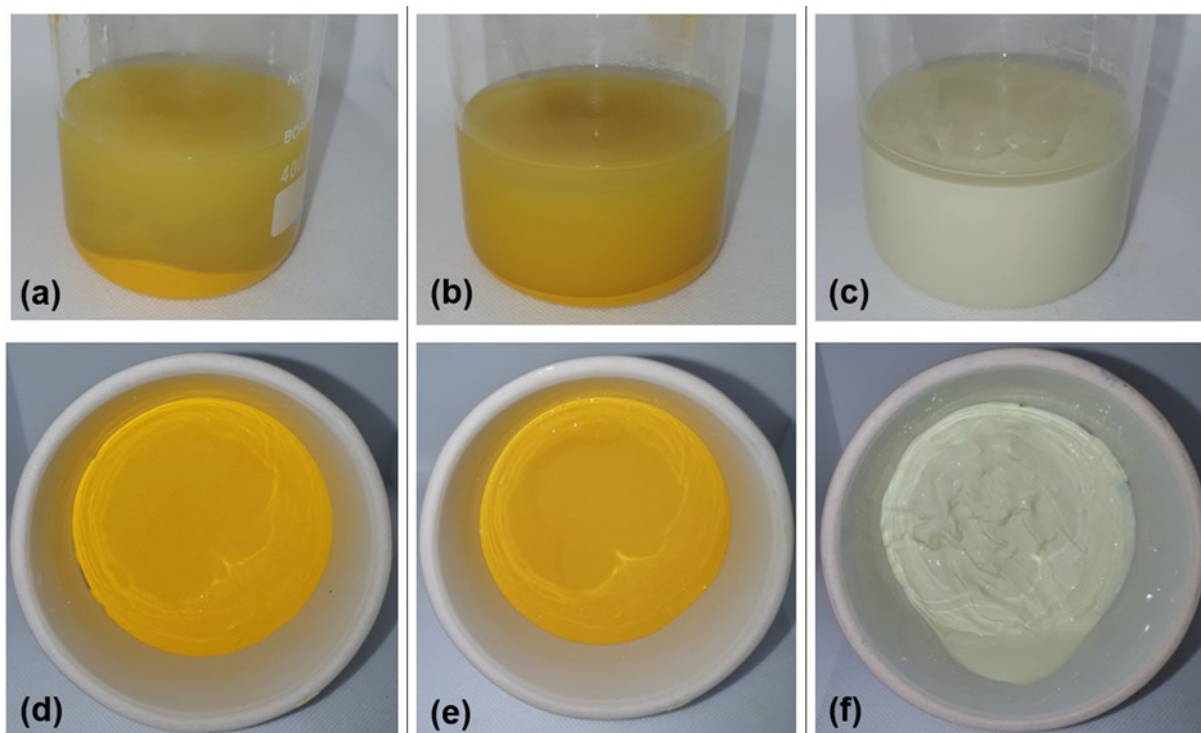
Figure 4. 3 H_2WO_4 precipitation in the resulting slurry after thermal decomposition and H_2WO_4 product after filtration: (a) slurry of the 1st cycle, (b) slurry of the 2nd cycle, (c) slurry of the 3rd cycle, (d) H_2WO_4 product of the 1st cycle, (e) H_2WO_4 product of the 2nd cycle, (f) H_2WO_4 product of the 3rd cycle.

Another challenge arose during drying the resulting filter cake, producing white $CaSO_4$ whiskers and less-crystallized, green, hard-formed mud **(Figure 4.4 (b))**. The green muddy solid product couldn't be effectively separated from the filter paper and weighed, as seen in **Figure 4.4 (a)**. To ascertain the crystallographic structure of thermal decomposition products, XRD analysis was conducted.
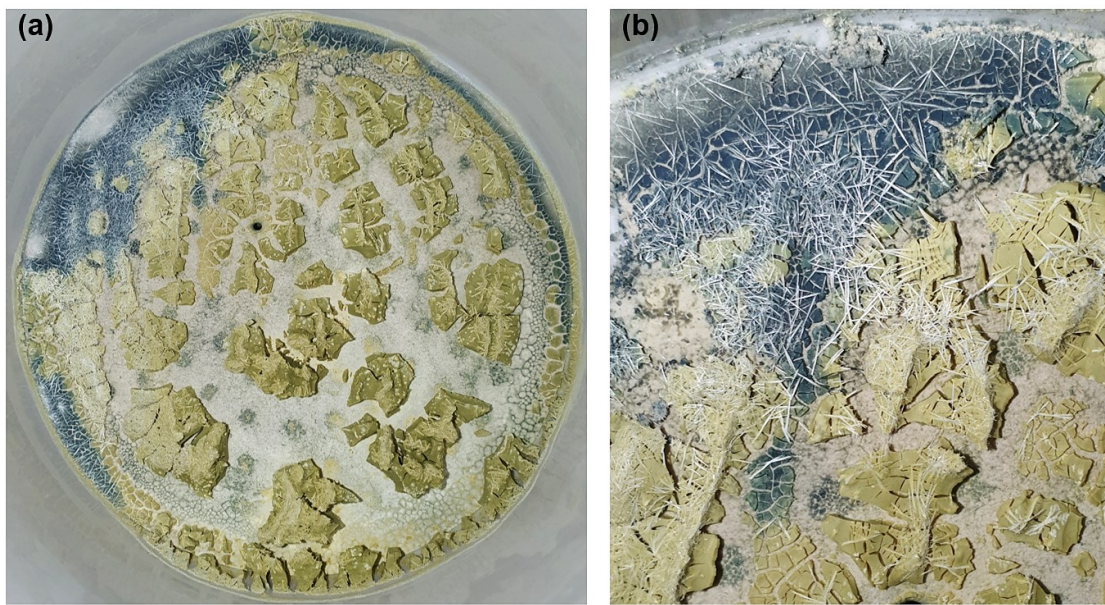
Figure 4. 4 The dried filter cake was obtained after the thermal decomposition of the 3rd cycle: (a) the dried filter cake, (b) white whiskers, and green mud on the filter cake.

The XRD patterns reveal that the diffraction peaks of cycle 1 and cycle 2 correspond to pure $WO_3 \cdot H_2O$, while no impurity phases are observed in the pattern, as shown in **Figure 4.5**. This implies that the thermal decomposition process could yield pure $WO_3 \cdot H_2O$ of the phase [11] when sufficient H_2SO_4 concentration was present. However, the diffraction peaks of the 3rd cycle notably differed from the initial 2 cycles and were identified as indexed to the hexagonal phases of tungsten oxide hydrate ($WO_3.0.33H_2O$). In the 3rd cycle, the appearance of the filter cake indicated inadequate crystallization, a conclusion supported by the XRD analysis results.
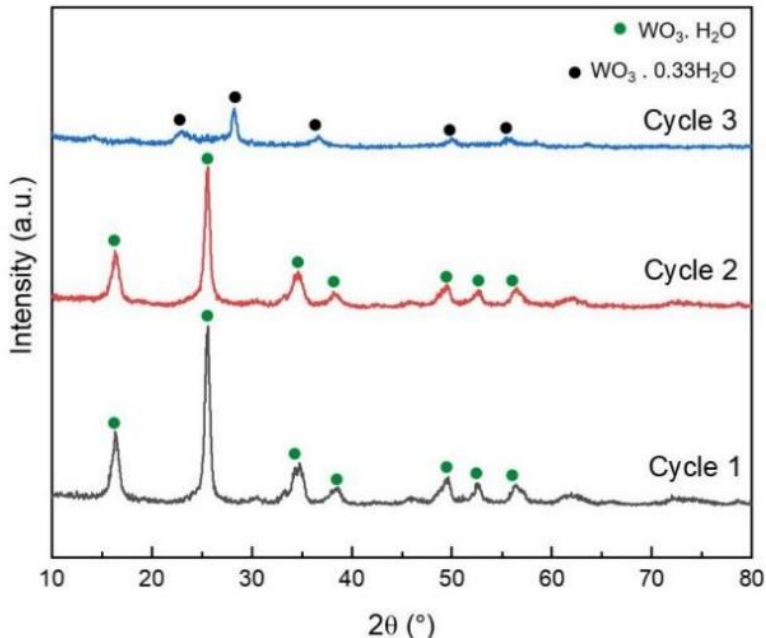
Figure 4. 5 XRD patterns of the resulting H_2WO_4 filter cakes after thermal decomposition were obtained by 3 cycles.

Table 4.1 exclusively summarizes the pH, volume, and weight of the recycled lixiviums of each cycle. The experiment commenced with a fresh leaching solution weighing 282.32 g and having a pH of -1.4. After the thermal decomposition and filtration, the 1st cycle yielded 223.06 g (202 mL) of transparent bright light-yellow recycled lixivium, as depicted in **Figure 4.6 (a)**. Similarly, the 2nd cycle produced 180.72 g (180 mL) of transparent bright dark-yellow recycled lixivium, shown in **Figure 4.6 (b)**. This decline in volume and weight during the 1st cycle, attributed to complete H_2O_2 consumption and a minor amount of H_2SO_4 (13.89% Ca content in the ore [13]), became notably pronounced in the 2nd cycle. This drastic decrease arises from the second H_2SO_4 depletion in the chemical reaction. Moreover, the pH of the recycled lixivium at the 1st cycle's conclusion increased to -0.45, and further to -0.42 in the 2nd cycle. This shift in pH is attributed to decreased H_2SO_4 concentration and increased water content due to H_2O_2 decomposition.
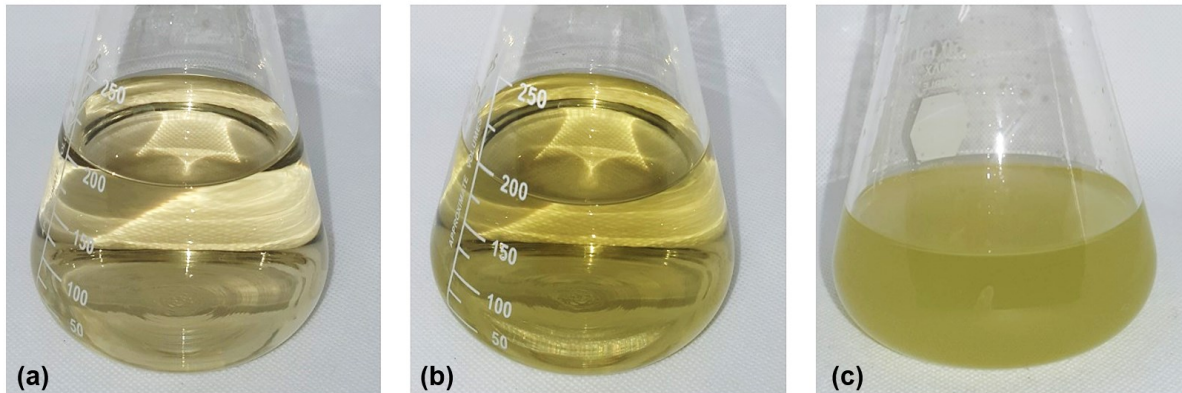
Figure 4. 6 Recycled lixivium after thermal decomposition:

(a) 1st cycle, (b) 2nd cycle, (c) 3rd cycle.

Conversely, the final cycle yielded a markedly turbid pale light-green recycled lixivium, as depicted in **Figure 4.6 (c)**. Due to nanoparticle clogging in the recycled lixivium, efficient volume and weight measurements were hindered. The final volume ended up being under 180 mL, with a weight of approximately 222.18 grams. Additionally, its pH value was measured at 0.08, marking the highest pH value recorded throughout the test. The pH elevation was caused by an increase in water level and a decrease in H_2SO_4 concentration. When the pH value was considered, the positive pH indicated H_2SO_4 fell below 1 mol/L, suggesting an insufficient surplus level for the reaction. Given the challenges, coupled with low leaching rates and yield, the decision was made to conclude the tests after the 3rd cycle.

Table 4. 1 Volume, weight, and pH values measurements during the lixivium recycle and reuse mechanism test.

1st cycle	Fresh leaching solution	V (1) (mL)	Weight (g)	pH (1)
		250	282.32	-1.4
	Recycled lixivium	V (1") (mL)	Weight (g)	pH (1")
		202	223.06	-0.45
2nd cycle	New leaching solution	V (2) (mL)	Weight (g)	pH (2)
		250	274.86	-1.02
	Recycled lixivium	V (2") (mL)	Weight (g)	pH (2")
		180	180.72	-0.42
3rd cycle	New leaching solution	V (3) (mL)	Weight (g)	pH (3)
		250	269.83	0.23
	Recycled lixivium	V (3") (mL)	Weight (g)	pH (3")
		<180	≈222.18	0.08

During the thermal decomposition experiments, a temperature of 90°C was maintained, a choice informed by the literature [13] as the optimal condition. This temperature was selected for its ability to accelerate particle generation and growth, facilitating the creation of yellow H_2WO_4 particles with the desired spherical shape and larger size. Contrary to the literature's suggestion that a 4-hour thermal decomposition could achieve a 99.3% W precipitation rate [13], the results of our mass balance show this duration was inadequate. As highlighted in **Chapter 3.1**, the achieved leaching efficiency, determined through ICP analysis, exceeded 97%. However, the conducted mass balance within this experiment pointed to a W crystallization efficiency of around 69%.

The preceding study [11] employed the same L/S ratio of 10 mL/g as referenced in [8], and it was found that 45 minutes of thermal decomposition at 95°C yielded 97% W crystallization. Additionally, in a different investigation [13] with an L/S ratio of 6 mg/L, it was reported that a 4-hour thermal decomposition at 90°C resulted in 99.3% W precipitation. While the specified optimal thermal decomposition duration holds for the experiment with an S/L ratio of 6 mg/L [13], the filtered lixivium was once again subjected to thermal decomposition to observe whether the yellow H_2WO_4 precipitation continued.

Notably, the continuous formation of yellow H_2WO_4 precipitates in the recycled lixivium **(Figure 4.7)** persisted even after an additional hour of thermal decomposition, implying an extended duration was needed. In response, the thermal decomposition time was extended to a total of 6 hours, resulting in more effective W crystallization. The 1st and 2nd cycles achieved 89.87% and 84.3% W crystallization, respectively. Thus, the thermal decomposition duration was optimized and set at 6 hours for synthetic ore leaching under conditions described in reference 1 [8]. This optimization emphasized the relationship between the L/S ratio and thermal decomposition duration.

Figure 4. 7 Yellow H_2WO_4 precipitates with extended thermal decomposition duration to 2 more hours.

In conclusion, the results reveal that through thermal decomposition, the recycling of the leaching solution allows for reusing the recycled lixivium in the 2nd cycle by simply supplementing the consumed H_2O2, without introducing additional H_2SO_4, under the specified operating conditions from reference 1 [8]. It's established that a maximum of 2 cycles can be effectively conducted using this process. This outcome is attributed to the critical role of H+ ions and initial H_2SO_4 concentration in the chemical reaction and crystallization processes [8].

During leaching, the leaching solution's acidity diminishes due to H_2SO_4 depletion. Concurrently, with H_2O_2 decomposition, water content increases, resulting in leaching solution dilution. Consequently, to create a fresh leaching solution after thermal decomposition under reference 1 [8] conditions, H_2O_2 supplementation alone isn't adequate; H_2SO_4 supplementation is also imperative to sustain the leaching process, including multiple cycles. As highlighted [13], combining both reagents allowed recycling and reuse for 5 cycles without any decrease in leaching efficiency.

Furthermore, the optimization of thermal decomposition duration involved an extension of the initially identified 4-hour optimum to a total of 6 hours. It was evident that as the solid content in the solution increased, a longer period was necessary for the precipitation of W in the form of H_2WO_4 through thermal decomposition. Consequently, in the context of synergistic leaching, adhering to the conditions of reference test 1 [8], the synthetic ore's optimized thermal decomposition time was established at 6 hours. This discovery underscores the significance of accounting for the L/S ratio's influence on thermal decomposition duration to achieve optimal outcomes in synthetic scheelite leaching.

The results of this test strongly support the notion that recycling and reusing lixivium significantly decreases reagent consumption and operational cost, aligning with the findings highlighted in Zhang et al.'s study [13]. Furthermore, these findings highlight the questioning and deep investigation of the reduction of H_2SO_4 concentration using the operating conditions of reference 1 [8] in synergistic leaching of $CaWO_4$ in H_2SO_4 and H_2O_2 solution. The optimization of H_2SO_4 concentration presents various advantages, encompassing reduced reagent consumption, lowered operating costs, and an enhanced environmentally conscious leaching process. An in-depth examination of optimization tests concerning reagent concentration, temperature, and leaching duration is provided in **Chapter 5**. As such, this comprehensive exploration offers valuable insights into the feasibility of optimizing synergistic leaching processes.

4.3 Summary

The lixivium recycle and reuse tests were conducted to gain insights into the thermal decomposition mechanism involved in leaching $CaWO_4$ using an H_2SO_4 and H_2O_2 solution. The experimental results yielded the following key conclusions:

- The significance of H_2SO_4 concentration on the crystallization characteristics of $CaSO_4$ and H_2WO_4 final products was underscored. Lower H_2SO_4 concentrations led to the formation of smaller, denser crystals with challenges in the filtration process. Leaching efficiency notably declined at reduced H_2SO_4 concentrations.

- Under the conditions outlined in reference 1 [8], it was established that lixivium could be recycled and reused twice without requiring H_2SO_4 supplementation. The first two cycles generated comparable final products and byproducts. Consequently, lixivium recycling not only reduces waste in operations but also curtails reagent consumption, and operating costs, and promotes an environmentally friendly approach.

- The investigation of the relationship between thermal decomposition time and L/S ratio revealed that higher solid ratios necessitate longer processing times. As a result, the initial 4-hour thermal decomposition time was optimized and extended to 6 hours for systems with higher solid ratios.

- The ability to reuse lixivium twice without supplemental H_2SO_4 suggests that H_2SO_4 concentration optimization can be accomplished within the framework of reference 1 [8] operating conditions. This optimization potential allows for reduced H_2SO_4 consumption, leading to a more environmentally sustainable leaching solution for synthetic scheelite leaching in an H_2SO_4-H_2O_2 mixed solution.

In conclusion, this study offers valuable insights into the recycling mechanism and significance of lixivium, contributing to a comprehensive understanding of the process. Additionally, it aims to enhance the efficiency and productivity of the thermal decomposition process.

CHAPTER 5 OPTIMIZATION STUDY ON SYNERGISTIC LEACHING METHOD

This chapter aims to build upon the results presented in **Chapter 4** by exploring the potential optimization of operational parameters within the synergistic leaching process for synthetic scheelite, utilizing a mixed acid solution of H_2SO_4 and H_2O_2. The study delves into the feasibility of reducing the H_2SO_4 concentration below the levels stipulated in reference 1 [8], intending to potentially cut down operating costs and foster a more sustainable leaching approach.

Moreover, as discussed in **Chapter 3.1**, the operational conditions of the reference 1 [8] test are open to optimization. Existing studies [8], [11], [13] conducted under this novel W leaching method have predominantly focused on understanding the kinetics of synergistic leaching and identifying optimal operational conditions. However, these studies have often blurred the line between conditions applied to natural and synthetic ores. Thus, a comprehensive examination of the optimization potential for synthetic scheelite leaching and an investigation of its operational conditions are necessary.

The present chapter addresses this gap by assessing the optimization's impact and identifying optimal operational conditions for synthetic scheelite leaching. This assessment is divided into three key sections: reagent concentration optimization, temperature optimization, and leaching duration optimization. Notably, no adjustments were made to the stirring rate and L/S ratio during this optimization study. The decision to omit stirring rate optimization is grounded in the understanding that its influence on final leaching efficiency is minimal [101]. Furthermore, the L/S ratio is already set at its maximum, as indicated in previous studies [8], [11]. In addition, the final leaching efficiencies obtained from the optimization tests were compared to the 95.98% leaching efficiency obtained from the conducted validation test of reference 1 [8]. Therefore, the optimization focus was directed towards more impactful parameters to achieve the desired results.

5.1 Concentration Optimization

In **Chapter 3**, the impracticality of decreasing H_2O_2 concentration through a suggested 2-step method was highlighted. On the other hand, **Chapter 4** demonstrated the potential of executing synergistic leaching with H_2SO_4 concentrations lower than the specified levels in reference 1 [8], even though the optimal concentration was set at 3 mol/L. Notably, reagent concentration significantly influences reaction rates in solid-liquid heterogeneous systems [11].

Building on these insights, this chapter aims to assess the viability of employing less concentrated H_2SO_4 and H_2O_2 within the synergistic leaching system and to ascertain its impact on leaching efficiency. Furthermore, this experiment aims to propose an eco-friendlier and more cost-efficient leaching process that upholds high-efficiency levels while decreasing reagent consumption.

5.1.1 Experimental

The experimental procedure involved conducting complete leaching cycles excluding thermal decomposition, using the operating conditions specified in reference 1 [8] as discussed in **Chapter 3.1**. For the reagent concentration optimization tests, experiments were conducted using 250 mL scale leaching setups within sealed Pyrex® reaction flasks. These flasks were heated under precise temperature control provided by a water bath, with magnetic stirring for agitation. In each experiment, a blend of H_2SO_4–H_2O_2 mixed-acid solution was introduced into the reaction vessel and elevated to the desired temperature, maintaining accuracy within ± 0.5 °C. Once the desired conditions were attained, the reaction was initiated by adding a specific amount of synthetic scheelite (L/S: 10 mL/g), and the timing commenced. After the completion of the leaching process, the resulting slurry was allowed to cool within the vessel. Subsequently, filtration was conducted using Whatman grade 5 filter paper to remove by-product $CaSO_4$ from the PTA, followed by thorough washing with DI water. The collected residue from the filtration process was then subjected to drying in an oven set at 70 °C for 24 hours. Post-drying, the weight of the residue was determined using an electronic balance. The W content in the pregnant solution was determined through ICP analysis, and the final leaching efficiency was calculated by adding the W content in the wash waters, considering the outcomes from **Chapter 3.1**.

Table 5.1 outlines 6 distinct sets of experimental conditions incorporating optimized H_2SO_4 and H_2O_2 concentrations. Throughout these experiments, the focus was on systematically decreasing the H_2SO_4 reagent concentration as per the prescribed operational parameters elucidated in reference 1 [8]. Notably, only the H_2SO_4 concentration was modified, while keeping other parameters—such as H_2O_2 concentration, L/S ratio, temperature, leaching duration, and stirring rate—unchanged by reference 1 [8].

Table 5. 1 H_2SO_4 and H_2O_2 concentration optimization tests conditions.

Conditions	Test 1	Test 2	Test 3	Test 4	Test 5	Test 6
H_2SO_4 (mol/L)	2	1	2	1	0.5	1
H_2O_2 (mol/L)	1.5	1.5	1	1	1	0.5
L/S ratio (mL/g)	10	10	10	10	10	10
Temperature (°C)	45	45	45	45	45	45
Leaching duration (min)	90	90	90	90	90	90
Stirring rate (r/min)	400	400	400	400	400	400

To elaborate, the initial experiment, labeled as Test 1, involved a reduction in the H_2SO_4 concentration from 3 mol/L to 2 mol/L. Subsequently, Test 2 was executed by employing the minimal amount of H_2SO_4 established in the literature to achieve high leaching efficiency [8]. In the subsequent phase of the experiment, Test 3 and Test 4 were executed, utilizing a reduced H_2O_2 concentration of 1 mol/L instead of the previously used 1.5 mol/L [8]. The intention behind these tests was to evaluate the leaching efficiency of Test 1 and Test 2 under conditions of lower H_2O_2 concentration. Importantly, the H_2SO_4 concentrations from Test 1 and Test 2 were retained, and no adjustments were made to the L/S ratio, temperature, leaching duration, or stirring rate. Lastly, during the final stage of the experiment, Test 5 and Test 6 were conducted by combining H_2SO_4 and H_2O_2 concentrations of 1 mol/L and 0.5 mol/L respectively. This allowed for an evaluation of the effects stemming from the minimum concentrations outlined in the literature on the leaching system [8], [13].

5.1.2 Results and Discussion

Based on visual observation, the leaching process of Test 1, 2, 3, 4, and 6 produced similar transparent light-yellow colored PTAs as shown in **Figure 5.1 (a), (b), (c), (d) and (f)**, except Test 5. As depicted in **Figure 5.1 (e)**, Test 5 resulted in a PTA with a green and turbid appearance, indicating a deficiency in the H_2SO_4 concentration within the leaching solution. Despite the turbidity, the filtration process proceeded without any clogging due to the presence of less crystallized fine particles, a phenomenon explained in **Chapter 4**. This finding supports the notion that diminishing the H_2SO_4 concentration leads to a decrease in available H_2SO_4 for the reaction involving $CaWO_4$. Consequently, it was observed that the leaching efficiency was adversely

affected at lower H_2SO_4 concentrations [8]. These visual observations were further corroborated by the results of ICP analysis.

Figure 5. 1 PTAs after leaching obtained from reagent optimization tests: (a) Test 1, (b) Test 2, (c) Test 3, (d) Test 4, (e) Test 5, (f) Test 6.

In each test, the visual observation revealed consistent appearances of white $CaSO_4$ filter cakes, as depicted in **Figure 5.2 (a), (b), (c), (d), (e), and (f)**, with no indications of yellow H_2WO_4 precipitates. However, Test 5 stood out as an exception, where although not detected in the $CaSO_4$ filter cake, yellow H_2WO_4 precipitates were found at the bottom of the flask after the cooling process, as displayed in **Figure 5.3**. The presence of yellow H_2WO_4 precipitates in the slurry, aligning with the color and turbidity of the PTA, offers further support to the conclusion that the leaching solution lacked sufficient H_2SO_4 concentration to effectively drive the leaching reaction.

In contrast, the absence of yellow H_2WO_4 precipitates in the slurry of Test 6 underscores the pivotal role of maintaining an adequate level of H_2SO_4 concentration in achieving successful synergistic leaching.

Furthermore, the decrease in acid concentration within the aqueous medium resulted in the formation of distinct fine particle-sized structures in the $CaSO_4$ product. Notably, the products obtained from Test 5 and Test 6 exhibited finer grain sizes and a more viscous consistency compared to the typical results. This observed phenomenon can be attributed to the impaired crystallization process, leading to the development of relatively small, disorganized, and densely packed particles. This behavior aligns with the discussion presented in **Chapter 4**, where the effects of decreasing acidity in the leaching solution were elucidated [8]. This phenomenon underscores the sensitivity of the leaching process to changes in acid concentration and underscores the critical importance of maintaining appropriate acidity levels to achieve optimal outcomes.

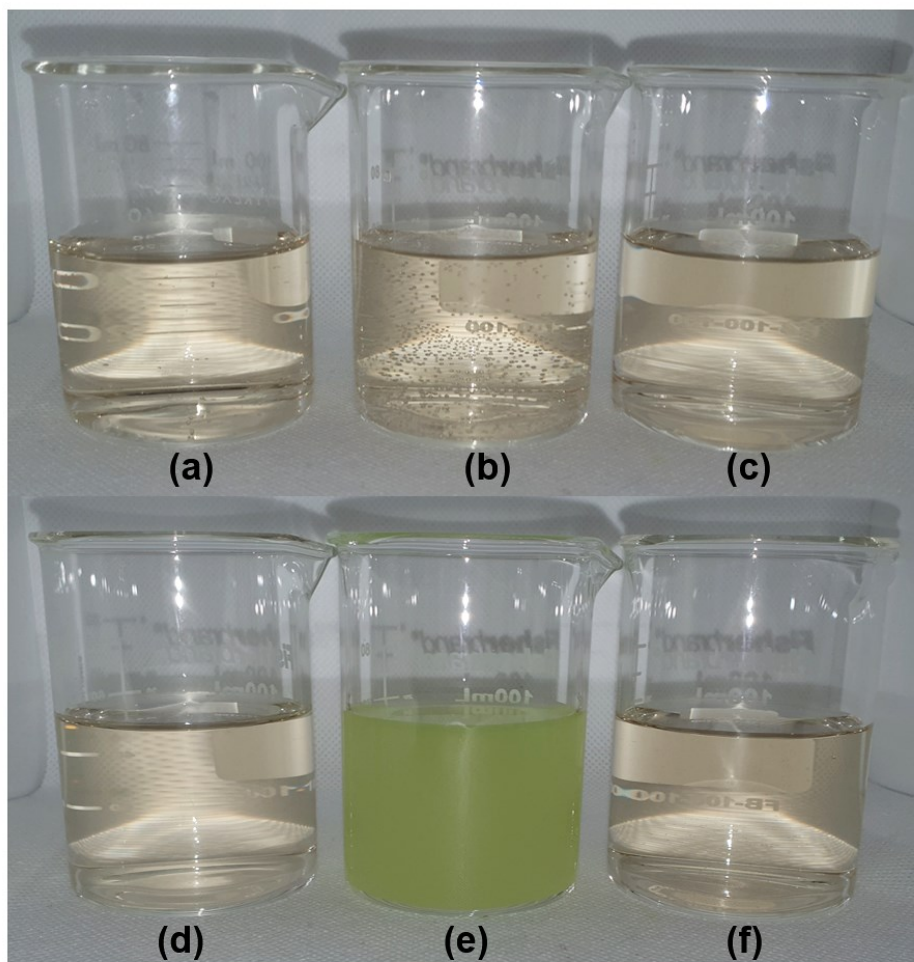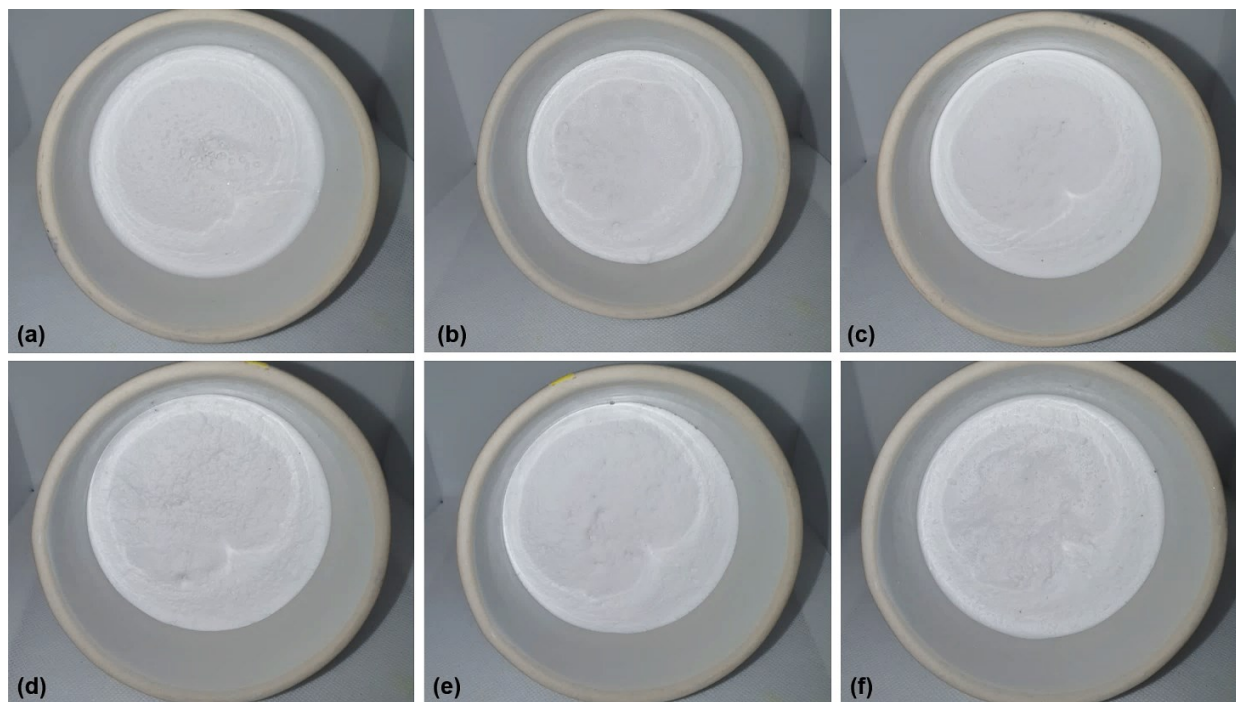**Figure 5. 2** $CaSO_4$ filter cakes after leaching obtained from reagent optimization tests: (a) Test 1, (b) Test 2, (c) Test 3, (d) Test 4, (e) Test 5, (f) Test 6.
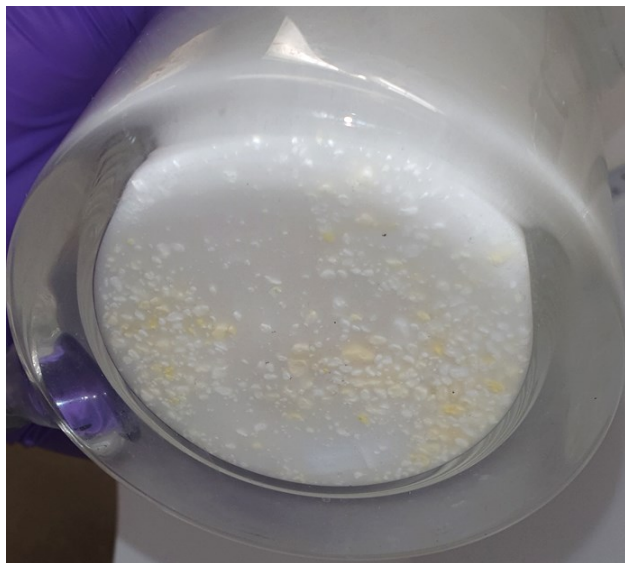
Figure 5. 3 Yellow H_2WO_4 precipitation at the bottom of the slurry after the cooling down process in Test 5.

Figure 5.4 serves as a comprehensive summary of the final leaching efficiency obtained from the reagent concentration optimization tests. The ICP analysis results for Test 1 showed a leaching efficiency of 90.43%, which closely approximated the expected performance compared to reference 1 [8], with a leaching efficiency of 95.98%. Notably, the leaching efficiency did not exhibit a significant decrease as initially reported [8], a phenomenon that aligns with the findings discussed in **Chapter 4**.

Similarly, Test 2 exhibited a leaching efficiency of 89.32%, a value notably higher than expected, despite reducing the H_2SO_4 concentration to only one-third of the amount specified in reference 1 [8]. The consistency in results between these two tests and their closeness to the reference 1 [8] values could be attributed to the utilization of synthetic ore instead of natural ore. This underscores the pivotal role of ore composition in influencing leaching behavior and underscores the necessity for customized optimization strategies.

Building on the promising outcomes of Test 1 and Test 2, the experimentation continued by conducting Test 3 and Test 4, which involved a reduction in the H_2O_2 concentration from 1.5 mol/L to 1 mol/L. Surprisingly, both tests remarkably exhibited closely matched leaching efficiencies of 89.84% and 89.67%, respectively. Notably, even though Test 4 utilized a lower H_2SO_4 concentration of 1 mol/L, the leaching efficiency remained nearly identical to that of Test 3. This

compelling consistency in leaching efficiencies suggests the presence of a surplus amount of H_2SO_4 in the solution, which seems sufficient for the effective conversion of $CaWO_4$ [101].

Moreover, the striking similarity in the results of Test 3, Test 4, and Test 2 further underscores the significance of having an appropriate initial concentration of H_2O_2 in facilitating the leaching reaction effectively. The literature has indicated that an increase in the number of active molecules in the solution (-O-O-) and the enhancement of the frequency of effective intermolecular collisions per unit of time contribute to the formation of PTA, ultimately leading to improved leaching efficiency of W per unit time. According to the reported findings, the leaching efficiency was enhanced from 99.5% to 99.9% as the initial concentration of H_2O_2 was elevated from 0.8 mol/L to 1.2 mol/L [8]. To summarize, the extraction efficiency of W is favorably influenced by an elevation in the H_2O_2 concentration [11].

Encouraged by the promising results from the initial 4 tests, Test 5 was performed with the lowest H_2SO_4 concentration (0.5 mol/L) reported [8], and 1 mol/L H_2O_2. As anticipated, the visual observations concurred with the findings, resulting in a low efficiency of 54.62%. It is noteworthy that reference 1 [8] reports a final leaching efficiency of 41.1% when using a combination of 0.5 mol/L H_2SO_4 and 2.5 mol/L H_2O_2 in synergistic leaching conducted on natural ore. Despite utilizing the maximum concentration of H_2O_2 (2.5 mol/L) [11] as reported, the achieved leaching efficiency is considerably low. Additionally, the same study highlights that the leaching efficiency surpasses 90% when employing H_2SO_4 concentrations of 1 mol/L or higher, coupled with 2.5 mol/L H_2O_2. In essence, the results of Test 5 mirror the documented findings, highlighting the pivotal role of the initial concentration of H_2SO_4 in synergistic leaching. This underscores the notion that H_2SO_4 concentration should be maintained above 1 mol/L within this leaching system to achieve effective results. This finding corroborates **Chapter 4** results, emphasizing the importance of maintaining a surplus H_2SO_4 concentration.

Concluding the series of tests, Test 6 was executed to examine the outcomes of combining the minimum recommended quantities of H_2SO_4 (1 mol/L) and H_2O_2 (0.5 mol/L) [13]. Surprisingly, this combination yielded a leaching efficiency of 89.2%, despite using the specified minimal reagent concentrations. Notably, reference 1 [8] documents that when conducting synergistic leaching on natural ore using 0.5 mol/L H_2O_2 in conjunction with 3 mol/L H_2SO_4, the final leaching efficiency reaches 95.9%. Intriguingly, Test 6 achieved a high efficiency comparable to the other test results, except for Test 5, despite employing an H_2SO_4 concentration that is one-third of the reported

value. This outcome contrasts initial expectations and highlights the complex interplay of factors within the leaching process.
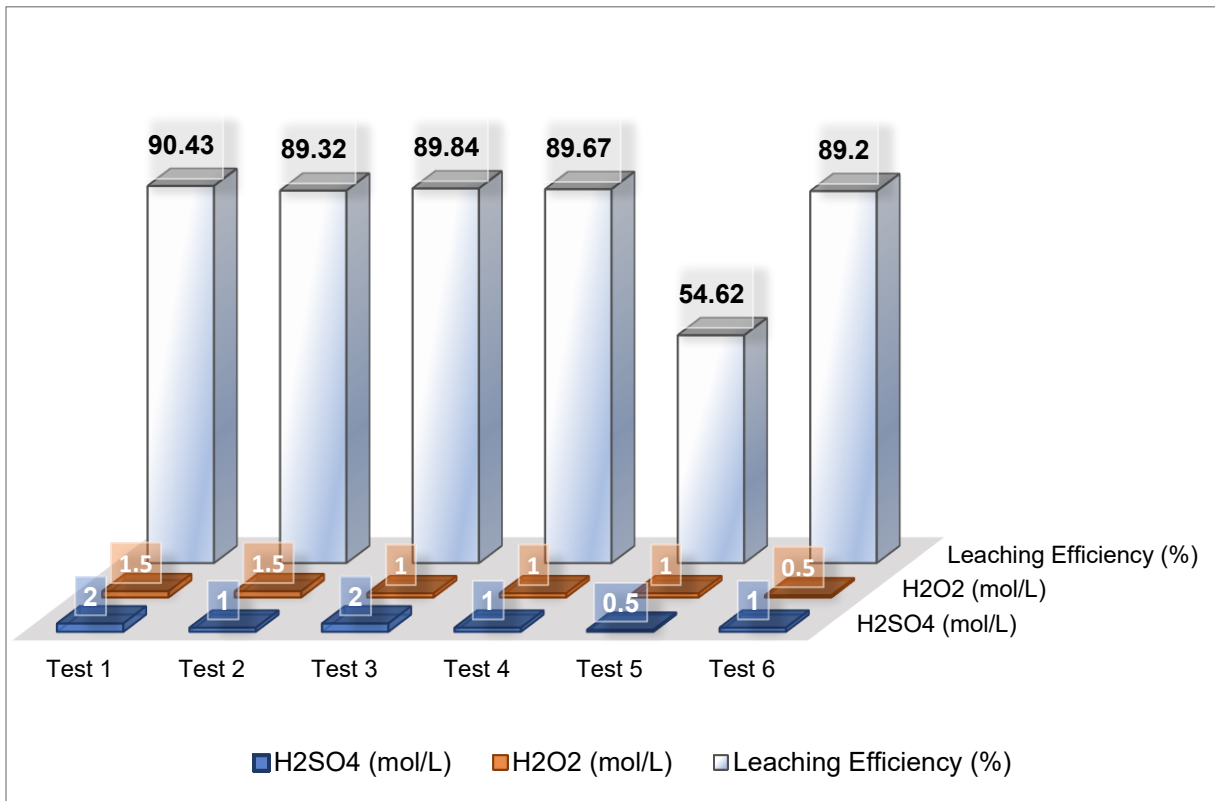
Figure 5. 4 Final leaching efficiency of reagent optimization tests based on ICP characterization.

To summarize, the reagent optimization tests yielded several key findings. The consistent leaching results in tests 1, 2, 3, 4, and 6 were primarily attributed to the use of synthetic ore, maintaining other parameters unchanged. The exploration of various combinations of reagent concentrations, specifically targeting the optimal concentrations outlined in this study (3 mol/L H_2SO_4 and 1.5 mol/L H_2O_2) [8], showcased a minor decline in the final leaching efficiency. This reduction proved to be much less significant than anticipated, particularly in contrast to the leaching efficiency reported in reference 1 [8], which utilized natural ore.

Furthermore, Test 5 emphasized the critical significance of maintaining H_2SO_4 concentration above 1 mol/L to ensure effective leaching. Additionally, the results of Test 6 highlighted the importance of initiating the leaching process with adequately balanced reagent concentrations to

attain satisfactory reaction outcomes. Based on the comprehensive findings, it can be concluded that reagent concentrations can be optimized through further parameter testing, without compromising the attainment of desirable leaching efficiency. This insight holds the potential to pave the way for a more efficient and sustainable leaching process.

The insights gained from these findings carry significant implications for enhancing the optimization of the synergistic leaching process for synthetic scheelite. These results not only suggest the potential advantages of reducing reagent consumption to achieve cost-effectiveness and environmental sustainability but also provide a comparative perspective on the applicability of operating conditions established for natural ore to the synthetic ore scenario. In essence, this research offers a pathway for process enhancement and optimization, with the potential to boost overall efficiency. Nonetheless, to achieve a more comprehensive understanding, further exploration is necessary to uncover the effects of optimizing other parameters on leaching efficiency. Building upon this foundation, **Chapter 5.2** takes a deeper dive into the analysis of temperature optimization and its implications for enhancing the leaching efficiency of synthetic scheelite. Through this detailed investigation, a more comprehensive perspective on the process and its optimization potential can be attained.

5.2 Temperature Optimization

As highlighted in **Chapter 3.1**, the higher leaching efficiency of reference test 2 [11] was attributed to its elevated temperature and longer duration compared to reference test 1 [8]. Furthermore, the potential for optimizing reference test 1 [8] parameters in comparison to reference test 2 [11] was underlined. **Chapter 5.1** demonstrated the possibility of optimizing reagent consumption in the leaching process. Expanding on the preceding chapters, this chapter aims to explore the feasibility of employing higher temperatures within the reagent-optimized synergistic leaching system established in **Chapter 5.1**. Through systematic experimentation and analysis, this research aims to comprehensively understand how temperature optimization can further amplify leaching efficiency for synthetic scheelite, contributing to a more efficient process.

5.2.1 Experimental

The experimental procedure involved conducting complete leaching cycles excluding thermal decomposition using the operating conditions specified in reference 1 [8], as discussed in **Chapter 3.1**. For the temperature optimization tests, 250 mL scale leaching experiments were

executed within a sealed Pyrex® reaction vessel. The vessel was thermostatically heated through a water bath and kept in continuous agitation using a magnetic stirrer. In each trial, a mixed-acid solution of H_2SO_4–H_2O_2 was introduced into the vessel and gradually heated to the target temperature, maintaining accuracy within ± 0.5 °C. Following temperature stabilization, the leaching process was initiated by adding a specified quantity (L/S: 10 mL/g) of synthetic scheelite, and timing commenced. Once the leaching period was complete, the resulting slurry was allowed to cool to ambient temperature. Subsequently, the slurry was subjected to filtration using Whatman grade 5 filter paper to extract the $CaSO_4$ by-product from the pregnant solution. A thorough rinse with DI water was performed on the filter cake. The residue obtained from this process was then dried in an oven set at 70 °C for 24 hours and weighed using an electronic balance. The tungsten (W) content in the pregnant solution was quantified via ICP analysis. The final leaching efficiency was determined by incorporating the amount of W present in the wash waters, based on the findings from **Chapter 3.1**.

For the temperature optimization experiments, the leaching temperature was raised from the reference value of 45°C [8] to 60°C [11]. It is worth noting that 60°C represents the upper limit for effective H_2O_2 leaching without undergoing thermal decomposition, as established by previous research [11]. The specifics of the experimental conditions are summarized in **Table 5.2**. In this investigation, two test conditions were chosen for further exploration based on the outcomes of the reagent optimization study discussed in **Chapter 5.1**: Test 1 and Test 2.

The selection of Test 1 was motivated by its notable performance in the reagent optimization study, while Test 2 was singled out for employing the highest H_2O_2 concentration of 1.5 mol/L. As previously highlighted, the initial H_2O_2 concentration significantly influences the leaching process, impacting both leaching efficiency and the crystal structure of $CaSO_4$ [11]. Furthermore, in temperature optimization experiments, a higher H_2O_2 concentration provides better reliability and performance at elevated temperatures, considering the thermal decomposition behavior of H_2O_2. Ensuring an H_2O_2 concentration of 1.5 mol/L in these tests is essential for maintaining thermal stability at higher temperatures, as lower concentrations might be more susceptible to decomposition**.**

Table 5. 2 Temperature optimization test conditions.

Conditions	Test 7	Test 8
H_2SO_4 (mol/L)	2	1
H_2O_2 (mol/L)	1.5	1.5
L/S ratio (mL/g)	10	10
Temperature (°C)	60	60
Leaching duration (min)	90	90
Stirring rate (r/min)	400	400

5.2.2 Results and Discussion

Based on visual observation, there were no notable alterations observed in the resulting PTAs and $CaSO_4$ filter cakes when the temperature was elevated from 45°C to 60°C in Test 7 and Test 8. Both tests yielded transparent, light-yellow colored PTAs that closely resembled each other, as illustrated in **Figure 5.2 (a)** and **(b)**. Similarly, visual observations of the leaching process indicated that consistent white $CaSO_4$ filter cakes were produced in each test, maintaining their characteristic appearance, as depicted in **Figure 5.5 (a) and (b)**. Furthermore, no presence of yellow H_2WO_4 precipitates was detected in any of the tests.

(a) **(b)**
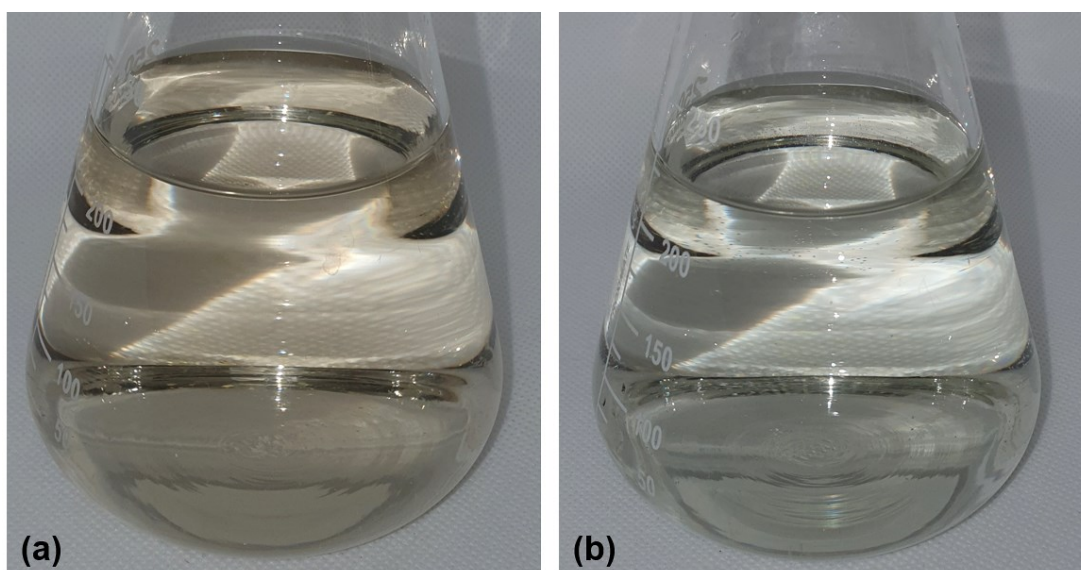
Figure 5. 5 PTAs after leaching obtained from temperature optimization tests: (a)Test 7, (b) Test 8.
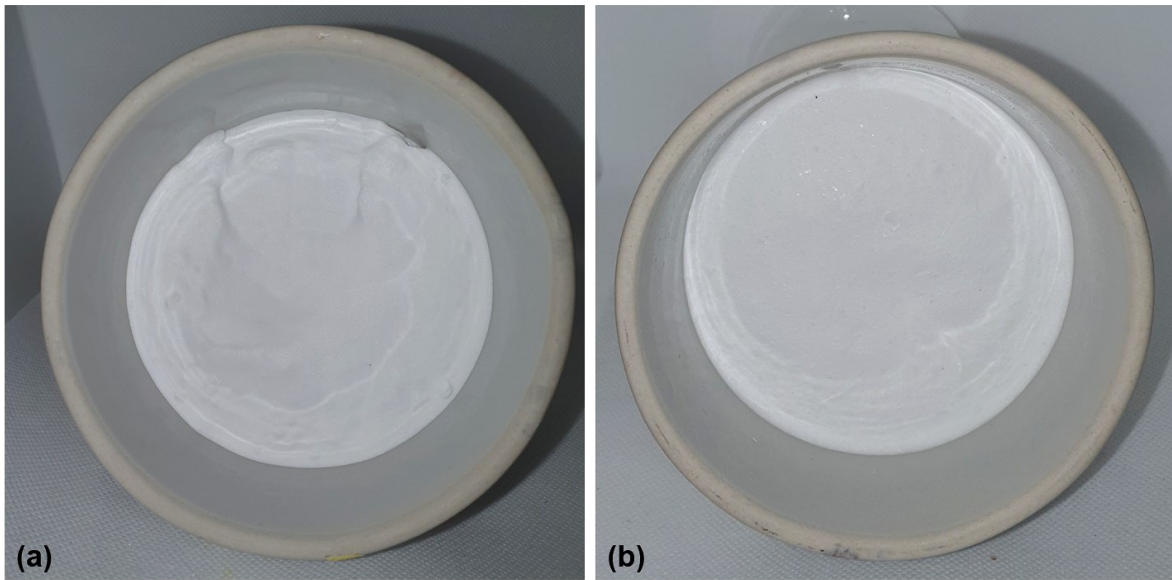
Figure 5. 6 CaSO$_4$ filter cakes after leaching obtained from leaching duration optimization tests: (a) Test 9, (b) Test 10.

Figure 5.7 offers as a comprehensive summary of the final leaching efficiency derived from the temperature optimization tests. Based on the ICP analysis results, both Test 7 and Test 8 exhibited higher leaching efficiencies compared to those observed in the previous chapter. In **Chapter 5.1**, the recorded leaching efficiencies for Test 1 and Test 2 were 90.43% and 89.32%, respectively. It is established that an increase in temperature enhances the leaching rate [11]. Consequently, Test 7 and Test 8 yielded leaching efficiencies of 92.23% and 91.68%, respectively. Remarkably, the consistency in these results and their proximity to the reference 1 [8] values can be attributed to the utilization of synthetic ore instead of natural ore, considering that no parameter apart from the leaching temperature was modified.

.
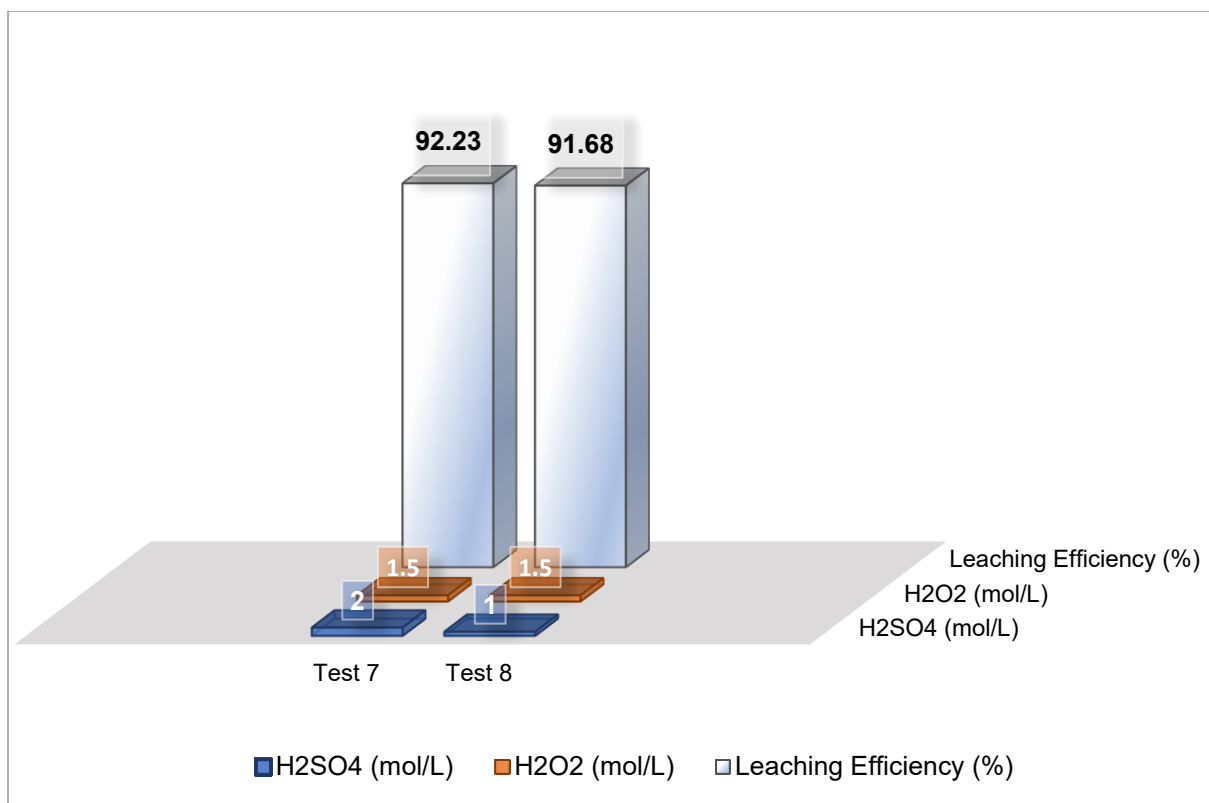
Figure 5. 7 Final leaching efficiency of temperature optimization tests based on ICP analysis.

In conclusion, optimizing the temperature within the reagent-optimized leaching system has yielded positive results by enhancing the leaching rate, leading to an overall increase in final efficiency. This increased efficiency, and similarity in final efficiencies for both tests are not only attributed to the utilization of synthetic ore but are also significantly influenced by the adept utilization of reagents at the appropriate surplus initial concentrations. The comprehensive findings emphasize that temperature optimization, when combined with the optimization of other parameters, can be successfully pursued to enhance leaching efficiency without compromising effectiveness.

The findings of this study significantly contribute to enhancing our understanding of optimizing the leaching process for synthetic scheelite. Additionally, this research offers a comparative insight into the temperature conditions specified in the literature for natural ore and their impact on leaching efficiency when applied to synthetic ore. In summary, this investigation holds promise for identifying avenues to improve the leaching process and enhance efficiency. However, to attain a more comprehensive understanding, further research is warranted to explore the effects of leaching duration on leaching efficiency. Building on this knowledge, **Chapter 5.3** delves

deeper into the investigation of duration optimization's impact on the leaching efficiency of synthetic scheelite, providing a comprehensive analysis of the process.

5.3 Leaching Duration Optimization

Chapter 3.1 clarified that the superior leaching efficiency of reference test 2 [11] resulted from its higher temperature and prolonged duration, distinguishing it from reference test 1 [8]. Additionally, the potential for optimizing operational parameters of reference 1 [8] in comparison to reference test 2 [11] was emphasized. **Chapter 5.1** verified the possibility of optimizing reagent consumption within the leaching process, while **Chapter 5.2** demonstrated the positive impact of raising the temperature to 60°C on the reaction. Building on these earlier chapters, this chapter aims to examine leaching duration in the synergistic leaching system and explore its effect on efficiency. By conducting systematic experiments, this research seeks to provide a comprehensive understanding of how optimizing leaching duration can further enhance the efficiency of the reagent and temperature-optimized process for leaching synthetic scheelite.

5.3.1 Experimental

The experimental procedure involved complete leaching cycles without thermal decomposition, following the specified operating conditions from reference 1 [8], as discussed in **Chapter 3.1**. Leaching duration tests were conducted in 250 mL scale experiments using a sealed Pyrex® reaction cell. The reaction flask was heated accurately using a water bath and stirred constantly with a magnetic stirrer. Each experiment began with introducing a mixed-acid solution of H_2SO_4–H_2O_2 into the flask, heated to the desired temperature with ± 0.5 °C accuracy. The leaching process commenced by adding a specific amount of synthetic scheelite (L/S: 10 mL/g) and initiating the timer. After completing the leaching process, the resulting slurry cooled to room temperature, followed by filtration using Whatman grade 5 filter paper to separate the $CaSO_4$ by-product from PTA. Thorough washing with DI water was performed, and the washed residue underwent drying in a 70 °C oven for 24 hours, weighed using an electronic balance. The W content in the pregnant solution was analyzed through ICP, and the final leaching efficiency was calculated by adding the W content in the wash waters, as per **Chapter 3.1** results**.**

Table 5.3 presents the experimental parameters utilized for optimizing leaching durations. In the context of this investigation, two specific test conditions, Test 7 and Test 8, were singled out for

detailed exploration, guided by the findings from **Chapter 5.2**. Initially, Test 9 was carried out with a reduced leaching duration of 60 minutes, deviating from the prescribed 90 minutes [8]. This adjustment aimed to assess the leaching efficiency of Test 7 within a shorter reaction period. Subsequently, Test 10 was conducted with an extended leaching time of 120 minutes, in contrast to the original 90 minutes, to assess the leaching efficiency of Test 8 with a prolonged duration. While solely focusing on optimizing the leaching duration, other parameters (H_2O_2 concentration, L/S ratio, temperature, and stirring rate) remained consistent with reference 1 [8].

Table 5. 3 Leaching duration optimization tests conditions.

Conditions	Test 9	Test 10
H_2SO_4 (mol/L)	2	1
H_2O_2 (mol/L)	1.5	1.5
L/S ratio (mL/g)	10	10
Temperature (°C)	60	60
Leaching duration (min)	60	120
Stirring rate (r/min)	400	400

5.3.2 Results and Discussion

Visual observation revealed that both Test 9 and Test 10 produced similar transparent, light-yellow colored PTAs, as depicted in **Figure 5.8 (a) and (b)**. Nonetheless, a subtle difference was noted, with the PTA from Test 9 appearing slightly darker in yellow appearance compared to Test 10. In contrast, the appearance of the white $CaSO_4$ filter cakes displayed variability, as illustrated in **Figure 5.9 (a) and (b)**. In Test 9, a noticeable accumulation of yellow H_2WO_4 precipitate was observed on the $CaSO_4$ filter cake. This indicates that the 60-minute leaching duration was insufficient to achieve thorough leaching under the designated operational conditions. Conversely, Test 10 yielded a white $CaSO_4$ filter cake devoid of yellow H_2WO_4 precipitates. This outcome highlights that the extended leaching duration in Test 10 successfully facilitated a more comprehensive leaching reaction compared to Test 9.
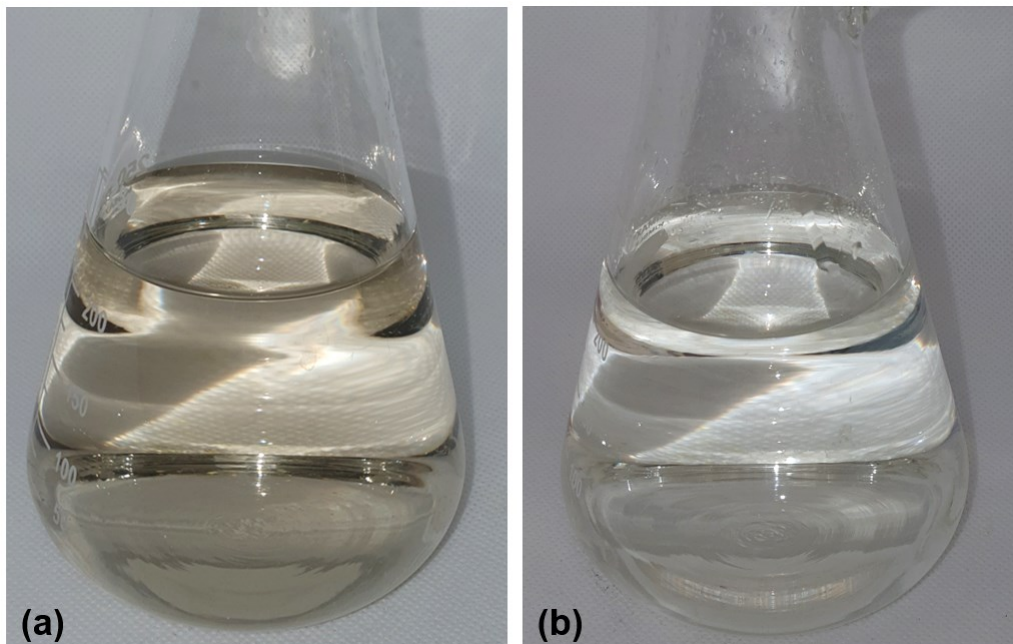
Figure 5. 8 PTAs after leaching obtained from leaching duration optimization tests: (a) Test 9, (b) Test 10.
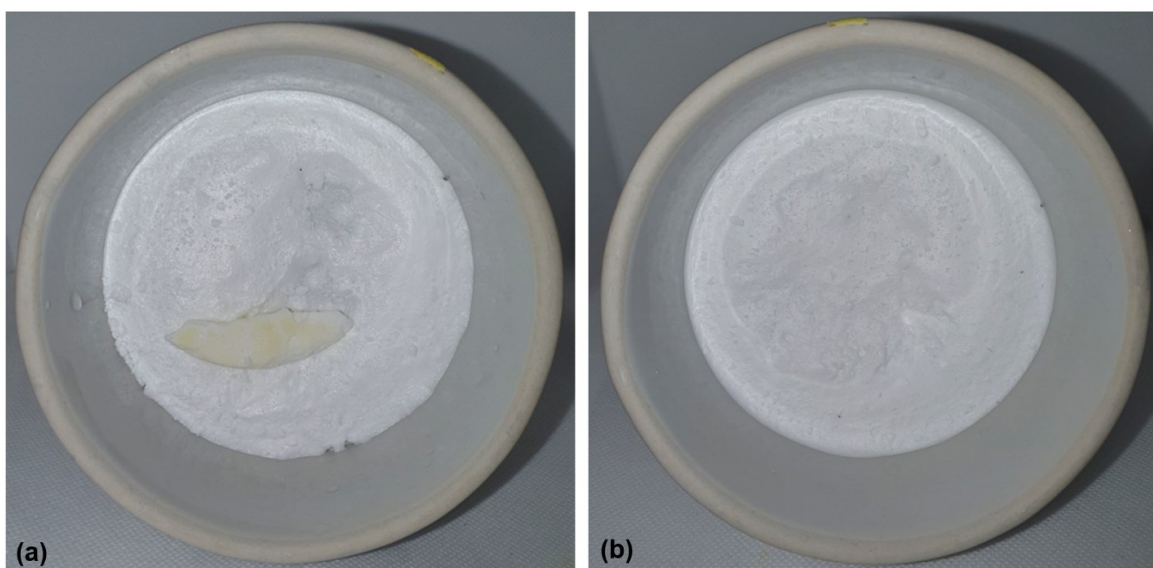
Figure 5. 9 CaSO$_4$ filter cakes after leaching obtained from leaching duration optimization tests: (a) Test 9, (b) Test 10.

Figure 5.10 provides a comprehensive overview of the final leaching efficiency outcomes from the leaching duration optimization tests. Test 9, conducted with a shortened leaching duration compared to Test 7 (which demonstrated superior reagent optimization performance in **Chapter**

5.1), exhibited a decreased efficiency of 72.8% from the original 92.23%. Visual observations and ICP results collectively indicate that a leaching time of 60 minutes fails to deliver effective leaching performance under the given operational conditions. This underscores the significance of adhering to literature recommendations [8], which assert that a leaching duration surpassing 90 minutes is crucial, irrespective of ore type, to ensure complete reactions and attain high yields.

On the other hand, Test 10 yielded an enhanced efficiency of 95.91%. Notably, under identical reagent conditions and temperature, the counterpart test performed in **Chapter 5.2** yielded an efficiency of 91.68%. The contrast between the outcomes of Test 8 and Test 10 emphasizes the necessity for a leaching duration exceeding 90 minutes at these optimized operational parameters to accomplish a thorough reaction with high efficiency.
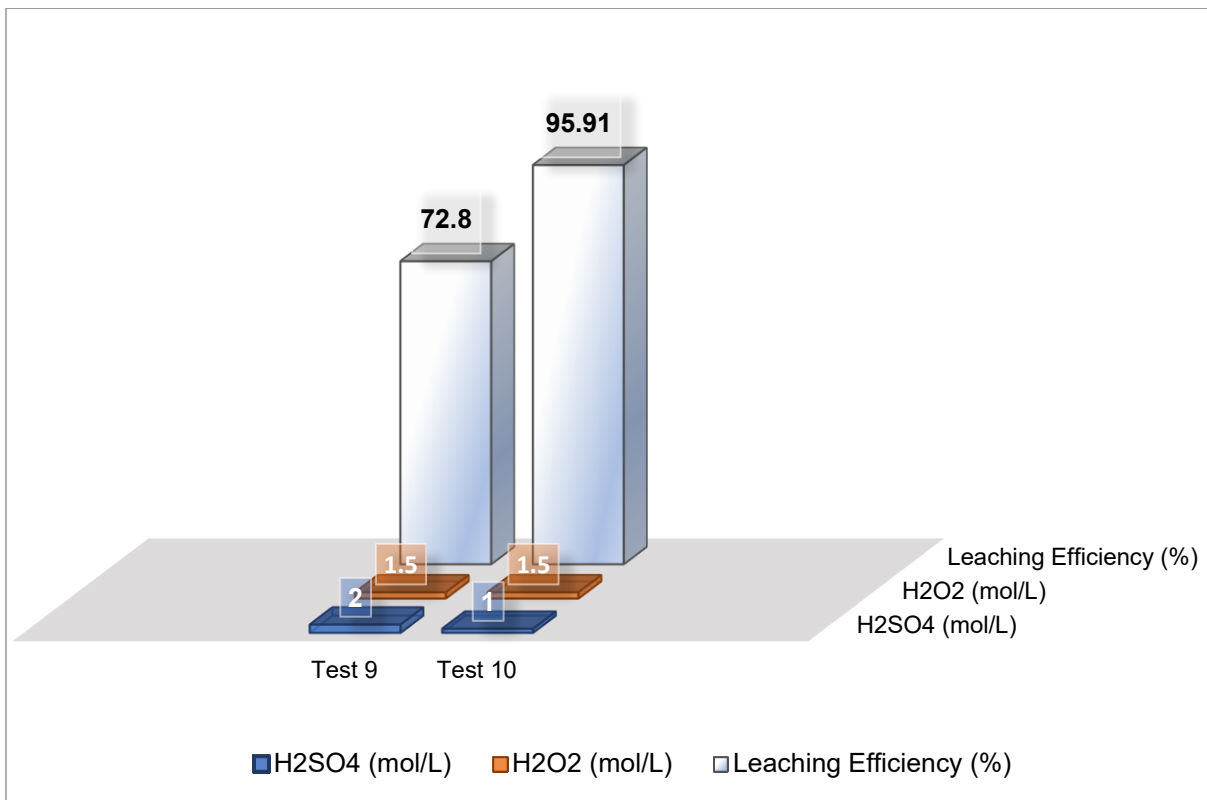
Figure 5. 10 Final leaching efficiency of leaching duration optimization tests based on ICP analysis.

In conclusion, the optimization of the reagent- and temperature-optimized leaching system in terms of leaching duration has yielded a positive impact on the leaching rate, leading to increased final efficiency. The elevated leaching efficiency observed in Test 10 is not solely attributed to the

use of synthetic ore but is also significantly influenced by the skilled management of reagents at suitable initial concentrations. The leaching efficiency of 95.91% obtained in **Chapter 5.3** is very close to the 95.98% leaching efficiency obtained from the reference 1 [8] test conducted within the scope of the validation tests. The comprehensive findings emphasize that through systematic parameter optimization, leaching duration can be fine-tuned without compromising satisfactory leaching efficiency.

These study findings contribute significantly to the advancement of our understanding of optimizing the leaching process for synthetic scheelite. Moreover, this research provides a comparative perspective on the leaching durations recommended in the literature for natural ore and their relevance to enhancing leaching efficiency in the context of synthetic ore. To summarize, this inquiry holds the potential to uncover strategies for process improvement and heightened efficiency.

5.4 Summary

The investigation into optimizing operational parameters for leaching synthetic scheelite in an H_2SO_4 and H_2O_2 solution centered around three key factors: reagent concentration, temperature, and leaching duration. The conclusions drawn from the experimental outcomes are as follows:

- The significance of the initial concentrations of H_2SO_4 and H_2O_2, and their influence on leaching efficiency and final product characteristics, was highlighted. Within the context of synergistic leaching for synthetic scheelite, reducing the H_2SO_4 concentration to one-third of the established level (3 mol/L) was feasible. Conversely, maintaining an H_2O_2 concentration of 1.5 mol/L proved advantageous for promoting effective leaching reactions and crystallization. This tailored reagent combination resulted in a modest reduction of approximately 5% in leaching efficiency. This finding underscores the potential for achieving high-efficiency leaching through a synergistic optimization of reaction conditions and other operational parameters. Notably, this optimized process offers the dual benefits of reducing chemical consumption, making it a more environmentally friendly approach, and ensuring cost-effectiveness.

- The optimization of temperature from 45°C to 60°C in the reagent-optimized system yielded a notable enhancement in leaching efficiency, with improvements ranging from 2% to 3%.

- Extending the leaching duration emerged as a beneficial strategy for establishing optimal conditions conducive to a highly efficient reaction within the reagent-optimized system. Combining increased leaching time with temperature optimization led to further improvements in leaching efficiency. Remarkably, the results indicated that equivalent efficiency levels can be attained by reducing the H_2SO_4 concentration from the recommended 3 mol/L in reference 1 [8] to 1 mol/L for synthetic scheelite while elevating the temperature from 45 to 60°C and extending leaching duration from 90 to 120 minutes.

Table 5.4 presents a comprehensive overview of the conducted optimization tests alongside their corresponding leaching efficiencies. In summation, the optimal conditions for leaching synthetic scheelite in an H_2SO_4 and H_2O_2 solution are as follows: H_2SO_4 concentration of 1 mol/L, H_2O_2 concentration of 1.5 mol/L, leaching temperature of 60°C, leaching duration of 120 minutes, and a stirring speed of 400 rpm. These optimized conditions yielded a remarkable leaching efficiency of 95.91%. However, it is imperative to undertake further exploration to gauge the implications of this optimization approach on natural ore. Such research holds the potential to offer valuable insights aimed at boosting the efficiency and productivity of the process.

Table 5. 4 Summary of the operating parameters in optimization test with leaching efficiency results.

Conditions	Test 1	Test 2	Test 3	Test 4	Test 5	Test 6	Test 7	Test 8	Test 9	Test 10
H_2SO_4 (mol/L)	2	1	2	1	0.5	1	2	1	2	1
H_2O_2 (mol/L)	1.5	1.5	1	1	1	0.5	1.5	1.5	1.5	1.5
L/S ratio (mL/g)	10	10	10	10	10	10	10	10	10	10
Temperature (°C)	45	45	45	45	45	45	60	60	60	60
Leaching duration (min)	90	90	90	90	90	90	90	90	60	120
Stirring rate (r/min)	400	400	400	400	400	400	400	400	400	400
Leaching efficiency (%)	90.43	89.32	89.84	89.67	54.62	89.2	92.23	91.68	72.8	95.91

CHAPTER 6 CONCLUSIONS AND FUTURE RECOMMENDATIONS

In conclusion, this study embarked on a comprehensive exploration of optimizing the synergistic leaching process for synthetic scheelite using a mixed H_2SO_4-H_2O_2 acid solution. The research involved a diverse range of experiments designed to assess the feasibility of a sequential 2-step leaching approach, unravel the mechanisms of lixivium recycling and reuse, and ultimately achieve optimization. A focal point of this investigation was the systematic examination of operational parameter optimization, aimed at advancing the current comprehension of scheelite leaching. The study has yielded significant findings and highlighted avenues for future research, encapsulating both key discoveries and areas that merit deeper exploration.

6.1 Conclusions

- This study underscores the significance of H_2O_2 in the leaching process. The synergistic leaching approach involves the rapid formation of insoluble solid products, H_2WO_4 and $CaSO_4$, upon ore addition. H_2O_2 functions as a complexing agent, preventing H_2WO_4 precipitation and facilitating W to PTA conversion. However, the proposed 2-step method, which aims to convert H_2WO_4 to PTA in a subsequent step, presents challenges. The 2-step process requires extended time due to slow reaction in the second step, surpassing the recommended duration for synergistic leaching. Moreover, the presence of precipitated H_2WO_4 on unreacted $CaWO_4$ particles inhibits further reaction, making it difficult to reduce H_2O_2 retention time. In comparison, synergistic leaching outperforms the 2-step method by achieving higher efficiency and yields. The prolonged reaction time of the latter approach leads to energy loss and decreased productivity, while synergistic leaching offers satisfactory results without necessitating complete H_2WO_4 conversion, ultimately enhancing process efficacy.

- The study underscores the influence of H_2SO_4 concentration on the crystal characteristics of $CaSO_4$ and H_2WO_4 products. Reduced H_2SO_4 concentration results in smaller, denser crystals, which pose filtration challenges and reduce leaching efficiency. In line with reference 1 [8] conditions, lixivium recycling without additional H_2SO_4 supplementation is viable for two cycles, yielding comparable final products and byproducts. This approach promotes waste reduction, lowers reagent consumption, enhances cost-effectiveness, and aligns with eco-friendly practices. Exploring thermal decomposition time and L/S ratio reveals that higher solid ratios require more time. Initially set at 4 hours, thermal

decomposition time was optimized to 6 hours for higher solid ratios. The possibility of reusing lixivium twice without additional H_2SO_4 supports the optimization of H_2SO_4 concentration using reference 1 [8] conditions. This optimization reduces H_2SO_4 consumption, contributing to a more environmentally sustainable synthetic scheelite leaching process in an H_2SO_4-H_2O_2 mixed solution.

- The study highlights the impact of initial H_2SO_4 and H_2O_2 concentrations on leaching efficiency and product characteristics. Within the context of synergistic leaching for synthetic scheelite, a reduction of H_2SO_4 concentration by one-third (from 3 mol/L) is feasible, while maintaining H_2O_2 at 1.5 mol/L is advantageous for effective leaching and crystallization. Moreover, temperature optimization within the reagent-optimized systems, shifting from 45°C to 60°C, demonstrates a positive impact, enhancing leaching efficiency by approximately 2-3%. Additionally, extending the leaching duration emerges as a favorable strategy for ensuring optimal conditions within the reagent-optimized system. In conclusion, it has been demonstrated that the optimized system is achieved by reducing the H_2SO_4 concentration from 3 mol/L to 1 mol/L, increasing the temperature from 45°C to 60°C, and extending the leaching duration from 90 minutes to 120 minutes. The achieved leaching efficiency of 95.91% obtained is very close to the 95.98% leaching efficiency obtained from the reference 1 [8] test conducted within the scope of the validation test.

6.2 Future Work

Based on the findings, further research is warranted to address the following aspects:

- Identification of newly optimized thermal decomposition conditions for a leaching system employing the proposed optimal leaching conditions.
- Determination of optimal operating conditions for both natural and synthetic ore scenarios.
- Exploration of strategies to enhance the feed ratio for improved process efficiency.

REFERENCES

[1]   Y. Lei, F. Sun, X. Liu, and Z. Zhao, "Understanding the wet decomposition processes of tungsten ore: Phase, thermodynamics and kinetics," *Hydrometallurgy*, vol. 213, p. 105928, 2022, doi: https://doi.org/10.1016/j.hydromet.2022.105928.

[2]   A. Koutsospyros, W. Braida, C. Christodoulatos, D. Dermatas, and N. Strigul, "A review of tungsten: From environmental obscurity to scrutiny," *J Hazard Mater*, vol. 136, no. 1, pp. 1–19, 2006, doi: https://doi.org/10.1016/j.jhazmat.2005.11.007.

[3]   X. Yang, "Beneficiation studies of tungsten ores – A review," *Miner Eng*, vol. 125, pp. 111–119, 2018, doi: https://doi.org/10.1016/j.mineng.2018.06.001.

[4]   Q. LIU, T. TU, H. GUO, H. CHENG, and X. WANG, "Complexation extraction of scheelite and transformation behaviour of tungsten-containing phase using H2SO4 solution with H2C2O4 as complexing agent," *Transactions of Nonferrous Metals Society of China*, vol. 31, no. 10, pp. 3150–3161, 2021, doi: https://doi.org/10.1016/S1003-6326(21)65724-2.

[5]   J. I. Martins, J. L. F. C. Lima, A. Moreira, and S. C. Costa, "Tungsten recovery from alkaline leach solutions as synthetic scheelite," *Hydrometallurgy*, vol. 85, no. 2, pp. 110–115, 2007, doi: https://doi.org/10.1016/j.hydromet.2006.08.007.

[6]   L. Wan, L. Yang, Y. Chen, L. Zhao, and H. Li, "Synthesis of scheelite with wolframite and calcium carbonate by a direct solid-state synthesis route," *Int J Refract Metals Hard Mater*, vol. 48, pp. 301–304, 2015, doi: https://doi.org/10.1016/j.ijrmhm.2014.09.023.

[7]   L. Wan, X. Huang, D. Deng, H. Li, and Y. Chen, "Synthesis of scheelite from sodium tungstate solution by calcium hydroxide addition," *Hydrometallurgy*, vol. 154, pp. 17–19, 2015, doi: https://doi.org/10.1016/j.hydromet.2015.03.010.

[8]   C. Yin, L. Ji, X. Chen, X. Liu, and Z. Zhao, "Efficient leaching of scheelite in sulfuric acid and hydrogen peroxide solution," *Hydrometallurgy*, vol. 192, p. 105292, 2020, doi: https://doi.org/10.1016/j.hydromet.2020.105292.

[9]   L. Shen, X. Li, D. Lindberg, and P. Taskinen, "Tungsten extractive metallurgy: A review of processes and their challenges for sustainability," *Miner Eng*, vol. 142, p. 105934, 2019, doi: https://doi.org/10.1016/j.mineng.2019.105934.

[10] L. Xiao *et al.*, "Tungsten extraction from scheelite hydrochloric acid decomposition residue by hydrogen peroxide," *Miner Eng*, vol. 179, p. 107461, 2022, doi: https://doi.org/10.1016/j.mineng.2022.107461.

[11] W. Zhang *et al.*, "Understanding the role of hydrogen peroxide in sulfuric acid system for leaching low-grade scheelite from the perspective of phase transformation and kinetics," *Sep Purif Technol*, vol. 277, p. 119407, 2021, doi: https://doi.org/10.1016/j.seppur.2021.119407.

[12] J. Li and Z. Zhao, "Kinetics of scheelite concentrate digestion with sulfuric acid in the presence of phosphoric acid," *Hydrometallurgy*, vol. 163, pp. 55–60, 2016, doi: https://doi.org/10.1016/j.hydromet.2016.03.009.

[13] W. Zhang, Y. Chen, J. Che, C. Wang, and B. Ma, "Green leaching of tungsten from synthetic scheelite with sulfuric acid-hydrogen peroxide solution to prepare tungstic acid," *Sep Purif Technol*, vol. 241, p. 116752, 2020, doi: https://doi.org/10.1016/j.seppur.2020.116752.

[14] P. Pędziwiatr, F. Mikołajczyk, D. Zawadzki, K. Mikołajczyk, and A. Bedka, "Decomposition of hydrogen peroxide - kinetics and review of chosen catalysts," *Acta Innovations*, pp. 45–52, Jun. 2018, doi: 10.32933/ActaInnovations.26.5.

[15] M. J. Nicol, "The role and use of hydrogen peroxide as an oxidant in the leaching of minerals. II. alkaline solutions," *Hydrometallurgy*, vol. 194, p. 105365, 2020, doi: https://doi.org/10.1016/j.hydromet.2020.105365.

[16] Y.-T. Park and K.-T. Lee, "Characterization of nanoparticulated WO3 electrochromic thin films prepared via precipitation reaction of peroxotungstic acid solution," *Opt Mater (Amst)*, vol. 121, p. 111577, 2021, doi: https://doi.org/10.1016/j.optmat.2021.111577.

[17] X. Zhu, X. Li, H. Zhang, and J. Huang, "International market power analysis of China's tungsten export market – from the perspective of tungsten export policies," *Resources Policy*, vol. 61, pp. 643–652, 2019, doi: https://doi.org/10.1016/j.resourpol.2018.11.005.

[18] T. Henckens, "Chapter 7 - Thirteen scarce resources analyzed," in *Governance of the World's Mineral Resources*, T. Henckens, Ed., Elsevier, 2021, pp. 147–380. doi: https://doi.org/10.1016/B978-0-12-823886-8.00007-5.

[19]   G. D. RIECK, "CHAPTER 1 - HISTORY, USE, ORES AND PRODUCTION," in *Tungsten and its Compounds*, G. D. RIECK, Ed., Pergamon, 1967, pp. 1–5. doi: https://doi.org/10.1016/B978-1-4832-0108-5.50004-5.

[20]   L. Shen, X. Li, and P. Taskinen, "Thermodynamics of Tungsten Ores Decomposition Process Options," Mar. 2018. doi: 10.1007/978-3-319-95022-8_206.

[21]   H. Wang *et al.*, "Efficient dissolution of tungstic acid by isopolytungstate solution based on the polymerization theory of tungsten," *Hydrometallurgy*, vol. 209, p. 105835, 2022, doi: https://doi.org/10.1016/j.hydromet.2022.105835.

[22]   G. Calvo, A. Valero, and A. Valero, "How can strategic metals drive the economy? Tungsten and tin production in Spain during periods of war," *Extr Ind Soc*, vol. 6, no. 1, pp. 8–14, 2019, doi: https://doi.org/10.1016/j.exis.2018.07.008.

[23]   M. Yang, X. Zhang, A. Grosjean, I. Soroka, and M. Jonsson, "Kinetics and Mechanism of the Reaction between H2O2 and Tungsten Powder in Water," *The Journal of Physical Chemistry C*, vol. 119, no. 39, pp. 22560–22569, Oct. 2015, doi: 10.1021/acs.jpcc.5b07012.

[24]   B. Barume, U. Naeher, D. Ruppen, and P. Schütte, "Conflict minerals (3TG): Mining production, applications and recycling," *Curr Opin Green Sustain Chem*, vol. 1, pp. 8–12, 2016, doi: https://doi.org/10.1016/j.cogsc.2016.07.004.

[25]   B. Zeiler, A. Bartl, and W.-D. Schubert, "Recycling of tungsten: Current share, economic limitations, technologies and future potential," *Int J Refract Metals Hard Mater*, vol. 98, p. 105546, 2021, doi: https://doi.org/10.1016/j.ijrmhm.2021.105546.

[26]   W. T. ELWELL and D. F. WOOD, "CHAPTER 2 - PHYSICAL AND CHEMICAL PROPERTIES," in *Analytical Chemistry of Molybdenum and Tungsten*, W. T. ELWELL and D. F. WOOD, Eds., in International Series of Monographs on Analytical Chemistry, vol. 47. Pergamon, 1971, pp. 5–11. doi: https://doi.org/10.1016/B978-0-08-016673-5.50006-5.

[27]   X. WANG *et al.*, "Review of tungsten resource reserves, tungsten concentrate production and tungsten beneficiation technology in China," *Transactions of Nonferrous Metals Society of China*, vol. 32, no. 7, pp. 2318–2338, 2022, doi: https://doi.org/10.1016/S1003-6326(22)65950-8.

[28]   J. Sun and B. C. Bostick, "Effects of tungstate polymerization on tungsten(VI) adsorption on ferrihydrite," *Chem Geol*, vol. 417, pp. 21–31, 2015, doi: https://doi.org/10.1016/j.chemgeo.2015.09.015.

[29]   "Tungsten," *British Geological Survey*. British Geological Survey, Jan. 2011. Accessed: May 09, 2022. [Online]. Available: https://www2.bgs.ac.uk/mineralsuk/download/mineralProfiles/tungsten_profile.pdf

[30]   B. Pracejus, "IV/D - Oxides with Metal : Oxygen = 1 : 2 (MO2 and related compounds)," in *The Ore Minerals Under the Microscope (Second Edition)*, B. Pracejus, Ed., Second Edition.Elsevier, 2014, pp. 790–867. doi: https://doi.org/10.1016/B978-0-444-62725-4.50016-8.

[31]   A. Shemi, A. Magumise, S. Ndlovu, and N. Sacks, "Recycling of tungsten carbide scrap metal: A review of recycling methods and future prospects," *Miner Eng*, vol. 122, pp. 195–205, 2018, doi: https://doi.org/10.1016/j.mineng.2018.03.036.

[32]   K. Shedd, "Tungsten Recycling in the United States in 2000," May 2022.

[33]   S. N. Bhosale, S. Mookherjee, and R. M. Pardeshi, "Current practices in tungsten extraction and recovery," *High temperature materials and processes*, vol. 9, pp. 147–162, 1990.

[34]   H. Liu, H. Liu, C. Nie, J. Zhang, B.-M. Steenari, and C. Ekberg, "Comprehensive treatments of tungsten slags in China: A critical review," *J Environ Manage*, vol. 270, p. 110927, 2020, doi: https://doi.org/10.1016/j.jenvman.2020.110927.

[35]   C. L. Rollinson, "1 - THE ELEMENT," in *The Chemistry of Chromium, Molybdenum and Tungsten*, C. L. Rollinson, Ed., in Pergamon International Library of Science, Technology, Engineering and Social Studies. Pergamon, 1973, pp. 742–749. doi: https://doi.org/10.1016/B978-0-08-018868-3.50011-2.

[36]   Z. , Han, A. , Golev, and M. Edraki, "A Review of Tungsten Resources and Potential Extraction from Mine Waste," *Minerals*, vol. 11, no. 7, p. 701, Jul. 2021.

[37]   M. Osvald *et al.*, "Laboratory investigations of the physical parameters influencing the in situ leaching of tungsten," *Geothermics*, vol. 89, p. 101992, 2021, doi: https://doi.org/10.1016/j.geothermics.2020.101992.

[38]   H. H. Ahn and M.-S. Lee, "Hydrometallurgical Processes for the Recovery of Tungsten from Ores and Secondary Resources," Apr. 2018, doi: 10.7844/kirr.2018.27.6.3.

[39]   J. Li *et al.*, "Wolframite geochronology and scheelite geochemistry of the Yangwuchang W-Au deposit and Dashegou W deposit in the Yangxie ore district, the North Qinling, China: Implications for W-Au mineralization," *Ore Geol Rev*, vol. 155, p. 105359, 2023, doi: https://doi.org/10.1016/j.oregeorev.2023.105359.

[40]   L. C. Hsu and P. E. Galli, "Origin of the Scheelite-Powellite Series of Minerals," *Economic Geology*, vol. 68, no. 5, pp. 681–696, Aug. 1973, doi: 10.2113/gsecongeo.68.5.681.

[41]   Y. Lu, S. Wang, and H. Zhong, "New insights into separating wolframite from calcium bearing minerals by flotation," *Journal of Industrial and Engineering Chemistry*, vol. 97, pp. 549–559, 2021, doi: https://doi.org/10.1016/j.jiec.2021.03.014.

[42]   S. K. Haldar, "Chapter 1 - Minerals and rocks," in *Introduction to Mineralogy and Petrology (Second Edition)*, S. K. Haldar, Ed., Second Edition.Oxford: Elsevier, 2020, pp. 1–51. doi: https://doi.org/10.1016/B978-0-12-820585-3.00001-6.

[43]   S. K. Haldar, "Chapter 12 - Mineral Processing," in *Mineral Exploration*, S. K. Haldar, Ed., Boston: Elsevier, 2013, pp. 223–250. doi: https://doi.org/10.1016/B978-0-12-416005-7.00012-X.

[44]   G. Ai, W. Huang, X. Yang, and X. Li, "Effect of collector and depressant on monomineralic surfaces in fine wolframite flotation system," *Sep Purif Technol*, vol. 176, pp. 59–65, 2017, doi: https://doi.org/10.1016/j.seppur.2016.11.064.

[45]   L. Dong, F. Jiao, W. Qin, and W. Liu, "Selective flotation of scheelite from calcite using xanthan gum as depressant," *Miner Eng*, vol. 138, pp. 14–23, 2019, doi: https://doi.org/10.1016/j.mineng.2019.04.030.

[46]   S. Shuai *et al.*, "Selective separation of wolframite from calcite by froth flotation using a novel amidoxime surfactant: Adsorption mechanism and DFT calculation," *Miner Eng*, vol. 185, p. 107716, 2022, doi: https://doi.org/10.1016/j.mineng.2022.107716.

[47]   J. Z. Kuang, Y. Yang, Z. Zou, W. Yuan, Z. Huang, and H. Cheng, "Effect of metal ions on the dispersion and agglomeration behavior of micro-fine wolframite," *Colloids Surf A Physicochem Eng Asp*, vol. 643, p. 128747, 2022, doi: https://doi.org/10.1016/j.colsurfa.2022.128747.

[48] A. O. Kalpakli, S. Ilhan, C. Kahruman, and I. Yusufoglu, "Dissolution behavior of calcium tungstate in oxalic acid solutions," *Hydrometallurgy*, vol. 121–124, pp. 7–15, 2012, doi: https://doi.org/10.1016/j.hydromet.2012.04.014.

[49] M. Robbins, "Fluorescent Forum," *Rocks & Minerals*, vol. 65, no. 5, pp. 455–459, 1990, doi: 10.1080/00357529.1990.11761711.

[50] N. Kupka and M. Rudolph, "Froth flotation of scheelite – A review," *Int J Min Sci Technol*, vol. 28, no. 3, pp. 373–384, 2018, doi: https://doi.org/10.1016/j.ijmst.2017.12.001.

[51] Z. Guan, K. Lu, Y. Zhang, H. Yang, and X. Li, "Mechanism of manganese ion interaction with the surface of scheelite and calcite and its effect on flotation separation," *Colloids Surf A Physicochem Eng Asp*, vol. 648, p. 129397, 2022, doi: https://doi.org/10.1016/j.colsurfa.2022.129397.

[52] C. Zhong, H. Wang, B. Feng, L. Zhang, Y. Chen, and Z. Gao, "Flotation separation of scheelite and apatite by polysaccharide depressant xanthan gum," *Miner Eng*, vol. 170, p. 107045, 2021, doi: https://doi.org/10.1016/j.mineng.2021.107045.

[53] J. I. Martins, "Leaching of Synthetic Scheelite by Nitric Acid without the Formation of Tungstic Acid," *Ind Eng Chem Res*, vol. 42, no. 21, pp. 5031–5036, Oct. 2003, doi: 10.1021/ie030008s.

[54] J. I. Martins, A. Moreira, and S. C. Costa, "Leaching of synthetic scheelite by hydrochloric acid without the formation of tungstic acid," *Hydrometallurgy*, vol. 70, no. 1, pp. 131–141, 2003, doi: https://doi.org/10.1016/S0304-386X(03)00053-7.

[55] W. Zhang, J. Li, Z. Zhao, S. Huang, X. Chen, and K. Hu, "Recovery and separation of W and Mo from high-molybdenum synthetic scheelite in HCl solutions containing H2O2," *Hydrometallurgy*, vol. 155, pp. 1–5, 2015, doi: https://doi.org/10.1016/j.hydromet.2015.03.020.

[56] J. I. Martins, A. Moreira, and S. C. Costa, "Leaching of synthetic scheelite by hydrochloric acid without the formation of tungstic acid," *Hydrometallurgy*, vol. 70, no. 1, pp. 131–141, 2003, doi: https://doi.org/10.1016/S0304-386X(03)00053-7.

[57] N. T. Nassar, T. E. Graedel, and E. M. Harper, "By-product metals are technologically essential but have problematic supply," *Sci Adv*, vol. 1, no. 3, p. e1400180, 2015, doi: 10.1126/sciadv.1400180.

[58] S. S. K. Kamal, P. K. Sahoo, J. Vimala, B. Shanker, P. Ghosal, and L. Durai, "Synthesis of high purity tungsten nanoparticles from tungsten heavy alloy scrap by selective precipitation and reduction route," *J Alloys Compd*, vol. 678, pp. 403–409, 2016, doi: https://doi.org/10.1016/j.jallcom.2016.03.303.

[59] T. Brown and P. Pitfield, "Tungsten," in *Critical Metals Handbook*, John Wiley & Sons, Ltd, 2014, pp. 385–413. doi: https://doi.org/10.1002/9781118755341.ch16.

[60] L. Shen *et al.*, "Wolframite Conversion in Treating a Mixed Wolframite–Scheelite Concentrate by Sulfuric Acid," *JOM: the journal of the Minerals, Metals & Materials Society*, vol. 70, pp. 161–167, Mar. 2017, doi: 10.1007/s11837-017-2691-1.

[61] S. Hairunnisha, G. K. Sendil, J. P. Rethinaraj, G. N. Srinivasan, P. Adaikkalam, and S. Kulandaisamy, "Studies on the preparation of pure ammonium para tungstate from tungsten alloy scrap," *Hydrometallurgy*, vol. 85, no. 2, pp. 67–71, 2007, doi: https://doi.org/10.1016/j.hydromet.2006.08.002.

[62] M. Weil and W.-D. Schubert, "The beautiful colours of tungsten oxides," *International Tungsten Industry Association: London, UK*, pp. 1–9, 2013.

[63] W. Guan, L. Zeng, G. Zhang, C. Zeng, G. Shang, and D. Wang, "Preliminary study on preparation of ammonium metatungstate from ammonium tungstate solutions using bipolar membrane electrodialysis," *Hydrometallurgy*, vol. 169, pp. 239–244, 2017, doi: https://doi.org/10.1016/j.hydromet.2017.01.013.

[64] J.-Q. Liu, Z.-L. Xu, and K.-G. Zhou, "Study on new method of the preparation of pure ammonium metatungstate (AMT) using a coupling process of neutralization–nanofiltration–crystallization," *J Memb Sci*, vol. 240, no. 1, pp. 1–9, 2004, doi: https://doi.org/10.1016/j.memsci.2004.03.027.

[65] R. Gero, L. Borukhin, and I. Pikus, "Some structural effects of plastic deformation on tungsten heavy metal alloys," *Materials Science and Engineering: A*, vol. 302, no. 1, pp. 162–167, 2001, doi: https://doi.org/10.1016/S0921-5093(00)01369-1.

[66] X. Cai, Y. Xu, M. Liu, B. Cao, and X. Li, "Study of the growth kinetics of in situ WC grains in tungsten carbide layers produced by a diffusion-controlled reaction," *Ceram Int*, vol. 48, no. 23, Part A, pp. 35290–35300, 2022, doi: https://doi.org/10.1016/j.ceramint.2022.08.131.

[67] P. Zhang, J. Wang, L. Wang, J. Li, and W. Jiang, "Dense tungsten carbide bulks by self-densification reaction sintering of nanodiamond with tungsten at 1700 °C," *Ceram Int*, vol. 49, no. 6, pp. 9287–9297, 2023, doi: https://doi.org/10.1016/j.ceramint.2022.11.095.

[68] X. Li, L. Shen, Q. Zhou, Z. Peng, G. Liu, and T. Qi, "Scheelite conversion in sulfuric acid together with tungsten extraction by ammonium carbonate solution," *Hydrometallurgy*, vol. 171, pp. 106–115, 2017, doi: https://doi.org/10.1016/j.hydromet.2017.05.005.

[69] C. Gong *et al.*, "The dissolution behavior of different forms of tungstic acid in hydrogen peroxide," *Hydrometallurgy*, vol. 202, p. 105598, 2021, doi: https://doi.org/10.1016/j.hydromet.2021.105598.

[70] T. Havlík, "Introduction," in *Hydrometallurgy*, T. Havlík, Ed., in Woodhead Publishing Series in Metals and Surface Engineering. Woodhead Publishing, 2008, pp. xi–xiii. doi: https://doi.org/10.1016/B978-1-84569-407-4.50020-7.

[71] N. Singh, J. Li, and X. Zeng, "Solutions and challenges in recycling waste cathode-ray tubes," *J Clean Prod*, vol. 133, pp. 188–200, 2016, doi: https://doi.org/10.1016/j.jclepro.2016.04.132.

[72] M. Nicol, "1 - Introduction," in *Hydrometallurgy*, M. Nicol, Ed., Elsevier, 2022, pp. 1–13. doi: https://doi.org/10.1016/B978-0-323-99322-7.00002-8.

[73] "Extractive Metallurgy | Introduction to Chemistry." https://courses.lumenlearning.com/introchem/chapter/extractive-metallurgy/ (accessed Jan. 03, 2022).

[74] L. Shen *et al.*, "Sustainable and efficient leaching of tungsten in ammoniacal ammonium carbonate solution from the sulfuric acid converted product of scheelite," *J Clean Prod*, vol. 197, pp. 690–698, 2018, doi: https://doi.org/10.1016/j.jclepro.2018.06.256.

[75] D. Gong, Y. Zhang, L. Wan, T. Qiu, Y. Chen, and S. Ren, "Efficient extraction of tungsten from scheelite with phosphate and fluoride," *Process Safety and Environmental Protection*, vol. 159, pp. 708–715, 2022, doi: https://doi.org/10.1016/j.psep.2022.01.029.

[76] Q. TENG, Z. YANG, and H. WANG, "Recovery of vanadium and nickel from spent-residue oil hydrotreating catalyst by direct acid leaching-solvent extraction," *Transactions of Nonferrous Metals Society of China*, vol. 33, no. 1, pp. 325–336, 2023, doi: https://doi.org/10.1016/S1003-6326(22)66110-7.

[77]   Y. Chen, G. Huo, X. Guo, and Q. Wang, "A sustainable process for tungsten extraction from wolframite concentrate," *Int J Refract Metals Hard Mater*, vol. 107, p. 105903, 2022, doi: https://doi.org/10.1016/j.ijrmhm.2022.105903.

[78]   J. I. Martins, "Leaching Systems of Wolframite and Scheelite: A Thermodynamic Approach," *Mineral Processing and Extractive Metallurgy Review*, vol. 35, Feb. 2014, doi: 10.1080/08827508.2012.757095.

[79]   Y. Chen, G. Huo, X. Guo, and Q. Wang, "Sustainable extraction of tungsten from the acid digestion product of tungsten concentrate by leaching-solvent extraction together with raffinate recycling," *J Clean Prod*, vol. 375, p. 133924, 2022, doi: https://doi.org/10.1016/j.jclepro.2022.133924.

[80]   G. H. Xuin, D. Y. Yu, and Y. F. Su, "Leaching of scheelite by hydrochloric acid in the presence of phosphate," *Hydrometallurgy*, vol. 16, no. 1, pp. 27–40, 1986, doi: https://doi.org/10.1016/0304-386X(86)90049-6.

[81]   G. He *et al.*, "Leaching kinetics of scheelite in hydrochloric acid solution containing hydrogen peroxide as complexing agent," *Hydrometallurgy*, vol. 144–145, pp. 140–147, 2014, doi: https://doi.org/10.1016/j.hydromet.2014.02.006.

[82]   S. Gürmen, S. Tımur, C. Arslan, and I. Duman, "Acidic leaching of scheelite concentrate and production of hetero-poly-tungstate salt," *Hydrometallurgy*, vol. 51, no. 2, pp. 227–238, 1999, doi: https://doi.org/10.1016/S0304-386X(98)00080-2.

[83]   J. Li *et al.*, "Efficient extraction of tungsten, calcium, and phosphorus from low-grade scheelite concentrate," *Miner Eng*, vol. 181, p. 107462, 2022, doi: https://doi.org/10.1016/j.mineng.2022.107462.

[84]   C. Kahruman and I. Yusufoglu, "Leaching kinetics of synthetic CaWO4 in HCl solutions containing H3PO4 as chelating agent," *Hydrometallurgy*, vol. 81, no. 3, pp. 182–189, 2006, doi: https://doi.org/10.1016/j.hydromet.2005.12.003.

[85]   W. Zhang, J. Yang, Z. Zhao, W. Wang, and J. Li, "Coordination leaching of tungsten from scheelite concentrate with phosphorus in nitric acid," *J Cent South Univ*, vol. 23, no. 6, pp. 1312–1317, 2016, doi: 10.1007/s11771-016-3181-2.

[86]   W. Zhang, J. Li, and Z. Zhao, "Leaching kinetics of scheelite with nitric acid and phosphoric acid," *Int J Refract Metals Hard Mater*, vol. 52, pp. 78–84, 2015, doi: https://doi.org/10.1016/j.ijrmhm.2015.05.017.

[87]   Z. Zhongwei and J. Li, "Method for extracting tungsten from scheelite," Jul. 08, 2014

[88]   J. Li *et al.*, "Extraction of tungsten from scheelite concentrate using a methanesulfonic acid-phosphoric acid coleaching process followed by solvent extraction with N1923," *Hydrometallurgy*, vol. 213, p. 105917, 2022, doi: https://doi.org/10.1016/j.hydromet.2022.105917.

[89]   Z. Zhao *et al.*, "Extracting tungsten from scheelite concentrate with caustic soda by autoclaving process," *Hydrometallurgy*, vol. 108, no. 1, pp. 152–156, 2011, doi: https://doi.org/10.1016/j.hydromet.2011.03.004.

[90]   X. Chen, F. Guo, Q. Chen, X. Liu, and Z. Zhao, "Dissolution behavior of the associated rare-earth elements in scheelite using a mixture of sulfuric and phosphoric acids," *Miner Eng*, vol. 144, p. 106057, 2019, doi: https://doi.org/10.1016/j.mineng.2019.106057.

[91]   C. Cao, X. Qiu, Y. Li, L. Yang, Z. Pang, and Z. Yuan, "Study on leaching behaviour of tungstates in acid solution containing phosphoric acid," *Hydrometallurgy*, vol. 197, p. 105392, 2020, doi: https://doi.org/10.1016/j.hydromet.2020.105392.

[92]   T. M. Nagiev, "6 - The Phenomena of Interference in Chemical and Biochemical Redox Reactions with Hydrogen Peroxide," in *Coherent Synchronized Oxidation Reactions by Hydrogen Peroxide*, T. M. Nagiev, Ed., Amsterdam: Elsevier, 2007, pp. 185–228. doi: https://doi.org/10.1016/B978-044452851-3/50007-8.

[93]   L. Shen, H. Sippola, X. Li, D. Lindberg, and P. Taskinen, "Thermodynamic Modeling of Calcium Sulfate Hydrates in a CaSO4–H2SO4–H2O System from 273.15 to 473.15 K up to 5 m Sulfuric Acid," *J Chem Eng Data*, vol. 65, no. 5, pp. 2310–2324, May 2020, doi: 10.1021/acs.jced.9b00829.

[94]   X. Liu *et al.*, "Recovery of tungsten from acidic solutions rich in calcium and iron," *Hydrometallurgy*, vol. 204, p. 105719, 2021, doi: https://doi.org/10.1016/j.hydromet.2021.105719.

[95] X. Liu *et al.*, "Acidic decomposition of scheelite by organic sodium phytate at atmospheric pressure," *Miner Eng*, vol. 172, p. 107125, 2021, doi: https://doi.org/10.1016/j.mineng.2021.107125.

[96] F. A. Forward and A. I. Vizsolyi, "Process for the production of tungstic acid," US3193347A, 1965

[97] L. Yang, X. Zhang, C. Cao, X. Huang, and L. Wan, "Sustainable and efficient leaching of tungsten from scheelite using the mixture of ammonium phosphate, ammonia and calcium fluoride," *Hydrometallurgy*, vol. 210, p. 105846, 2022, doi: https://doi.org/10.1016/j.hydromet.2022.105846.

[98] J. Pazinato, M. Villetti, O. Mertins, E. Da Silva, and I. Garcia, "Insights on Structuration of Peroxotungstic Acid in Aqueous Media," *J Braz Chem Soc*, vol. 30, Mar. 2018, doi: 10.21577/0103-5053.20180196.

[99] B. Pecquenard, H. Lecacheux, S. Castro-Garcia, and J. Livage, "Electrochromic properties of peroxopolytungstic acid thin films," *J Solgel Sci Technol*, vol. 13, pp. 923–927, 1998.

[100] S. Nasrazadani and S. Hassani, "Chapter 2 - Modern analytical techniques in failure analysis of aerospace, chemical, and oil and gas industries," in *Handbook of Materials Failure Analysis with Case Studies from the Oil and Gas Industry*, A. S. H. Makhlouf and M. Aliofkhazraei, Eds., Butterworth-Heinemann, 2016, pp. 39–54. doi: https://doi.org/10.1016/B978-0-08-100117-2.00010-8.

[101] L. Shen, "Technology and theory of producing APT from tungsten concentrates by sulfuric acid conversion-ammonium salt leaching," 2019.